

COMBINATORIAL REGULATION OF SHARED TARGET GENES

**BY
LMD AND MEF2**

DISSERTATION

zur Erlangung des Doktorgrades der Naturwissenschaften

**Doctor rerum naturalium
(Dr. rer. nat.)**

dem Fachbereich Biologie
der Philipps-Universität Marburg-
-Entwicklungsbiologie-

vorgelegt von

Paulo Miguel Fernandes Cunha
aus Barcelos, Portugal

Marburg/ Lahn 2010

This analysis was carried out at the European Molecular Biology Laboratory (EMBL) in Heidelberg, under the supervision of Dr. Eileen Furlong.

Vom Fachbereich Biologie
der Philipps-Universität Marburg als Dissertation am 14.07.2010 angenommen.

Erstgutachterin: Prof. Dr. Renate Renkawitz-Pohl
Zweitgutachterin: Prof. Dr. Susanne Önel

Tag der mündlichen Prüfung: 20.07.2010

**COMBINATORIAL REGULATION
OF SHARED TARGET GENES
BY
LMD AND MEF2**

Table of Contents

TABLE OF CONTENTS	4
FIGURES AND TABLES	7
1. SUMMARY	9
ABBREVIATIONS.....	10
2. INTRODUCTION	14
2.1. REGULATION OF GENE EXPRESSION IN DEVELOPMENT	14
2.2. <i>DROSOPHILA MELANOGASTER</i> AS A PRIME MODEL ORGANISM FOR THE STUDY OF DEVELOPMENTAL BIOLOGY	17
2.3. OVERVIEW OF MUSCLE DEVELOPMENT IN <i>DROSOPHILA MELANOGASTER</i>	18
2.3.1. The mesoderm is specified by signaling leading to invagination of a patch of ventral blastoderm	19
2.3.2. The mesoderm is subdivided by cues secreted from the overlying ectoderm	22
2.3.3. Specification of Founder Cells (FCs) and Fusion Competent Myoblasts (FCMs).....	23
2.3.4. Myotubes are formed by the process of Myoblast Fusion between FCs and FCMs	25
2.3.5. Terminal differentiation of myotubes to functional muscle fibers	30
2.4. COMPARISON WITH VERTEBRATE DEVELOPMENT	34
2.4.1. The somite is patterned by diffusible signaling molecules from nearby structures	34
2.4.2. Muscle development in vertebrates is controlled by master regulators of the MyoD family of Muscle Regulatory Factors (MRF)	35
2.5. <i>MYOCYTE ENHANCING FACTOR 2 (MEF2)</i> IS ESSENTIAL FOR MYOBLAST FUSION AND TERMINAL DIFFERENTIATION IN <i>DROSOPHILA</i>	38
2.5.1. <i>Mef2</i> is expressed in all muscle cells.....	38
2.5.2. <i>Mef2</i> loss-of-function leads to a complete block of myoblast fusion and terminal differentiation	39
2.5.3. <i>Mef2</i> regulates several genes involved in different aspects of muscle development ...	39
2.6. <i>LAME DUCK (LMD)</i> A ZN-FINGER TRANSCRIPTION FACTOR ESSENTIAL FOR FCM SPECIFICATION AND MYOBLAST FUSION.....	41
2.6.1. <i>lmd</i> is expressed specifically in FCMs during the time of myoblast fusion.....	41
2.6.2. <i>lmd</i> loss-of-function results in a lack of FCM differentiation and block of fusion.	42
2.6.3. <i>lmd</i> is a member of the Gli family of TFs, and can directly activate <i>Mef2</i>	43
2.6.4. The activity of Lmd is regulated by distinct posttranscriptional mechanisms	44

2.7. SYNERGISTIC COOPERATION ON COMMON ENHANCERS ALLOWS COMPLEX SPATIO-TEMPORAL REGULATION	46
3. AIM OF THE PROJECT.....	47
4. MATERIALS AND METHODS	48
4.1. MATERIALS	48
4.1.1. Instruments	48
4.1.2. Chemicals	49
4.1.3. Miscellaneous materials	50
4.1.4. Oligonucleotides.....	51
4.1.5. Antibodies.....	56
4.1.6. Plasmids.....	56
4.1.7. Software.....	56
4.1.8. Media, solutions and buffers	57
4.1.9. Fly lines	59
4.2. METHODS	60
4.2.1. Molecular Biology and Biochemistry.....	60
4.2.2. Histological techniques.....	61
4.2.3. Quantitative Real-Time Polymerase Chain Reaction (qPCR).....	63
4.2.4. Cell culture and Luciferase assays.....	64
4.2.5. ChIP-on-chip and Expression profiling.....	65
5. RESULTS	68
5.1. ANALYSIS OF <i>LMD</i> EXPRESSION PROFILING AND CHIP-ON-CHIP DATA	68
5.1.1. Genomic regions bound by <i>Lmd</i> <i>in vivo</i>	68
5.1.2. Known direct target genes are identified, underscoring the accuracy of the ChIP-on-chip results.....	70
5.1.3. Defining direct targets from ChIP-bound regions	71
5.1.4. Extensive co-regulation of target genes by <i>lmd</i> and <i>Mef2</i> via common enhancers.....	72
5.1.5. <i>Lmd</i> and <i>Mef2</i> CRM occupancy has different effects on target gene expression.....	73
5.2. <i>LMD</i> AND <i>MEF2</i> REGULATE TARGET GENES <i>IN VIVO</i> IN A SYNERGISTIC OR ANTAGONISTIC MANNER	75
5.3. DELIMITING ENHANCERS FROM CHIP BOUND REGIONS FOR <i>IN VIVO</i> AND <i>IN VITRO</i> STUDIES..	79
5.3.1. Scanning the sequences with a <i>Mef2</i> PWM reveals the presence of several putative <i>Mef2</i> binding sites	80
5.3.2. Conservation of sites in other <i>Drosophila</i> species helps to reduce false-positives.....	80
5.3.3. qPCR shows enrichment of <i>Lmd</i> Chromatin Immunoprecipitates in the vicinity of <i>Mef2</i> sites	81
5.4. CHARACTERIZATION OF NOVEL ENHANCERS.....	82

5.5.	LOSS OF <i>LMD</i> AND <i>MEF2</i> DIFFERENTIALLY AFFECTS REPORTER ACTIVITY <i>IN VIVO</i>	87
5.6.	<i>LMD</i> CO-REGULATES ENHANCERS WITH <i>MEF2</i> IN A COOPERATIVE, ADDITIVE OR INHIBITORY MANNER	91
5.6.1.	<i>lmd</i> can act as a transcriptional repressor	92
5.6.2.	<i>lmd</i> and <i>Mef2</i> can act additively to activate target genes	94
5.6.3.	<i>Lmd</i> and <i>Mef2</i> can act cooperatively to activate target genes	96
6.	DISCUSSION	98
6.1.	A SYSTEMATIC GENOMIC APPROACH IDENTIFIES DIRECT TARGET GENES OF <i>LMD</i>	98
6.2.	THE INTEGRATION OF DIVERSE TECHNIQUES PROVIDES INFORMATION FROM DIFFERENT PERSPECTIVES	99
6.3.	COMBINATORIAL BINDING ON SHARED ENHANCERS LEADS TO ADDITIVE, COOPERATIVE OR REPRESSIVE EFFECTS	100
6.4.	<i>LMD</i> AS A TRANSCRIPTIONAL REPRESSOR	101
7.	CONCLUSIONS	104
8.	APPENDIX	105
8.1.	NON-OVERLAPPING REGIONS BOUND BY <i>LMD</i>	105
8.2.	EXPRESSION PROFILING OF <i>LMD</i>	108
8.3.	DIRECT TARGET GENES OF <i>LMD</i> AND <i>MEF2</i>	119
9.	REFERENCES	124
	ACKNOWLEDGMENTS	132
	DECLARATION	134
	PUBLICATIONS	135
	<i>CURRICULUM VITAE</i>	136

Figures and Tables

Figures

Figure 1 - General architecture of a eukaryotic gene locus.....	15
Figure 2 – Somatic, Visceral and Heart, the three major types of muscle in <i>Drosophila</i> larvae.	18
Figure 3 - The blastoderm is subdivided by a gradient of nuclear Dorsal concentration.....	21
Figure 4 - The mesoderm is sub-specified both by the expression of genes in the mesoderm and by signaling from the overlying ectoderm.	22
Figure 5 - Progenitor cells are specified via integration of Ras signaling and Delta/Notch lateral inhibition.	24
Figure 6 - Model of myoblast fusion in <i>Drosophila</i>	28
Figure 7 - Fusion-Restricted Myogenic-Adhesive Structures (FuRMAS).	30
Figure 8 - The vertebrate somite is patterned by secreted signaling molecules of the same families as in <i>Drosophila</i> mesoderm patterning.	35
Figure 9 - Model of interaction between MRFs and Mef2 on common enhancers.....	37
Figure 10 - Schematic overview of <i>lmd</i> and <i>Mef2</i> function during myogenesis and collected data-points.....	69
Figure 11 - Positive controls are recovered in the ChIP-on-chip data.....	70
Figure 12 - Overlap between fragments bound by Lmd and Mef2, as well as direct target genes of both TFs.	72
Figure 13 - k-means clustering of <i>lmd</i> and <i>Mef2</i> expression data.	73
Figure 14 - Ectopic Expression detected by colorimetric <i>in situ</i> hybridization.	76
Figure 15 - Ectopic Expression detected by fluorescent <i>in situ</i> hybridization.	77
Figure 16 - Enhancers were further refined by qPCR.	79
Figure 17 - Quantitative PCR results show enrichment of Lmd binding in the vicinity of different Mef2 binding sites.....	81
Figure 18 - Novel <i>tramtrack</i> (<i>ttk</i>) early and late enhancers.....	82
Figure 19 - <i>blown fuse</i> (<i>blow</i>) enhancer	83
Figure 20 – Novel <i>goliath</i> (<i>gol</i>) enhancer.	84
Figure 21 - Refined CG5080 enhancer.....	85
Figure 22 - Reporter lines previously characterized or refined in this study.	86
Figure 23 - <i>lmd</i> and <i>Mef2</i> are differentially required for enhancer activity <i>in vivo</i>	89
Figure 24 - <i>lmd</i> and <i>Mef2</i> are differentially required for enhancer activity <i>in vivo</i>	90
Figure 25 - Lmd can repress expression activated by Mef2 <i>in vitro</i>	92
Figure 26 - Additive activation of targets <i>in vitro</i> between Lmd and Mef2.....	94
Figure 27 - Cooperative response.	96

Tables

Table I – Probe labeling reaction for *in situ* hybridization..... 61

Table II - qPCR Reaction Mix..... 64

Table III - Non-overlapping regions obtained by merging all significantly enriched sequences.... 105

Table IV - Expression profiling of lmd. 108

Table V - Direct target genes list for lmd and Mef2, showing shared target genes. 119

1. Summary

The development of any multicellular organism involves the coordinated expression of different genes in complex spatio-temporal patterns. These complex patterns of gene expression result from the interplay between multiple transcription factors (TFs) and their co-factors, acting on specific *cis*-regulatory modules to activate or repress the affected locus. This study investigates the interaction between two essential regulators of myogenesis: the transcription factors *Myocyte enhancing factor 2* (*Mef2*) and *lame duck* (*lmd*). Mutations in either of these transcription factors results in a similar block of fusion phenotype, but the molecular basis for this similar phenotype is not yet understood.

The analysis started with ChIP-on-chip to identify the genomic location where each TF binds *in vivo*. Microarrays were used again to conduct expression profiling of loss-of-function mutants, and the combination of these two approaches yielded a list of direct target genes of the two TFs. Interestingly, the majority of enhancers bound by *Lmd* are also bound by *Mef2* at the same developmental timepoint. Likewise, almost 80% of the *lmd* direct target genes are also direct targets of *Mef2*, revealing an extensive co-regulation between the two TFs. A group of shared direct targets was then selected for further study; *Lmd* and *Mef2*, alone or in combination, were used to drive ectopic expression of these genes, resulting in both synergistic and antagonistic interactions.

The affected enhancer for each target was identified using a variety of predictions, and transgenic fly lines were created to demonstrate the capacity of the enhancers for correct expression *in vivo*. These enhancers were also analyzed in the mutant background of loss-of-function mutations and revealed specific requirements for each transcription factor. *Lmd* and *Mef2* were also tested *in vitro* for their effect on transcription from these enhancers, revealing additive, cooperative, and repressive interactions.

These results indicate that *lmd* is a temporal and tissue-specific modulator of *Mef2* activity, acting both as a transcriptional activator and repressor on a subset of the catalog of target genes of *Mef2*. More generally, it demonstrates a scenario of flexibility in the regulatory output of two transcription factors, leading to additive, cooperative and repressive interactions.

Abbreviations

°C	degrees Celsius
<i>Act57B</i>	<i>Actin 57B</i>
<i>Act87E</i>	<i>Actin 87E</i>
<i>ants</i>	<i>antisocial</i>
<i>ap</i>	<i>apterous</i>
<i>bap</i>	<i>bagpipe</i>
<i>Arf 51F</i>	<i>ADP ribosylation factor 51F</i>
ARF6	synonym for <i>Arf51F</i>
<i>bap</i>	<i>bagpipe</i>
BDGP	Berkeley Drosophila Genome Project
bHLH	basic-Helix-Loop-Helix
<i>bin</i>	<i>binious</i>
<i>blow</i>	<i>blown fuse</i>
BMP4	Bone Morphogenic Protein 4
bp	basepair(s)
BSA	Bovine Serum Albumine
<i>βTub60D</i>	<i>β-Tubulin at 60D</i>
ca.	Circa
<i>caps</i>	<i>Capricious</i>
<i>cact</i>	<i>Cactus</i>
CAT	Chloramphenicol Acetyltransferase
CDM	CED-5, Dock180, Myoblast city
cDNA	complementary DNA
CDS	coding sequence
<i>Ced-12</i>	<i>Ced-12</i>
ChIP	Chromatin Immuno-Precipitation
<i>ci</i>	<i>cubitus interruptus</i>
<i>Con</i>	<i>Connectin</i>
<i>Crk</i>	<i>Crk</i>
CRM	Cis-Regulatory Module
DIG	Digoxigenin
<i>Dl</i>	<i>Delta</i>
<i>dl</i>	<i>dorsal</i>
DNA	deoxyribonucleic acid
Dock180	Dedicator of cytokinesis 1
<i>dpp</i>	<i>decapentaplegic</i>
<i>drl</i>	<i>derailed</i>
<i>duf</i>	<i>dumbfounded</i> (synon. for <i>kirre</i>)
ECM	Extracellular Matrix

EDTA	Ethylene Diamine Tetraacetic Acid
EGF	Epidermal Growth Factor
ELMO	(synon. for <i>Ced-12</i>)
EM	Electron Microscopy
<i>en</i>	<i>engrailed</i>
EST	Expressed Sequence Tag
<i>eve</i>	<i>even-skipped</i>
<i>Fas3</i>	<i>Fascilin III</i>
FC	Founder Cell
FCM	Fusion Competent Myoblast
FDR	False Discovery Rate
FGF	Fibroblast Growth Factor
FuRMAS	Fusion-Restricted Myogenic-Adhesive Structure
G	gravitational constant
g	gram(s)
GEF	Guanine nucleotide Exchange Factor
GFP	Green Fluorescent Protein
<i>gol</i>	<i>goliath</i>
<i>grk</i>	<i>gurken</i>
<i>gro</i>	<i>groucho</i>
<i>hbs</i>	<i>hibris</i>
<i>hh</i>	<i>hedgehog</i>
<i>him</i>	<i>holes in muscles</i>
HRP	Horseradish Peroxidase
hrs	hours
IgSF	Immunoglobulin Super Family
I κ -B	Inhibitor of κ B
<i>irreC</i>	<i>irregular-chiasm-C</i> (synon. of <i>rst</i>)
Kb	kilobasepair
<i>kette</i>	<i>kette</i> (synon. of <i>Hem</i>)
<i>kirre</i>	<i>kin of irregular chiasm C</i> (synon. of <i>duf</i>)
<i>Kr</i>	<i>Krüppel</i>
l	litre
<i>l'sc</i>	<i>lethal of scute</i>
<i>lmd</i>	<i>lame duck</i>
LOESS	locally weighted regression and smoothing scatterplots
<i>loner</i>	<i>loner</i> (synon. of <i>siz</i>)
M	molar
MADS	MCM1, AGAMOUS, DEFICIENS and SRF domain
MAPK	Mitogen-Activated Protein Kinase
<i>mbc</i>	<i>myoblast city</i>
<i>Mef2</i>	<i>Myocyte enhancing factor 2</i>
<i>mck</i>	<i>muscle creatine kinase</i>
<i>Mhc</i>	<i>Myosin heavy chain</i>
min	minute(s)
μ l	microlitre(s)

ml	millilitre(s)
μM	micromolar
mM	millimolar
MRF	Muscle Regulatory Factor
mRNA	messenger Ribonucleic Acid
<i>Myog</i>	<i>Myogenin</i>
<i>N</i>	<i>Notch</i>
<i>nau</i>	<i>nautilus</i>
<i>Net-A</i>	<i>Netrin-A</i>
<i>Net-B</i>	<i>Netrin-B</i>
NFκ-B	Nuclear Factor of <i>kappa</i> light chain gene enhancer in B Cells
ng	nanogram(s)
NLS	Nuclear Localization Signal
nM	nanomolar
<i>osk</i>	<i>oskar</i>
<i>Pax</i>	<i>Paxilin</i>
PBS	Phosphate Buffered Saline
PCR	Polymerase Chain Reaction
PH	Pleckstrin Homology
<i>pip</i>	<i>pipe</i>
PKA	Protein Kinase A
PWM	Position Weight Matrix
qPCR	quantitative real-time Polymerase Chain Reaction
<i>Rac1</i>	<i>Ras-related C3 botulinum toxin substrate 1</i>
<i>Rac2</i>	<i>Ras-related C3 botulinum toxin substrate 2</i>
Ras	Rat sarcoma 2 viral oncogene
<i>rho</i>	<i>rhomboid</i>
<i>RNA</i>	<i>ribonucleic acid</i>
<i>robo</i>	<i>roundabout</i>
<i>rols</i>	<i>rolling pebbles</i>
Rols7	Rolling pebbles 7
<i>rst</i>	<i>roughest</i> (synon. of <i>irreC</i>)
RT	Room Temperature
RTK	Receptor Tyrosine Kinase
S2	Schneider 2
SAM	Significance Analysis of Microarrays
<i>sd</i>	<i>scalloped</i>
SEM	Standard Error of the Mean
<i>sim</i>	<i>single-minded</i>
<i>siz</i>	<i>schizo</i> (synon. of <i>loner</i>)
<i>sli</i>	<i>slit</i>
<i>slou</i>	<i>slouch</i>
<i>slp</i>	<i>sloppy-paired</i>
SM	Somatic Muscle
<i>sna</i>	<i>snail</i>
<i>sns</i>	<i>sticks and stones</i>

<i>sog</i>	<i>short-gastrulation</i>
<i>spz</i>	<i>spätzle</i>
<i>Sr</i>	<i>Stripe</i>
SRF	Serum Response Factor
<i>sug</i>	<i>sugarbabe</i>
TAE	tris-acetate ethylene diamine tetraacetic acid buffer
<i>tin</i>	<i>tinman</i>
TF	Transcription Factor
<i>Tl</i>	<i>Toll</i>
TF	Transcription Factor
<i>top</i>	<i>torpedo</i>
<i>ttk</i>	<i>tramtrack</i>
<i>twi</i>	<i>twist</i>
<i>vg</i>	<i>vestigial</i>
<i>vn</i>	<i>vein</i>
VM	Visceral Muscle
WASp	Wiskott-Aldrich Syndrome protein
WIP	WASp interacting Protein
<i>wntD</i>	<i>wnt inhibitor of Dorsal</i>
<i>wg</i>	<i>wingless</i>
<i>wt</i>	<i>wildtype</i>
<i>zen</i>	<i>zerknüllt</i>

2. Introduction

2.1. Regulation of gene expression in development

There are many questions on the mind of a developmental biologist contemplating the different arrays of organisms, tissues, cells. The diversity and complexity of the processes by which cells grow, divide, communicate, migrate and organize themselves into tissues, structures and organs raises questions about the coordination between these cells, and the nature of the processes that ultimately lead to an organized multicellular organism. However, taking one step back, a more fundamental question is: What is it that makes one cell different from another in a multicellular organism? This question can be more specifically rephrased as: How can the very same genome lead to such a diverse array of phenotypes of cells in different tissues? And how are these different readouts achieved in such a precise and organized fashion during development?

The answer to these questions lies in the many different ways to read the genome. The processing of information from a gene to the mature protein product is by no means an easy or linear process; it is a complex process involving many different layers of regulation. Some of these layers represent crucial steps in the flow of information, while others may be seen as fine-tuning events leading to the refinement of the final readout.

The readout of the genome can be affected epigenetically by chromatin structure remodeling (Turner, 2002), while mRNA splicing and stability in combination with the regulation of nuclear export control the composition and amount of mature mRNA available for translation in the cytoplasm. The processivity of the ribosome regulates translation, and the stability of the protein itself defines how much of the final effector is present in the cell. In addition, post-translational modifications further fine-tune protein function. Before any of these steps can happen, regulation of transcription is the first crucial step in the regulation of the readout of the genome, common to all known organisms from bacteria to complex multicellular organisms. Indeed, transcription is the primary

level of control for the expression of most eukaryotic genes (Wray et al., 2003) (Lodish et al., 2000).

Compared to the relative simplicity of the bacterial operon, regulation of transcription in eukaryotes is far more complex. The simple design of bacterial operons leads to the simultaneous transcription of a set of genes (usually involved in a common process) from a common promoter. Eukaryotes on the other hand, tend to regulate genes separately, with members of common biological pathways located in independent loci.

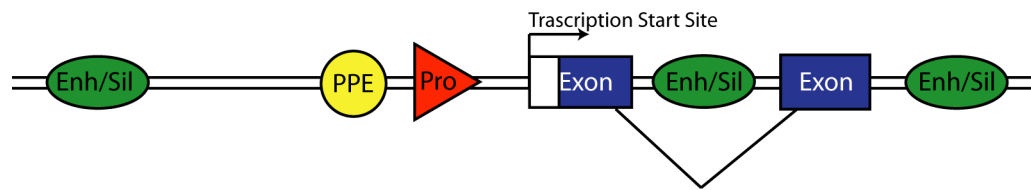


Figure 1 - General architecture of a eukaryotic gene locus.

The transcription machinery starts to assemble at the promoter (red triangle) and is aided by transcription factor binding immediately upstream in the upstream promoter proximal elements (yellow circle). The transcriptional start site (arrow) is located some 30-50 bp downstream. Transcription can be enhanced or repressed by enhancers/silencers (green ellipse) acting up to several thousand bp upstream or downstream, or even within introns.

Historically, three different DNA elements have been described for eukaryotic gene regulation, based on their distance to the transcriptional start site, as well as on interaction with different classes of proteins and functional characteristics of the modules (Figure 1). All three elements are *cis*-regulatory, acting on the same strand of DNA, as opposed to *trans*-acting elements like transcription factors (TFs) that can freely diffuse and act on a completely different and distant strand of DNA.

The promoter is the region of DNA to which the RNA polymerase and basal transcriptional machinery bind. It is located close (about 50 bp) upstream to the transcription start site and usually consists of a TATA box, initiator site or CpG island. The promoter proximal elements are elements that influence transcription through the binding of transcription factors, and are located about 100-200 bp upstream of the start site. They are sometimes considered part of the basal promoter (Blackwood and Kadonaga, 1998). Finally, there is a class of elements called enhancers due to the fact that even though they are not needed for basal

transcription, they are essential to enhance it. Similar elements can repress transcription (silencers). Enhancers/silencers are characterized by their ability to influence gene expression regardless of their orientation or relative position to the transcriptional start site. They can act over large distances (up to several thousand bp) and be located downstream, upstream, and even within introns of a gene (Figure 1) (Blackwood and Kadonaga, 1998) (Davidson, 2006).

These features make the identification of enhancers, also referred to as cis-regulatory-modules (CRMs), for a specific gene a difficult task. The term module emphasizes the fact that in many cases the precise spatio-temporal expression of a gene is actually the sum of individual contributions of distinct “modules”. A classical example is the *Myocyte enhancing factor 2 (Mef2)* gene. Mef2 protein is expressed in all myogenic cells throughout embryogenesis. Despite this seemingly simple pattern, this broad expression is the cumulative result of an impressive array of different CRMs spanning about 12 Kb of sequence, each responsible for a precise spatio-temporal band of expression in a different subset of mesodermal cells (Nguyen and Xu, 1998). Analysis of well-established CRMs shows that they typically comprise about 6-15 binding sites of 4-8 different transcription factors spanning a region of 50-500 bp of DNA. Thus a CRM is a cluster of TF binding sites that functions as a module to drive a specific spatio-temporal pattern in development (Davidson, 2006) (Arnone and Davidson, 1997)

2.2. *Drosophila melanogaster* as a prime model organism for the study of Developmental Biology

The fruit fly *Drosophila melanogaster* has been the subject of extensive study for almost a century (Rubin and Lewis, 2000). *Drosophila* is very well suited for the study of development due to its quick embryonic development (≈ 20 hours at 25 °C) and rapid generation time of about ten days. Fruit flies are also relatively inexpensive to maintain even in high numbers, being robust and tolerant of a wide range of environmental conditions. *Drosophila* is also very amenable to genetic studies, as they only have four chromosomes, one of which (the 4th) is very small and compact, containing few genes. Effectively, for experimental studies most geneticists only have to deal with three chromosomes, simplifying the mapping of genes and the ability to decipher their function *in vivo*. The fact that its genome lacks much of the redundancy often found in that of vertebrates has also proven to be a key advantage to its usefulness in the genomic era. Besides a sophisticated genetic toolkit, a wide range of well-established techniques is available, ranging from histological analysis to biochemical approaches, all coupled with a meticulously defined morphological mapping of embryonic development (Campos-Ortega and Hartenstein, 1997). In addition, the *Drosophila* research community shares a comprehensive pool of accumulated reagents. As a result, more knowledge has accumulated during the past 4-5 decades about *Drosophila melanogaster* than about virtually any other multicellular organism.

The genome of *Drosophila melanogaster* was sequenced at the turn of the millennium (Adams et al., 2000) allowing a new perspective on the study of gene function. Many other *Drosophila* species have since been fully sequenced (Richards et al., 2005) (Clark et al., 2007) allowing powerful comparative analysis between species. With the recent completion of the human genome, the high degree of conservation from flies to humans is now apparent, with $\sim 70\%$ of *Drosophila* genes having an ortholog in humans.

2.3. Overview of Muscle development in *Drosophila melanogaster*

The *Drosophila* muscle can be divided into three main classes according to structural and functional criteria. Somatic (SM) or body wall muscle is analogous to vertebrate skeletal muscle, and is present in a stereotypical array of 30 muscles per hemisegment used for locomotion and body structure (Figure 2 A). Visceral muscle (VM) lines the gut in an analogous way to vertebrate smooth muscle, and consists of interior circular rings covered by an exterior layer of longitudinal fibers (Figure 2 B). Heart muscle takes the form of the elongated dorsal vessel, and has many analogies to vertebrate cardiac muscle (Figure 2 C).

The different muscle types are derived from a common mesodermal origin but have subsequently taken different developmental paths. In brief, the mesoderm is specified by an array of transcription factors acting specifically in the ventral blastoderm. Cells in this ventral region invaginate into the interior of the embryo, dissociate from each other and begin to proliferate and migrate dorsally. The different types of muscles are sub-specified both by the action of segmentation genes and by signaling from the overlying ectoderm. The dorsal region of the mesoderm gives rise to visceral muscle and heart precursors, while the somatic muscle arises from cell lying more ventral to the cardiogenic mesoderm. Once specified, the SM myoblasts develop the ability to specifically recognize other muscle cells and fuse with each other, creating syncytial myotubes. These myotubes terminally differentiate and express the typical proteins of the contractile apparatus to become functional muscles.

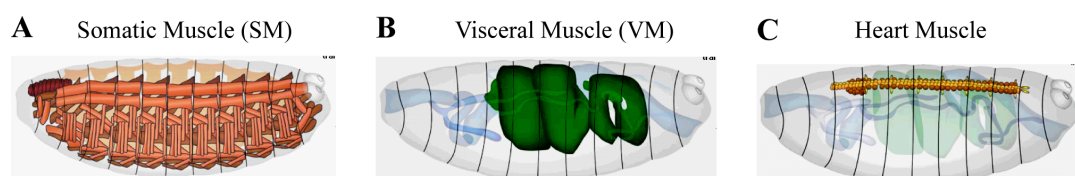


Figure 2 – Somatic, Visceral and Heart, the three major types of muscle in *Drosophila* larvae.

Schematic drawing of the three major types of muscle in *Drosophila* larvae, at stage 17. (A) Somatic Muscle. (B) Visceral Muscle. (C) Heart Muscle. Larvae are depicted with anterior to the left and dorsal at the top. Adapted from (Hartenstein, 2006)

2.3.1. The mesoderm is specified by signaling leading to invagination of a patch of ventral blastoderm

The first steps of *Drosophila* embryonic development differ from those in vertebrates in the fact that the first 13 rounds of nuclear division occur without cytokinesis, resulting in a syncytial blastoderm containing many nuclei sharing a common cytoplasm. As these divisions take place, the nuclei progressively migrate to the periphery of the embryo and form a rim at the edge of the embryo. Next, the nuclei are surrounded by in-growing cell membranes and cellularization takes place leading to the cellular blastoderm stage, characterized by a single epithelium of cells lining the embryo (Gilbert, 2006). The mesoderm originates from a ventral patch of cells from this epithelium that invaginate and spread dorsally. Simultaneously, they become progressively more sub-specified and eventually give rise to all three types of muscle, fat body, gonadal mesoderm and macrophages. The specification of this ventral patch is a complex process that can ultimately be traced back to the very specification of the embryonic dorso-ventral axis.

During oogenesis, the dorso-ventral axis of the embryo is established through intercellular communication between the oocyte and the surrounding somatic follicle cells. When the nucleus of the oocyte is located at an anterior-dorsal position, it allows the translation of *gurken* mRNA in this location only. *gurken* (*grk*) is a homologue of vertebrate EGF (Epidermal Growth Factor), and upon secretion from the oocyte binds to an EGF receptor coded by *torpedo* (*top*) in the follicle cells. This directs these cells to adopt a follicle dorsal fate, and inhibits them from expressing *pipe* (*pip*). Pipe is therefore synthesized in the ventral follicle cells only, and starts a proteolytic cascade in the perivitelline space leading to the cleavage of the signaling protein Spätzle specifically on the ventral side of the embryo. The cleaved Spätzle fragment is a ligand for the transmembrane receptor Toll, ubiquitously expressed in the embryo. Limited diffusion of Spätzle (Spz) in the perivitelline space leads to a graded activation of Toll (Tl), with the maximum at the ventral side and progressively decreasing dorsally. The gradient of Toll activation then directs a gradient activation of the transcription factor *dorsal*

(*dl*) which will in turn play a key role in the definition of a number of different regions along the dorso-ventral axis, among which the presumptive mesoderm.

Dorsal (NFκ-B ortholog) is usually sequestered in the cytoplasm by Cactus (Ik-B ortholog). Activation of Toll by Spätzle triggers an intracellular signaling cascade that results in the phosphorylation and degradation of Cactus, allowing Dorsal to move to the nucleus and become active, a pathway that parallels strikingly the signaling in vertebrate lymphocytes following the activation of the interleukin 1 receptor (part of the Toll-like receptor superfamily) (O'Neill, 2000). The gradient of Dorsal nuclear localization/activity sets up the expression of different sets of genes at different thresholds, ultimately defining different domains along the dorso-ventral axis (Figure 3) (Stathopoulos and Levine, 2002).

The basic Helix-Loop-Helix (bHLH) transcription factor *twist* (*twi*) is one of the first genes to be expressed in the presumptive mesoderm (Stathopoulos and Levine, 2002). Twist is a direct activator of a large number of other transcription factors essential for the proper development of virtually every type of muscle (*Mef2* (Cripps et al., 1998), *tin* (Yin et al., 1997), ...). Twist resides at the top of a cascade of genes regulating mesodermal development and is considered a master regulator of the mesoderm. Twist cooperates with its own activator, Dorsal, to cooperatively activate the transcription of *snail* (*sna*). Snail, itself a transcription factor, defines the boundaries of the presumptive mesoderm, delimiting it from the neurogenic ectoderm (Ip et al., 1992) by inhibiting neuroectodermal genes (Leptin, 1991). Dorsal and Twist also activate a novel Wnt family member called *wntD*, for *wnt inhibitor of Dorsal*. However, as *wntD* is itself inhibited by Snail in the presumptive mesoderm, its expression is limited to the lateral blastoderm. There it leads to a diminished nuclear import of Dorsal, helping to sharpen the borders of the presumptive mesoderm (Ganguly et al., 2005).

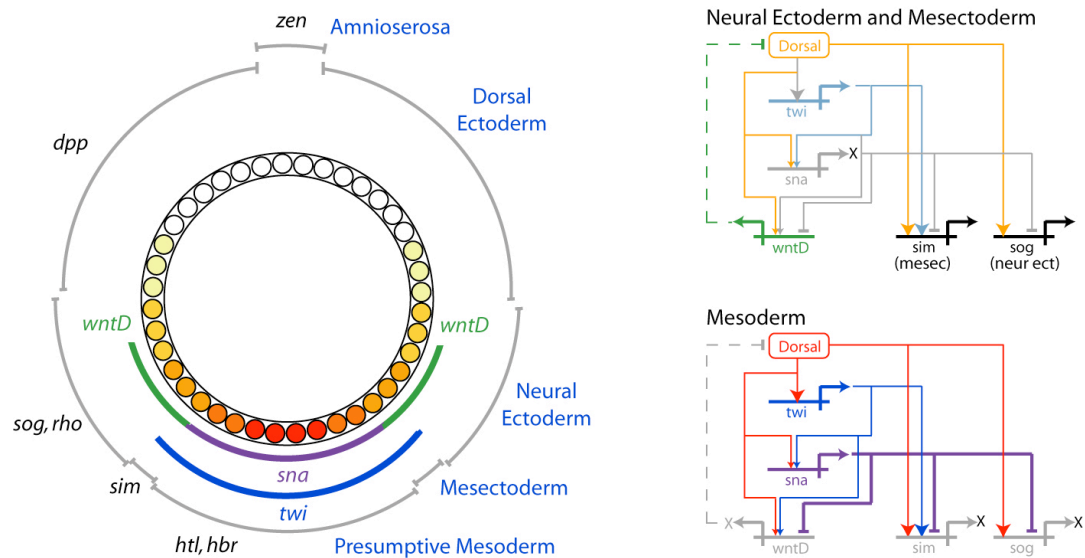


Figure 3 - The blastoderm is subdivided by a gradient of nuclear Dorsal concentration.

The presumptive mesoderm is specified in the ventral blastoderm by high levels of nuclear Dorsal. Dorsal activates Twist and both activate Snail. Snail acts as a repressor of many genes that would be activated by Dorsal or Twist and lead to a neural ectoderm fate. At more lateral positions, nuclear Dorsal concentration drops, leading to a decrease of Twist, and sharp absence Snail. The release of Snail inhibition, allows these cells to transcribe genes that respond to lower levels of Dorsal (high affinity sites) that specify the neural ectoderm. The steeper decline in Dorsal nuclear localization enhanced by the negative feedback loop of WntD on Dorsal. Direct lines show direct activation/repression while broken lines represent genetic interaction. Adapted from (Stathopoulos and Levine, 2002)

In summary, the blastoderm is subdivided by the nuclear Dorsal gradient interacting with members of its downstream transcriptional network, Twist and Snail. The target genes respond to the different concentrations of Dorsal through the architecture of their enhancers, integrating information from Twist, Snail as well as general co-activators/repressors (Stathopoulos and Levine, 2002). Our knowledge of the complex interplay between these factors, and the number of targets regulated has dramatically increased from two genome wide studies of this transcriptional network in early development (Sandmann et al., 2007) (Zeitlinger et al., 2007).

2.3.2. The mesoderm is subdivided by cues secreted from the overlying ectoderm

After gastrulation, the primitive mesoderm is a uniform layer of cells that has proliferated and migrated dorsally from its original ventral origin, spreading on each side of the embryo. At this stage, the cells are committed to a mesodermal cell fate, but are still pluripotent and therefore must still be sub-specified into the different muscle types and remaining mesodermal fates. This cell fate choice depends on the relative location of cells within each parasegment, which is subdivided into different fields both by the expression of mesodermal transcription factors and by the integration of signals from the overlying ectoderm. Each parasegment is divided in the anterior-posterior direction into two fields through the action of the pair-rule transcription factors *even-skipped* (*eve*) and *sloppy paired* (*slp*) (Figure 4). The *eve* domain corresponds to the anterior part and *slp* to the posterior. This division of each parasegment into two distinct fields is also reflected in the mesodermal expression of two domains of high (*slp* domain) and low (*eve* domain) twist expression at stage 11 (Riechmann et al., 1997). The parasegments are further defined by the action of the segment polarity genes *wingless* (*wg*) (posterior parasegment) and *engrailed* (*en*) and *hedgehog* (*hh*) (anterior parasegment). To subdivide the mesoderm in the dorsal-ventral direction, Decapentaplegic (Dpp), a member of the BMP family is secreted from the dorsal ectoderm. Dpp is essential for the specification of all tissue types derived from the dorsal mesoderm (Staehling-Hampton et al., 1994) (Frasch, 1995).

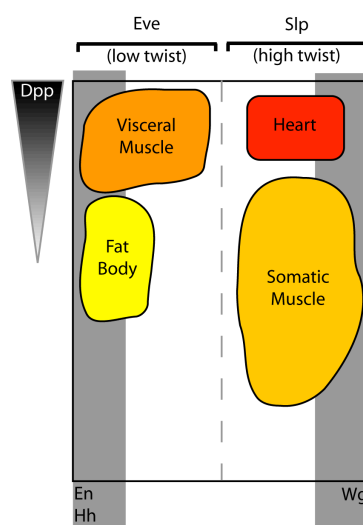


Figure 4 - The mesoderm is sub-specified both by the expression of genes in the mesoderm and by signaling from the overlying ectoderm.

Schematic drawing of the sub-specification of the mesoderm. Each segment is divided in the anterior-posterior axis by domains of *even-skipped* (anterior) and *sloppy paired* (posterior). The secreted molecules Wg and Hh act as segment polarity genes to further divide these domains. Dpp, secreted from the overlying ectoderm patterns the mesoderm in the dorso-ventral axis. The different muscle types arise from the integration of these signals in specific locations. Adapted from (Riechmann et al., 1997).

2.3.3. Specification of Founder Cells (FCs) and Fusion Competent Myoblasts (FCMs)

One of the remarkable features of skeletal muscle cells is their capacity to undergo cell-cell fusion. Final muscle fibers are therefore syncytia, with several nuclei sharing a common cytoplasm crossed by the contractile fibers that render the muscle functional. In *Drosophila*, it has long been established that cells contributing to the somatic muscle undergo myoblast fusion, whereas heart muscle cells do not. More recently it was shown that visceral muscle cells also undergo fusion, albeit to a different level than somatic muscle (Martin et al., 2001). One important aspect though, is that in *Drosophila*, myoblast fusion in both somatic and visceral muscle is an asymmetrical process. Each muscle fiber is seeded by an individual cell, the Founder Cell (FC), which then attracts and fuses with a determined number of Fusion Competent Myoblasts (FCM).

A number of mutants with blocked myoblast fusion continue to develop very thin muscles, containing only one nuclei, termed mini-muscles. This observation led to the Founder cell hypothesis, which suggested that there are two types of somatic muscle cells; one termed the Founder Cell which contains all of the necessary information to form a muscle, and a second cell type that was thought to be a naïve muscle cell with the capacity to fuse to FCs (termed Fusion Competent Myoblast). When myoblast fusion is blocked, FCs still migrate to their correct location, form their correct muscle attachment to the ectoderm, attract the appropriate motor neurons and express contractile proteins, showing that FCs have the necessary information to determine the character of their specific muscle.

The larval somatic muscle consists of a stereotypical array of 30 (Riechmann et al., 1997) muscles per hemisegment (A2-A7). Each muscle has characteristic properties including its location, size, shape and innervation (Figure 2 A). Each muscle is seeded by a FC expressing a particular combination of identity genes, such as *Krüppel* (*Kr*), *vestigial* (*vg*), *apterous* (*ap*), *slouch* (*slou*), *Toll* (*Tl*), *ladybird*, *Connectin* (*Con*), *even-skipped* (*eve*) (Baylies et al., 1998). The specific expression of these identity genes, together with the fact that many are known transcription factors, led to the hypothesis that these genes could instruct a

muscle to choose some of its specific characteristics (Baylies et al., 1998). Indeed, for particular cases a correspondence has been shown between identity gene loss and specific muscle loss or ectopic expression of the identity gene and the partial duplication of a specific muscle (Bourgouin et al., 1992) (Keller et al., 1997). It has also been shown that forced expression of an identity gene can impart its specific characteristics to a different muscle (Ruiz-Gomez et al., 1997).

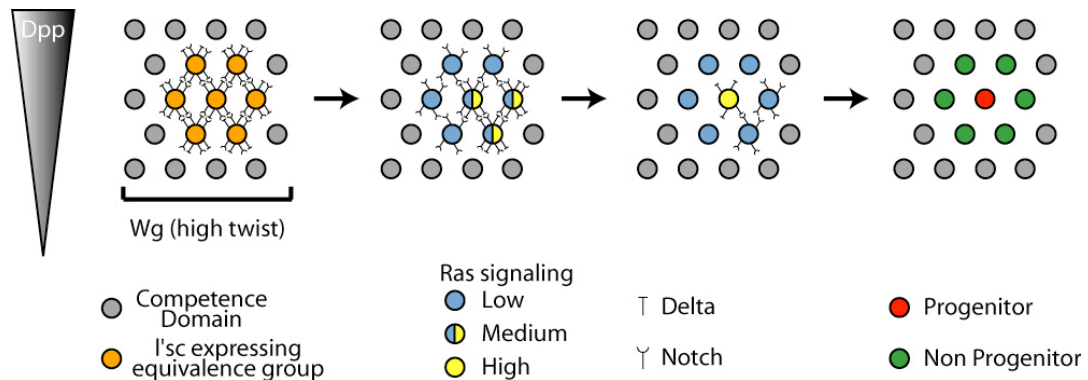


Figure 5 - Progenitor cells are specified via integration of Ras signaling and Delta/Notch lateral inhibition.

Schematic representation of Eve progenitor selection in the dorsal mesoderm. An equivalence group of cells expressing *l'sc* arises in a competence domain created by gradients of Dpp and Wg. The Ras/MAPK pathway is activated to intermediate levels in these cells, but cells try to inhibit the pathway in a juxtacrine fashion via Delta/Notch lateral inhibition. Finally, only one cell in the cluster reaches a high level of Ras signaling, becoming the progenitor cell. Adapted from (Carmena et al., 2002).

The specification of a FC is a complex process (Figure 5) that has been studied in detail for the dorsal *eve*-expressing cells (Halfon et al., 2000). In this case, a competence domain is created by the combined action of Dpp and Wg in the dorsal part of each hemisegment. A group of cells within this competence domain start to express the transcription factor *lethal of scute* (*l'sc*) and is rendered responsive to EGF and FGF signaling. Signaling downstream of FGF/EGF receptors activates the Ras/MAPK pathway in this equivalence group leading towards the selection of a progenitor cell fate. However, the Ras/MAPK signal is inhibited by juxtacrine Delta/Notch lateral signaling within the equivalence group, resulting in only one cell being selected as a progenitor cell (Carmena et al., 2002). The progenitor cell then divides asymmetrically, yielding either two different FCs or a FC and an adult muscle progenitor, or in the case of *eve*, a FC and a pericardial cell (Halfon et al., 2000). The adult muscle progenitor is marked by the

persistence of Twist expression and will remain undifferentiated until required during metamorphosis of the larva to the adult fly. The remaining cells from the equivalence group, where Notch signaling prevails over Ras/MAPK activation, become FCMs.

2.3.4. Myotubes are formed by the process of Myoblast Fusion between FCs and FCMs

Cell-cell fusion remains the least understood of the three types of membrane fusion events (the others being intracellular fusion of organelles and virus-cell fusion). Nonetheless, EM studies of the fusion process have revealed a defined sequence of events at the ultrastructural level. In a first step, FCMs extend filopodia and migrate towards FCs. After this first step of recognition and adhesion, paired vesicles of electron-dense margins form along the apposed membranes (prefusion-complex). These vesicles then resolve to electron-dense plaques, the cells align along their long axes, and finally the apposed membranes break down, forming fusion pores and allowing the formation of a multinucleated myotube (Doberstein et al., 1997).

A combination of genetic and biochemical studies have revealed a number of key players in the process. The molecules involved can be grouped in three broad categories: transmembrane receptors that mediate attraction/recognition, intracellular components that integrate the signals from the receptors and finally proteins that are capable of modifying the cytoskeleton leading to the process of fusion itself. On the transcriptional level, it is interesting to note that only two transcription factors have been identified that are essential for fusion of all somatic muscle: *Myocyte enhancing factor 2 (Mef2)*, expressed in both FCs and FCMs and required for myoblast fusion and muscle differentiation, and *lame duck (lmd)*, expressed in FCMs and necessary for FCMs differentiation. Mutation of either gene leads to a complete block of myoblast fusion in the somatic muscle.

2.3.4.1. Myoblast attraction and recognition is mediated by transmembrane receptors of the IgSF family

The transmembrane receptors *dumbfounded/kin of irregular chiasm C* (*duf/kirre*) (Ruiz-Gomez et al., 2000), *roughest/irregular chiasm C* (*rst/irreC*) (Strunkelnberg et al., 2001), *sticks and stones* (*sns*) (Bour et al., 2000) and *hibris* (*hbs*) (Dworak et al., 2001) (Artero et al., 2001) were identified almost simultaneously providing a handful of genes involved in the recognition between FCs and FCMs. *duf* and *sns* were also the first genes shown to be specifically expressed in FCs and FCMs respectively, providing a molecular mechanism for the founder cell model. *duf* and its paralog *rst* encode transmembrane proteins with an extracellular domain comprised of five Ig-like domains that share a relatively high degree of similarity (Strunkelnberg et al., 2001). The two genes act redundantly and only the simultaneous deletion of both genes leads to a complete block of fusion. Either gene can rescue the phenotype, and ectopic expression leads to attraction of FCMs (Strunkelnberg et al., 2001). *sns*, which encodes another transmembrane protein with extracellular Ig-like domains is expressed only in FCMs and is also essential for muscle fusion (Bour et al., 2000). Significantly, in both *duf+rst* double mutants and *sns* mutants one can find FCM extending filopodia, but with seemingly random orientations (Ruiz-Gomez et al., 2000). This is in contrast with other fusion mutants which seem to block fusion at a later stage, as FCMs are seen extending filopodia towards and making contact with FCs (Chen and Olson, 2001) (Chen et al., 2003). Together with evidence that Duf and Sns can mediate cell adhesion in cultured *Drosophila* S2 cells (Dworak et al., 2001), this confirms the role of these receptors in the initial recognition and adhesion between the two distinct cell populations. Hibris is also expressed in FCMs only but seems to act as a negative regulator of Sns, and could provide some fine tuning for the process (Artero et al., 2001).

2.3.4.2. The “fusion’ signal” is relayed from the membrane to the cytoskeleton by a number of signaling pathways

A second group of players are cytosolic proteins that transduce the signals from the membrane receptors to the cytoskeleton. Myoblast City (Mbc), a Dock180 family (CDM) member, is a cytoplasmic protein long known to be crucial to myoblast fusion (Rushton et al., 1995) (Erickson et al., 1997). This family has been proposed to form unconventional two-part Guanine nucleotide Exchange Factors (GEFs) with ELMO/CED-12 for the small GTPase Rac (Brugnera et al., 2002). That has recently been shown to be the case, with the identification of the *Drosophila* ELMO/CED-12 ortholog (Geisbrecht et al., 2008). Rac is a small GTPase involved in actin cytoskeleton rearrangements thought to be necessary for fusion. Indeed, the *Drosophila Rac1* has long been implicated in myoblast fusion (Luo et al., 1994), with later analysis uncovering a redundant role with *Rac2* (Hakeda-Suzuki et al., 2002). The link between Duf and Mbc has been found with the identification of the adaptor protein Ants/Rols7. This adaptor protein, expressed only in FCs, contains multiple potential protein interaction domains (Ankyrin, TRP, Coiled-coil) and was shown to bind to both the cytoplasmic domain of Duf and to Mbc in S2 cells. It is localized *in vivo* to distinct foci, and this localization is dependent on the presence of Duf or Rst, providing a link between the membrane receptors and actin cytoskeleton rearrangement (Rau et al., 2001) (Chen and Olson, 2001) (Menon and Chia, 2001). One intriguing fact is that in Ants/Rol7 mutants, a first wave of fusion is able to take place, and myofibers with 2-4 nuclei, called muscle precursors, are formed (Rau et al., 2001).

A second pathway working in parallel and cross-talking with the Ants/Rols7 pathway was unveiled with the characterization of *loner* (Chen et al., 2003) (also known as *schizo* (Hummel et al., 1999)). Loner is also a putative GEF with PH and Sec7 domains required for the first fusion event leading to the muscle precursor stage, as there is a complete block of fusion in *loner* mutants. As with Ants/Rols7, Loner is localized to distinct foci in a Duf/Rst dependent manner, but the Ants/Rol7 and Loner foci overlap only partially, and the localization of one is not dependent on the other (Chen et al., 2003). Sec7 domains are usually found in

GEFs for the ARF family of small GTPases, and in fact *Loner* can act as a GEF *in vitro* specifically for ARF6. ARF6 is expressed ubiquitously in the embryo, but a dominant negative form expressed in FCs leads to muscle fusion defects. ARF6 has been connected with the subcellular localization of Rac1, and in *loner* mutant embryos Rac1 seems to be delocalized to the cytoplasm as opposed to distinct loci (Chen et al., 2003). Therefore, these two signaling pathways impinge on the activation/localization of Rac1 to the sites of fusion, with the *Ants/Rol7* pathway being crucial for the progression beyond the muscle precursor stage. It is also interesting to note, that in visceral muscle, 2-3 and 3-5 nuclei were reported in circular and longitudinal fibers respectively (Martin et al., 2001), which could correspond to a status similar to precursor cell.

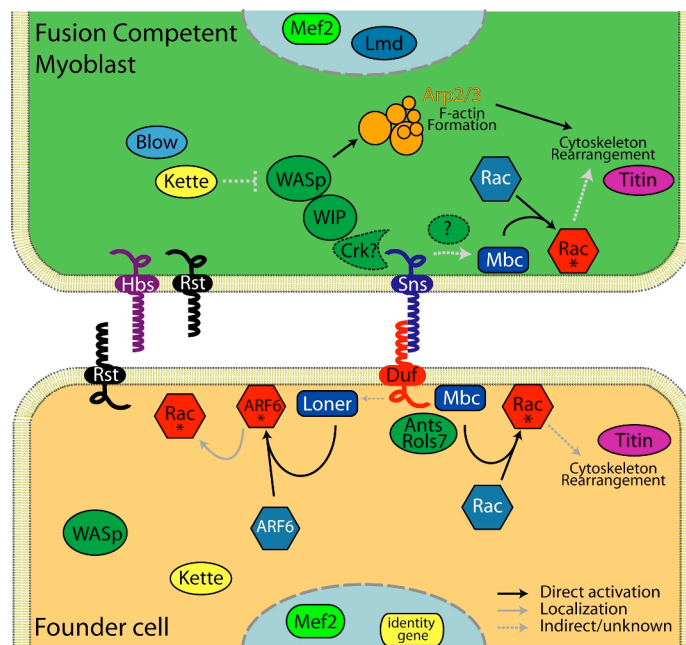


Figure 6 - Model of myoblast fusion in *Drosophila*.

Initial adhesion is mediated by transmembrane protein members of the IgSF. Duf is expressed in FCs only and interacts with Sns, expressed in FCMs only. In FCs, the intracellular domain of Duf can recruit the adaptor protein Ants/Rols7, which in turn mediates interaction with Mbc. Mbc (interacting with ELMO) is a GEF for Rac, activating and recruiting it to the membrane. Rac can then mediate changes to the actin cytoskeleton necessary for fusion. A second pathway in FCs involves Loner, again a GEF this time for ARF6. ARF6 has been shown to promote the localization of Rac to the

membrane, an important step for Rac function. In FCMs, WIP recruits WASp to foci of fusion in an Sns dependent manner, possibly through the small adaptor protein Crk. WASp is known to stimulate the Arp2/3 complex to start F-actin nucleation. *Drosophila* Titin (sls) is also involved in structural changes during the fusion process.

Two genes have been related to the transition from the precursor cell to the completely fused myotube. *blown fuse (blow)* (Doberstein et al., 1997) and *kette* (Schroter et al., 2004) are two cytosolic proteins whose mutants arrest fusion after the first 3-4 fusion events. *blow* mutants are unable to do the transition from prefusion complex to electron-dense plaques whereas in *kette* mutants, the electron-dense plaques do not resolve into fusion pores, and become abnormally

elongated. The fact that the two genes interact genetically during the second fusion step makes them good candidates to interact with the Ants/Rols7 pathway at this step, leading to transition from the prefusion complex to membrane breakdown (Schroter et al., 2004). On the other hand, *kette* genetically interacts with the recently characterized muscle fusion WIP/WASP pathway, necessary for progression beyond the precursor cell state (Schafer et al., 2007). WASp (Wiskott-Aldrich Syndrome protein) is a ubiquitously expressed protein known to activate the Arp2/3 complex to modulate F-actin nucleation. It is recruited to the foci of fusion by the FCM specific *Drosophila* WIP (WASp Interacting Protein)/Solitary(Sltr)/Verprolin 1(Vrp1). *In vitro*, WIP can interact with both the adaptor protein Crk and WASp, and Crk can bind the FCM receptor Sns (Kim et al., 2007) providing a possible connection *in vivo*. Accordingly, WIP is localized and F-actin enriched to fusion foci in a Sns dependent manner. There is conflicting data as to what the exact *in vivo* function of this F-actin nucleation is, but the pathway seems to be necessary for the transition beyond the precursor cell stage (Schafer et al., 2007) (Massarwa et al., 2007) (Kim et al., 2007).

Finally, the large protein Titin – also known as Sallimus (Sls) – long known to be necessary for sarcomere function in late differentiation, has meanwhile been found to play a role much earlier in myoblast fusion (Zhang et al., 2000).

2.3.4.3. Fusion-Restricted Myogenic-Adhesive Structures (FuRMAS) mediate Myoblast Fusion in *Drosophila melanogaster*

The genetic information described above has recently been supplemented with new studies including novel structural data, and a more detailed model of fusion has emerged. The transmembrane proteins Sns and Duf were found to be organized in a ring-structure at the contact points between FCMs and myotubes, with cytoplasmic components as Titin and F-actin forming a plug in the middle (Figure 7 A). Interestingly, Blow co-localizes with these actin plugs in FCMs after cell adhesion, while Ants/Rols7 is found interacting with Duf in the ring-structure in myotubes (Figure 7 B) (Kesper et al., 2007). This structure is involved in both

adhesion between myoblasts and the restriction of fusion to the inside of the ring; it has been named Fusion-Restricted Myogenic-Adhesive Structure (FuRMAS).

According to this model, F-actin polymerization and de-polymerization, involving the regulators described previously (Section 2.3.4.2), plays an important role in the progression of fusion. The branched F-actin plug leads to the enlargement of the FuRMAS (Figure 7 B) and electron-dense vesicles accumulate at the opposing membranes. As the FuRMAS expands, the FCM is pulled into the growing myotube (Figure 7 C) (Onel and Renkawitz-Pohl, 2009).

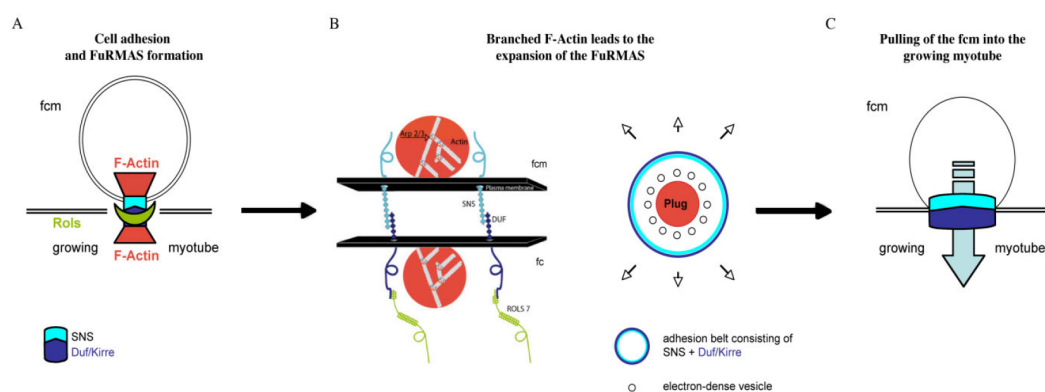


Figure 7 - Fusion-Restricted Myogenic-Adhesive Structures (FuRMAS).

Taken from (Önel and Renkawitz-Pohl, 2009)

FuRMAS have been compared to similar transient structures such as the immunological synapse, podosomes and invadopodia. The common bipartite architecture of a ring of cell-adhesion molecules and local F-actin branching could reflect a common way of restricting spatial and temporal communication between cells.

2.3.5. Terminal differentiation of myotubes to functional muscle fibers

During the last stages of differentiation, myotubes make contact with specific attachment points in the epidermis. Motoneurons are guided towards their recipient myotube, and form the functional neuromuscular junctions. In parallel,

structural proteins that make up the contractile apparatus are expressed and assembled into functional sarcomeres.

2.3.5.1. Migration towards attachment points in the epidermis is guided cues between the myotubes and tendon progenitor cells

Myotubes migrate towards and attach to epidermal tendon cell precursors as a result of bi-directional interplay between the two cell types. Tendon precursors are epidermal cells characterized by the expression of the triple Zinc-Finger TF Stripe (Sr), necessary and sufficient to determine tendon cell fate. However, final differentiation of tendon cells is dependent on attachment of myotubes providing a signal for tendon cell maturation (Volk, 2006). The nature of the cues guiding myotubes is not completely clear as yet, but several important components have been identified. Slit (Sli) and its receptor Roundabout (Robo) are involved in repelling muscles from the ventral midline of the embryo, preventing ventral muscles from crossing the ventral CNS. Conversely, later in development, Slit is used by segment border cells to attract Robo-expressing Ventral Longitudinal (VL) muscles (Kramer et al., 2001). Lateral Transverse (LT) muscles do not express Robo, and accordingly are not attracted to segment borders, extending instead in a dorso-ventral direction. The correct recognition by LT muscles of their Sr expressing tendon counterparts is instead dependent on the RTK Derailed (Drl), but the cue originating from these tendon cells has not yet been determined (Callahan et al., 1996). After correct attachment, the myotube secretes the Neuregulin-like ligand Vein (Vn), activating EGF receptors specifically in the tendon precursor and signaling its final maturation. Hemi-adherence junctions are formed between extracellular matrix (ECM) and both the tendon cell and the myotube resulting in stable attachments capable of withstanding the force of muscle contraction (Volk, 2006).

2.3.5.2. Axons are guided towards myotubes and form neuromuscular junctions (NMJ)

The 30 muscles of each hemisegment (A2-A7) are innervated specifically by 35 motoneurons (Nicholson and Keshishian, 2006). While motoneurons can initially develop on their own, they require the presence of myotubes to find their correct final positioning. At this step, both the growing motoneurons and myotubes extend filipodia probing for correct contact. The IgSF member protein Sidestep, present on the membrane of all myotubes, is generally required for the guidance of motoneurons towards myotubes, but other factor are present in specific muscles, [Fascilin III (Fas3), Connectin (Con), Capricious (caps), Netrin-A (Net-A) or Netrin-B (Net-B)], allowing the identification of specific targets by motoneurons (Nicholson and Keshishian, 2006). Toll and Robo were also implicated in mediating repulsion of motoneurons. Correct contacts lead to the formation of the neuromuscular junction (NMJ), with the assembly of post- and presynaptical complexes and the localization of Glutamate receptor (GluR) to the synapses. This is in sharp contrast to vertebrates, where acetylcholine is the neurotransmitter of choice for neuromuscular junctions, with glutamate used as the major excitatory neurotransmitter of the central nervous system.

2.3.5.3. The contractile apparatus is organized into sarcomeres, leading to functional myofibers

The main function of muscle is to convert chemical energy into the mechanical energy required for contraction. Muscle contraction can be seen as highly coordinated and efficient development of the common theme of ATPase motor proteins moving along actin filaments (Lodish et al., 2000). Ultrastructural information has been obtained from vertebrate and insect muscles, in particular from the adult indirect flight muscle (IFM) of *Drosophila* and the large waterbug *Lethocerus sp.*. The structure and most of the components of contractile apparatus show remarkable conservation from insets to vertebrates, where myofibrils are organized in repeating units of contraction called sarcomeres (Vigoreaux, 2006).

The sarcomeres are formed by an array of thick filaments, consisting mainly of the ATPase motor protein Myosin, interspersed with thin actin-based filaments, on which the thick Myosin filaments move. The thick filaments consist mainly of Myosin, but include other components such as Para-Myosin (PM), mini-paramyosin (mPm), flightin (fln) (Vigoreaux, 2006) and myofilin (Mf) (Qiu et al., 2005). The thin filaments are formed mainly by actin, troponin and tropomyosin (Vigoreaux, 2006). Very large proteins such as Titin help organize both thick and thin filaments (in addition to its earlier role in myoblast fusion (Zhang et al., 2000)).

2.4. Comparison with Vertebrate development

The use of model organisms, in one way or another, is as old as biology itself. The advantages of using an organism without the constant complications of redundancy arising from gene duplications are evident when comparing muscle development in *Drosophila* to that in vertebrates.

2.4.1. The somite is patterned by diffusible signaling molecules from nearby structures

As in *Drosophila*, all muscle in vertebrates is derived from the mesoderm. The heart, smooth muscle lining the digestive tract (analogous to visceral muscle) and the muscles lining the blood vessels (without equivalence in *Drosophila*) are derived from the Lateral Plate Mesoderm (LPM). All skeletal muscles (analogous to *Drosophila* somatic muscle) of vertebrates (with the exception of some head muscles) arises from the paraxial mesoderm. The paraxial mesoderm is a strip of mesodermal cells running in an anterior-posterior orientation on each side of the embryo parallel to the main axis formed by the neural tube and the notochord (Figure 8). The paraxial mesoderm is then segmented in the anterior-posterior direction into a defined number (for every species) of structures called somites. Most *in vivo* studies of vertebrate myogenesis have focused on the subsequent patterning of somites (Gilbert, 2006).

Like the mesoderm of *Drosophila*, the vertebrate somite receives inputs from nearby structures, including the overlying epidermis and notocord. It is striking to note that despite the obvious structural differences, the same pathways of secreted molecules that pattern the *Drosophila* mesoderm are used as well to pattern the vertebrate somite: Wnt [Wg] signaling from the neural tube and overlying epidermis, Sonic hedgehog (Shh) [Hh] signaling from the notochord, and Bone Morphogenic Protein 4 (BMP4) [Dpp] from the lateral plate mesoderm. Transcription factors of the paired box (PAX) and sine oculis related (SIX) families are also expressed in different regions of the somite (Richardson et al.,

2008) and the interplay of these signaling pathways and regulatory molecules leads to the patterning of the somite and activation of master regulators of muscle development (section 2.4.2) (Taylor, 2006). The ventral-most region called the sclerotome will form cartilage and bone, while the central dorsal dermatome will form the dermis. The dorsal medial region (closer to the neural tube) will form the epaxial muscles of the back (innervated by dorsal nerves). The dorsal lateral region will form the hypaxial muscles and limbs (innervated by ventral nerves).

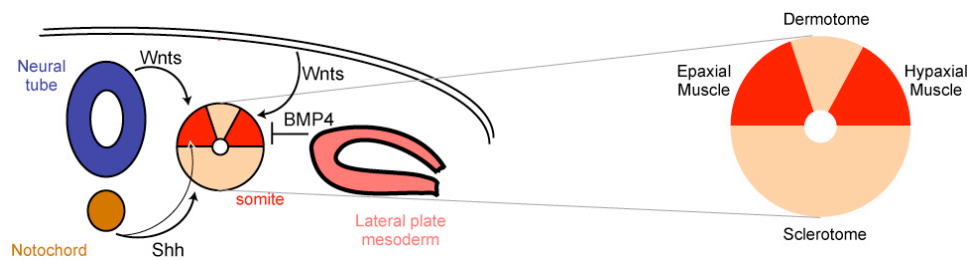


Figure 8 - The vertebrate somite is patterned by secreted signaling molecules of the same families as in *Drosophila* mesoderm patterning.

Wnt/Wg, Shh/Hh and BMP4/Dpp signaling pathways are used in *Drosophila* as well as in vertebrate mesoderm sub-specification. In vertebrates, they pattern the somites leading to specification of Sclerotome (cartilage, bone), dermis, Epaxial (dorsal) and Hypaxial (ventral, limb) muscle.

2.4.2. Muscle development in vertebrates is controlled by master regulators of the MyoD family of Muscle Regulatory Factors (MRF)

Muscle Regulatory Factors (MRFs) are a family of four basic helix-loop-helix transcription factors (bHLH) acting as master regulators of vertebrate muscle development (MyoD, Myf5, Myogenin and MRF4).

MyoD was first identified in the mouse fibroblast line 10T1/2 by its ability to convert these cells to the myogenic fate (Davis et al., 1987) (Davis et al., 1987). This striking effect was the first example of a single gene being able to drive a complex program of differentiation, and therefore acting as a master switch (Berkes and Tapscott, 2005). Nonetheless, the presence of four closely related proteins in the same family required *in vivo* genetic characterization to determine the individual contributions of each gene. There is substantial functional

redundancy between *MyoD* and *Myf5*, as mutation of either gene causes only mild muscle defects (Rudnicki et al., 1992) (Braun et al., 1992), whereas in a double mutant setting there is a complete absence of muscle (Rudnicki et al., 1993). *Myogenin* (*Myog*) can be activated by both *MyoD* and *Myf5* *in vitro*, and is expressed later in development. In *Myog* mutants, muscle mass is severely reduced, with many mononucleate myoblasts but very few differentiated muscle fibers (Hasty et al., 1993). Therefore, *Myog* seems to act downstream of *MyoD* and *Myf5* and is required for proper muscle differentiation and fusion. *MRF4* has been the least studied MRF, and was thought to act only late during differentiation. More recently it has been shown to act as well during earlier determination (Kassar-Duchossoy et al., 2004).

MRFs bind to the enhancers of many muscle-specific genes by forming heterodimers with the ubiquitously expressed E-box family of bHLH transcription factors and binding to E-box motifs (CANNTG). These heterodimers act cooperatively with the Mef2 family of TFs, another family of proteins required for proper myogenesis.

As with *MyoD*, Mef2 was first identified in vertebrate cell culture as a factor from C2 myoblasts that could binding to an enhancer of the *muscle creatine kinase* (*mck*) gene (Gossett et al., 1989). The Mef2 family of transcription factors contain an N-terminal MADS-box binding domain, followed by a novel conserved Mef2 domain, specific to this family (Olson et al., 1995). Mef2 family members form homo- or heterodimers that bind the canonical sequence YTA(W)₄TAR that is present in virtually every muscle gene (Black and Olson, 1998). Nevertheless, Mef2 family members are not able to induce myogenesis of transfected fibroblasts on their own, but can instead dramatically increase the myogenic effect of MRF family members. Remarkably, this synergistic activation results from direct protein-protein interactions between the “myogenic” bHLH of the MRF of an MRF/E-Box dimer and both the MADS and Mef2 domains of Mef2. That allows either Mef2 or MRF/E-Box to independently bind their respective sequences, and use the others transactivation domain to promote transcription (Molkentin et al., 1995).

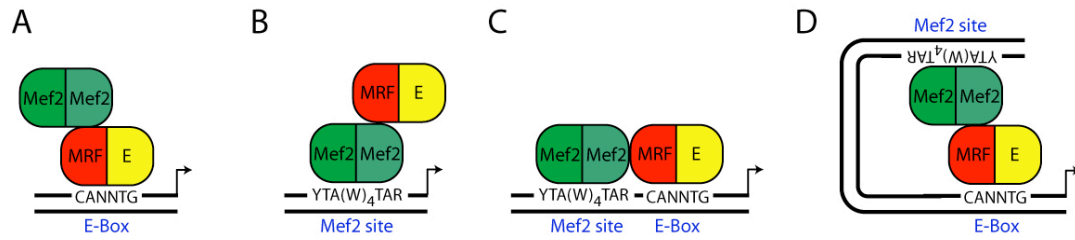


Figure 9 - Model of interaction between MRFs and Mef2 on common enhancers.

(A) MRF/E-protein heterodimers bind to E-box motifs and recruit Mef2 dimers via direct protein-protein interaction between the MRF and Mef2. This allows the transactivation domain of Mef2 to promote transcription without direct binding of Mef2 to the enhancer. (B) Conversely, Mef2 can bind to its site and recruit the MRF/E-protein dimer. (C) On enhancers containing both E-Box and Mef2 sites direct interaction between MRF/E-Box dimers and Mef2 dimers leads to synergistic activation, potentially facilitating the physical linking of distant enhancers (D). Adapted from (Molkentin et al., 1995).

The determination of the exact function of this family *in vivo* in vertebrates has been complicated by the occurrence of four paralogs (Mef2A-D) with overlapping expression and redundancy in various muscle tissues. Studying the single *Mef2* ortholog in *Drosophila* has therefore contributed significantly to our understanding of *Mef2* function (Section 2.5).

In *Drosophila* the only member of the MRFs family is the gene *nautilus* (*nau*), a TF with about 90% identity to the other MRFs in its bHLH domain, but otherwise quite divergent. However, *nau* is expressed in a restricted fraction of the mesoderm, and seems to act as an identity gene in only a subset of muscle fibers (Balagopalan et al., 2001). Instead, a different member of the bHLH family of TFs, Twist, performs the role of a functional MRF in *Drosophila* (Taylor, 2006). Apart from its essential role early during gastrulation (section 2.3.1), Twist acts as the myogenic switch in *Drosophila*, sitting at the top of an extensive cascade during myogenic specification, and directly activating a number of important genes for muscle development, including *Mef2* (Cripps et al., 1998). High levels of Twist are required for somatic myogenesis (section 2.3.2), and block the formation of other mesodermal derivatives. Similar to vertebrate MRFs, ectopic expression of Twist in the ectoderm is sufficient to drive these cells into myogenesis (Baylies and Bate, 1996). In parallel to the vertebrate system, Twist and Mef2 tightly co-regulate a great number of muscle genes on common enhancers (Sandmann et al., 2006b), tempting speculation on whether Twist could interact with Mef2 in a similar cooperative way.

2.5. *Myocyte enhancing factor 2 (Mef2)* is essential for myoblast fusion and terminal differentiation in *Drosophila*

2.5.1. *Mef2* is expressed in all muscle cells

Following the discovery of the Mef2 family in vertebrate cell culture, a single *Mef2* gene was identified in *Drosophila* by screening a cDNA library with a probe for the unique MADS-MEF2 sequence (Lilly et al., 1994) (Nguyen et al., 1994). Both the MADS-box and Mef2 domains of *Drosophila* Mef2 are highly conserved, while the rest of the protein shows little homology to other Mef2 family members. *In vitro* translated Mef2 protein can bind the vertebrate *mck* enhancer and drive expression from this enhancer in CAT assays when transfected in S2 cells. During development, *Mef2* is first detected in the ventral furrow, at cellular blastoderm stage 6 (according to (Campos-Ortega and Hartenstein, 1997)) and at stage 8 *Mef2* is clearly restricted to the mesoderm. At stage 10, as the mesoderm segregates into somatopleura (SM precursors) and splanchnopleura (VM and heart precursors), *Mef2* can be detected in both cell layers, as well as in the cephalic mesoderm, precursor of pharyngeal muscle. At stage 12 *Mef2* expression starts to decline in the VM and heart precursors but can be still be detected in the dorsal vessel as well as SM even in late stages of embryonic development (Lilly et al., 1994) (Nguyen et al., 1994). An antibody against Mef2 protein revealed a nuclear localization, consistent with the function of Mef2 as a TF (Lilly et al., 1995) (Bour et al., 1995). *Mef2* is therefore a mesodermal gene specifically expressed in all muscle cell precursors of every muscle type, and not in other mesodermal derivatives, such as fat body or pericardial cells. As noted before (section 2.1), this broad expression is actually the cumulative result of the action of multiple CRMs (Nguyen and Xu, 1998).

2.5.2. *Mef2* loss-of-function leads to a complete block of myoblast fusion and terminal differentiation

Mutation of the single *Mef2* gene in *Drosophila* results in lethality with severe muscle defects. There is a complete block of myoblast fusion, the SM fails to differentiate and the midgut is bloated, apparently due to the absence of differentiated VM. Terminal differentiation is compromised, as judged by the almost complete lack of expression of *Myosin Heavy Chain (Mhc)* in the dorsal vessel, SM and VM. These defects do not seem to stem from a block in the specification of mesodermal progenitors, as markers of specification of heart and VM [*tinman (tin)*, *bagpipe (bap)* and *Fasciclin 3 (Fas 3)*] are expressed normally. The FC identity genes *nau*, *ap*, and *slou* are also expressed at the right locations, but the labeled FCs remain in unorganized clusters, unable to fuse, and syncytia cannot be formed. Thus, *Mef2* is the only known gene required for terminal differentiation in every muscle type to date.

2.5.3. *Mef2* regulates several genes involved in different aspects of muscle development

Mef2 is genetically downstream of *twist* and *snail*, and the activation by *twist* was shown to be direct (Cripps et al., 1998). A comprehensive study of *Mef2* activity throughout development has now shown that *Mef2* directly regulates target genes at all stages of muscle development (Sandmann et al., 2006b), and the integration of *twist* in the regulation of the same enhancers draws exciting parallels to the regulation of MRFs and *Mef2* family members of common targets in vertebrates.

Interestingly, *Mef2* can activate itself, and this mechanism of autoregulation probably allows *Mef2* to reinforce the muscle phenotype throughout a myogenesis (Cripps et al., 2004). *Mef2* was also shown to directly activate targets like *Tropomyosin I (Tmn I)* (Lin et al., 1996) (Lin and Storti, 1997), *β -Tubulin60D* (*β Tub60D*) (Damm et al., 1998), *Muscle LIM protein at 60A (Mlp60A)* and *Muscle*

LIM protein at 84B (Mlp84B) (Stronach et al., 1999), and *Actin57B* (Kelly et al., 2002). Most of these genes have a structural role, either in the cytoskeleton or as part of the contractile apparatus, and can therefore account in part for the defects in terminal differentiation seen in *Mef2* mutants. However, the broad spatio-temporal expression of *Mef2* hints at a more general role in myogenesis, from early through late stages of development.

2.6. *lame duck (lmd)* a Zn-Finger transcription factor essential for FCM specification and myoblast fusion

2.6.1. *lmd* is expressed specifically in FCMs during the time of myoblast fusion

lame duck (Duan et al., 2001) (also known as *gleeful* (Furlong et al., 2001a) and *minc* (Ruiz-Gomez et al., 2002)) is a Zn-Finger transcription factor of the Gli superfamily. *lmd* is expressed between stages 10 and 14, noticeably during the time of muscle fusion. It is first detected at late stage 10 in the primordia of the visceral mesoderm (VM). This expression continues through stage 11 and *lmd* is apparently expressed in both FCs and FCMs of the VM (Ruiz-Gomez et al., 2002). At this stage there is a transition of expression from the VM to the somatic mesoderm. In the somatic mesoderm, however, expression is mainly restricted to FCMs, with little if any expression in somatic FC as judged by rP298 co-staining. By stage 12 *lmd* expression is lost from the VM and continues in the SM until stage 13-14. At stage 15 *lmd* RNA can only be found in the gonadal mesoderm (Ruiz-Gomez et al., 2002). The expression pattern of Lmd obtained with an antibody raised against the N-terminal domain of the protein is similar to the RNA pattern obtained by *in-situ* hybridization of *lmd* (Duan et al., 2001). It should be noted that *lmd* is expressed only in the types of muscle known to undergo muscle fusion (somatic, visceral) but not of the muscle types that do not fuse (heart) (Duan et al., 2001), with the gonadal mesoderm being the exception (Ruiz-Gomez et al., 2002). Interestingly, *lmd* is expressed immediately before and during fusion.

2.6.2. *lmd* loss-of-function results in a lack of FCM differentiation and block of fusion.

lmd mutants show a general block of pharyngeal and somatic muscle fusion, whereas the VM and heart apparently develop normally (Duan et al., 2001). The phenotype can be reasonably rescued with the expression of *Lmd* driven by Twist-Gal4 (Ruiz-Gomez et al., 2002).

In *lmd* mutants, the early pan-mesodermal expression of Mef2 is normal, indicating that early muscle specification is unaffected, which is in accordance with *lmd*'s relatively late expression pattern. However, later expression of Mef2 in somatic muscle is severely reduced. FCs can be detected with the FC-specific rP298-lacZ line, and the specification of individual FCs appears unaffected as judged by the expression of the identity genes *Kr*, *ladybird* and *nau*. Consistently with this normal specification, MHC stains reveal the presence of mononucleated mini-muscles. The FCs acquire their specific identity, finding their appropriate position, elongating, attaching to the ectoderm and expressing myosin, but there is no fusion with any FCMs. On the other hand, the FCM-specific marker *sns* is not expressed in the SM of *lmd* mutant embryos. Therefore, the reduction of Mef2 in the somatic muscle seems to be due to loss of Mef2 staining in the FCM population. However, this reduction is not caused by a loss of these cells as undifferentiated FCMs can still be detected by their abnormally prolonged *twist* expression. While wild-type FCMs lose *twist* expression upon differentiation at stage 11-12, *lmd* mutant FCMs do not differentiate and retain *twist* staining up to stage 14. Furthermore, in *Notch* (*N*) and *Delta* (*Dl*) mutants, where the specification of FCMs is unfavored (section 2.3.3) *lmd* expression is severely diminished (Ruiz-Gomez et al., 2002). Therefore, *lmd* mutants appear to have a defect in the correct differentiation of FCMs.

The phenotype of *lmd* mutant embryos differs significantly from those of other fusion genes. In *sns*, *duf+rst*, *mbc*, *blow*, *ants/rols7* mutants, FCMs continue to express Mef2 and MHC, indicating that the cells have differentiated but failed to fuse. In *lmd* mutants, segregation of FCs and FCMs occurs, as judged by FC development, but the differentiation of FCMs is blocked at an early stage and the

cells fail to both reduce *twist* expression and maintain *Mef2* expression. These cells do not develop into fully differentiated FCMs, revealing a specific differentiation program in this cell type.

Visceral muscle (VM) appears to be unaffected in *lmd* mutants, even though the TF is expressed there, as judged both by the expression of general muscle markers like *Mef2* and MHC. Gut constrictions are normal, as is the expression of VM specification markers *bagpipe* (*bap*) and *Fasciclin III* (*Fas3*). Interestingly, FCM-specific *sns* is completely abolished in the SM but not in the VM of the *lmd* mutants, again suggesting that the VM and SM have different transcriptional programs regulating myoblast fusion (Ruiz-Gomez et al., 2002). *Sns* is the FCM receptor mediating recognition before fusion (section 2.3.4.1), and the *lmd* loss-of-function phenotype in SM is probably mediated at least in part by the SM-specific loss of *Sns*. Heart muscle development is also normal as judged by morphology, *Mef2* and MHC expression (Duan et al., 2001).

2.6.3. *lmd* is a member of the Gli family of TFs, and can directly activate *Mef2*

lmd encodes a protein with 866 a.a. that contains five C2H2-type zinc finger domains. These zinc finger domains share considerable homology to the Gli family of transcription factors. The homology is restricted to the Zn-fingers, in particular Zn-fingers 3-5, with high divergence in the first two fingers and no homology in the remaining protein. The Lmd protein is therefore considered to be a member of the Gli superfamily of transcription factors, which also includes the *Drosophila* gene *cubitus interruptus* (*ci*) (Duan et al., 2001) (Ruiz-Gomez et al., 2002).

Ci/Gli are the main effectors of the Hedgehog signaling pathway in *Drosophila* and in vertebrates and are known to act both as activators and repressors of transcription. The protein is proteolytically cleaved in the absence of signaling, and acts as a transcriptional repressor. Signaling inhibits the cleavage and the complete protein acts as an activator (Jia and Jiang, 2006).

2.6.4. The activity of Lmd is regulated by distinct posttranscriptional mechanisms

In contrast to Mef2, Lmd protein can be found both in the nucleus and in the cytoplasm of FCMs. Furthermore, Lmd was shown to activate the transcription of *Mef2* by directly binding to the IEd5 (Nguyen and Xu, 1998) enhancer, and there was a correlation between nuclear localization of Lmd and activation of Mef2 *in vivo*: where Lmd is strictly cytoplasmic there is no detectable Mef2 (Duan et al., 2001). This showed Lmd to be a direct activator of Mef2, but also hinted at a dynamic regulation of Lmd's activity at least in part dependent on its nuclear localization.

Further studies have shown that Lmd's activity can be modulated by distinct posttranscriptional mechanisms (Duan and Nguyen, 2006). A nuclear localization sequence (NLS) present in the Zn-Finger domain is responsible for the nuclear import of Lmd. An N-terminal "I" domain and a C-terminal "II" domain are involved in cytoplasmic retention of the protein. It is not yet clear whether these domains act by masking the NLS (directly or indirectly), or/and if they could be involved in interaction with the microtubule network leading to cytoplasmic retention. In either case, a putative unknown activating factor would suppress these two domains, allowing Lmd to move to the nucleus and become active. The subcellular localization of Ci was shown to be regulated by microtubule dependent and independent mechanisms (Wang and Jiang, 2004), and a similar mechanism could potentially be used to regulate Lmd.

The regulation of activity by localization is crucial for the correct function of Lmd. Reintroducing the full length protein leads to extensive rescue of the mutant phenotype. Overexpression of the protein throughout the mesoderm with a *twist*-Gal4 driver produces only mild defects, indicating that the excess protein can be conveniently regulated by the mechanisms in place. Conversely, exclusively nuclear - hence constitutively active - truncated forms cause severe defects when over-expressed, and have poor rescue capabilities, indicating posttranscriptional regulation of Lmd via the "I" and "II" regulatory modules is essential.

Lmd also contains a putative SH3 domain binding site, as well as a putative PKA phosphorylation site. Mutation of either site leads to a hyperactive protein without disturbing its intracellular localization. It is tempting to draw parallels with the regulation of Ci, where phosphorylation by PKA leads to proteolysis of the activating Ci-155 to repressive Ci-75, with the PKA site mutant being a hyperactive protein (Price and Kalderon, 1999). However, a cleaved form of Lmd could not be detected by Western blot, and increased or decreased PKA function in the mesoderm does not seem to cause any obvious muscle defects. Hence it is likely that an unknown kinase is responsible for regulation at this PKA site, and it might work without promoting cleavage of Lmd (Duan and Nguyen, 2006).

In summary, Lmd activity is regulated by its nuclear localization and by changes at two sites that modulate the protein's activity independently of nuclear localization. This complex regulation, shows some parallels to the regulation of Ci, raising the question whether Lmd could also have a dual role as both activator and repressor, as is the case of the other member members of the Gli superfamily.

2.7. Synergistic cooperation on common enhancers allows complex spatio-temporal regulation

While *Mef2* has been considered a gene essential for terminal differentiation and myoblast fusion, its broad spatio-temporal expression throughout development suggested a more general role in myogenesis. Looking at the array of targets recently identified, it becomes apparent that *Mef2* activates different batteries of genes in different temporal windows (Sandmann et al., 2006b). It has been suggested that rising levels of *Mef2* could account in part for this effect: as development progresses, the concentration of active *Mef2* would increase and satisfy the higher requirements of late target genes (Elgar et al., 2008). However, it was also found that *Twist* is involved in the regulation of early targets of *Mef2* on common enhancers (Sandmann et al., 2006b). The spatio-temporal overlap of the two factors reinforces each other, increasing the specificity of the regulation.

Additional interactions have been reported between *Mef2* and other factors acting on common enhancers. Both *GATA4* (Morin et al., 2000) and *Hand1* (Morin et al., 2005) can act synergistically with the *Mef2* family to activate enhancers functional during vertebrate heart development. In *Drosophila* muscle development, it has recently been found that *Mef2* cooperates with *vestigial (vg)* and *scalloped (sd)* to activate genes in different subsets of developing myoblasts (Deng et al., 2009). A very interesting report on the function of *holes in muscles (him)* has shown this gene to be a repressor of *Mef2* gene activation by recruiting the general repressor Groucho (Gro) (Liotta et al., 2007). All of these interactions allow or prevent the broadly expressed *Mef2* from activating genes in precise spatio-temporal locations. It is likely that other factors are required to explain the specificity of *Mef2* gene activation in other different myoblast populations.

The transcription factor *lmd* has a more restricted expression pattern in mid-embryogenesis than that of *Mef2*. *lmd* is expressed specifically in FCMs and is required for the specification of this population. In addition, both *lmd* and *Mef2* mutant embryos suffer from a similarly severe block of myoblast fusion, making *lmd* a prime candidate to act as a modulator of *Mef2*'s activity in the fusion competent myoblast population.

3. Aim of the project

The aim of this project was to get a better understanding of the connection between combined regulation of a common process by two transcription factors (resulting in an identical specific phenotype) and combinatorial input these two transcription factors binding to shared enhancers. I assessed the contribution of each transcription factor on common enhancers using different *in vivo* and *in vitro* approaches to better understand the logics of target gene regulation.

The process chosen for analysis, myoblast fusion, is the process by which founder cells and fusion competent myoblasts fuse in *Drosophila melanogaster* forming the syncytial myotubes that will then differentiate into larval muscle. This process has been shown to integrate the inputs of two transcription factors, *Mef2* and *lmd*, with the interesting point that loss-of-function mutations in either of them leads to a similar complete block in myoblast fusion. More transcription factors have been identified whose loss-of-function mutation affects different muscle groups (“identity genes”), but *lmd* and *Mef2* are the only known transcription factors that affect all muscle fusion, indicating a general role in regulation the process.

The study starts with an analysis of stage-specific expression profiling and ChIP-on-chip data for both *Mef2* and *lmd* collected by Thomas Sandmann in the Furlong lab. Comparing the target list of the two TFs it was clear that most of the targets of *lmd* where also regulated by *Mef2* on a common enhancers. It was also striking to see that both *Mef2* and *lmd* seemed to be able to activate and repress the expression of genes in this data set. A number of questions highlight the aims of this study:

What is the individual input of each TF on a common enhancer? How do these inputs relate to the final result of enhancer/gene regulation? Do *lmd* and *Mef2* act cooperatively or simply additively? Can *Lmd* or *Mef2* act as direct transcriptional repressors?

The final aim of this project was to learn more about the nature of combinatorial regulation by different transcription factors on common enhancers, in the context of a developmental process.

4. Materials and Methods

4.1. Materials

4.1.1. Instruments

Name	Vendor
1.0x Objective Planapo	Leica
10x ocular (35mm, 2.5x, 4"x5")	Zeiss
16x/0.50 Plan-Neofluar Objective	Zeiss
20x/0.50 Plan-Neofluar Objective	Zeiss
ABI PRISM 7500 Sequence Detection System	Applied Biosystems
Analytical scales, AE50	Mettler
Axiophot Light Microscope	Zeiss
Centrifuges 5415D, 5417C, 5810	Eppendorf
FireCam 1.1.1 software	Leica
Electrophoresis chamber Mini-Sub Cell GT	BioRad
Electrophoresis chamber Wide Mini-Sub Cell GT	BioRad
Nanodrop Spectrophotometer ND-1000;	Nanodrop Technologies
Nanodrop 3.1.0 Software	Coleman Tech. Inc.
Rotary Mixer (Model 34526)	Snijder
Shaker table Gyrotory (Model G2)	New Brunswick Scientific
Shaker table Nutator (220V)	Adams
Speed-Vac Concentrator 5301	Eppendorf
Stereo Microscope MZ 16 FA	Leica
Stereo Microscope Stemi SV6	Zeiss
Stereo Microscope Lamps KL 1500 LCD	Schott
Thermal Cycler PTC-200 Multicycler DNA engine	MJ Research Peltier
Thermal Cycler PTC-225 DNA Engine Tetrad	MJ Research Peltier
Water bath Thermomix 5BU	B.Braun Biotech Internat.
Water bath GD100	Grant
Water bath MP	Julabo
Confocal Microscope Leica SP5	Leica
Confocal Microscope Software	Leica
VICTOR® Light 1420 Luminescence Counter	PerkinElmer
VICTOR software	PerkinElmer

4.1.2. Chemicals

Name	Catalog nr.	Vendor
10x UTP-mix (BioPrime CGH Kit)	18095-011	Invitrogen
Agarose (LMP)	15517-022	Gibco
Ampicillin	A9518	Sigma
Biorad protein assay	500-0001	Biorad
Boric acid (99.5%)	B7660	Sigma
Bovine Serum Albumine (BSA, fraction V)	A-7906	Sigma
Cellfectene [®]	10362-010	Invitrogen
Chloroform	C2432	Sigma
Cy3-dUTP fluorophore	PA53022	Amersham Biosciences
Cy5-dUTP fluorophore	PA55022	Amersham Biosciences
DAB substrate	1718096	Roche
DEPC treated water	9920	Ambion
DMSO	8.02912.10	Merck
deoxynucleoside-5'-triphosphate (dNTPs) for PCR	1 277 057	Roche
DNase I (RNase free)	0776785	Roche
EDTA	E6758	Sigma
Ethanol		Merck
Ethidium bromide	E-1385	Sigma
Exo-Klenow fragment DNA polymerase I (40 U/μl, BioPrime CGH Kit)	18095-011	Invitrogen
Formamide	F5786	Sigma
Formaldehyde (16%, methanol)	18814	Polyscience Europe
Glycogen	901393	Roche
Glycerol	4043-00	J.T.Baker
Hydrogen peroxide	H1009	Sigma
n-heptane	H9629	Sigma
NP 40 (= IGEPAL)	13021	Sigma
Methanol	106009	Merck
Pepstatin	P5318	Sigma
Pfu DNA-polymerase (native)	600135	Stratagene
Phenyl methyl sulfonyl fluoride (PMSF)	P7626	Sigma
Powerscript reverse transcriptase	639500	Clontech
Proteinase K	745723	Roche
2-propanol	1.09634.2500	Merck
RNA Polymerase SP6	M0207	New England Biolabs
RNA Polymerase T3	1031163	Roche
RNA Polymerase T7	881767	Roche
RNase A	1006693	Qiagen
RNase inhibitors	15518-012	Invitrogen
Sodium acetate	9740	Ambion

Sodium chloride	1.06404.5000	Merck
Sodium dodecyl sulfate	L6026	Sigma
SSC (20x)	9765	Ambion
Sybr-Green PCR Master Mix	4309155	Applied Biosystems
Taq-DNA polymerase		EMBL
T4 DNA-ligase	799099	Roche
Tris-base	T6791	Sigma
Triton-X-100	T8787	Sigma
TSA –Plus Fluorescence Palette System	NEL 760	Perkin Elmer
Tween-20	P-7949	Sigma
Restriction endonucleases		New England Biolabs
Western Blocking Reagent	11 921 673 001	Roche

4.1.3. Miscellaneous materials

Name	Catalog nr.	Vendor
1 kb-Ladder	N3232L	New England Biolabs
100 bp-Ladder	N3231L	New England Biolabs
ABIprism 96-well optical reaction plates	4306737	Applied Biosystems
AeroDuster 100		Servisol
BioPrime CGH Genomic DNA Labeling System	18095-011	Invitrogen
Brown microcentrifuge tubes (1.5 ml)	1-6180	NeoLab
Brushes (various sizes)	9.172.050	Buddeberg
<i>E.coli</i> DH5 α , chemocompetent	18265-017	Invitrogen
Filter Durapore 0.22 μ m		Millipore
Fisher finest premium glass cover slips (24x60-1)	12-548-5P	Fisher Scientific
Forceps (110 mm, straight)	E-7009	NeoLab
Glass coplin chars and slide holders		Sigma-Aldrich
Diamond pen	1-7621	NeoLab
Hybridisation chambers		Corning
Microscope glass slides (76x26 mm)		Menzel Glaeser
MinElute PCR Purification Kit	28066	Qiagen
MinElute Reaction Clean-up Kit	28204	Qiagen
Normal Goat Serum (NGS)		Vector Labs
Parafilm	PM-996	Pechiney
PCR tubes (0.5 ml, thin walled)	0030 124.502	Eppendorf
PCR tubes (0.2 ml, thin walled)	0030 124.332	Eppendorf
Phase-lock heavy gel tubes (2 ml)	0032-005-152	Eppendorf
Protein A sepharose beads (PAS, CL4B)	P9424	Sigma
QIAprep Spin Miniprep Kit (250)	27106	Qiagen

QIAquick PCR purification kit	28104	Qiagen
QIAquick minelute PCR purification kit	28104	Qiagen
Safe-Lock Tubes 1.5 ml	28004	Eppendorf
Safe-Lock Tubes 2.0 ml	0030 120.094	Eppendorf
Siliconized microcentrifuge tubes (1.6 ml)	710176	Biozym
Vectastain Elite ABC Kit	PK-6100	Vector Laboratories

4.1.4. Oligonucleotides

4.1.4.1. Primers for enhancer cloning

Name	Sequence	Restriction site
Act57B-KpnI-F	AATGGTACCTCCCCACCGTAACGAACC	Kpn I
Act57B-SacI-F	AATGAGCTCTCCCCACCGTAACGAACC	Sac I
Act57B-SacI-R	AAAGAGCTCAAGTATCGCCGCGTTGGTACTC	Sac I
Act57B-NheI-F	AATGCTAGCTCCCCACCGTAACGAACC	Nhe I
Act57B-NheI-R	AAAGCTAGCAAGTATCGCCGCGTTGGTACTC	Nhe I
Act57B-XhoI-R	AAACTCGAGAAGTATCGCCGCGTTGGTACTC	Xho I
bTub60D-KpnI-F	TAAGGTACCGATGGCTGTGTATCCATGAGATAC	Kpn I
bTub60D-SacI-R	ATTGAGCTCTTCAAACGTCAGTTTTGGACG	Sac I
bTub60D-SacI-F	TAAGAGCTCGATGGCTGTGTATCCATGAGATAC	Sac I
bTub60D-NheI-R	ATTGCTAGCTTCAAACGTCAGTTTTGGACG	Nhe I
bTub60D-NheI-F	TAAGCTAGCGATGGCTGTGTATCCATGAGATAC	Nhe I
bTub60D-XhoI-R	ATTCTCGAGTTCAAACGTCAGTTTTGGACG	Xho I
blow-KpnI-F	AAAGGTACCGGGATGTCGTAATGACAC	Kpn I
blow-SacI-R	CGGGAGCTCGGCTTCTAAATAGTATTGTATC	Sac I
blow-SacI-F	AAAGAGCTCGGGATGTCGTAATGACAC	Sac I
blow-NheI-R	CGGGCTAGCGGCTTCTAAATAGTATTGTATC	Nhe I
blow-NheI-F	AAAGCTAGCGGGATGTCGTAATGACAC	Nhe I
blow-XhoI-R	CGGCTCGAGGGCTTCTAAATAGTATTGTATC	Xho I

Name	Sequence	Restriction site
CG5080-XhoI-F	TAGCT CGAGG CTGGAAAGGGTAGGG	Xho I
CG5080-NheI-R	AAT GCTAGCT GGATGCAGCCCATG	Nhe I
CG5080-NheI-F	CAG GCTAGC GCTGGAAAGGGTAGGG	Nhe I
CG5080-MluI-R	AAT ACGCGT TGGATGCAGCCCATG	Mlu I
CG5080-MluI-F	TAG ACGCGT GCTGGAAAGGGTAGGG	Mlu I
CG5080-KpnI-R	GAC GGTACCT GGATGCAGCCCATG	Kpn I
CG9005-KpnI-F	TTT GGTACCT GGTGCTCTTCTTCCTCCAC	Kpn I
CG9005-SacI-R	AAC GAGCTCC ATAAATGAAATGTAACGAACTCG	Sac I
CG9005-SacI-F	TTT GAGCTCT GGTGCTCTTCTTCCTCCAC	Sac I
CG9005-NheI-R	AAC GCTAGCC ATAAATGAAATGTAACGAACTCG	Nhe I
CG9005-NheI-F	TTT GCTAGCT GGTGCTCTTCTTCCTCCAC	Nhe I
CG9005-XhoI-R	AAC CTCGAGC ATAAATGAAATGTAACGAACTCG	Xho I
9416(373)-KpnI-F	AA AGGTACCG CCATTTCAAATGATGATCG	Kpn I
9416(373)-SacI-R	AA AGAGCTCC CATATTTATATTCGGCATTTTGG	Sac I
9416(373)-SacI-F	AA AGAGCTCG CCATTTCAAATGATGATCG	Sac I
9416(373)-NheI-R	AA AGCTAGCC CATATTTATATTCGGCATTTTGG	Nhe I
9416(373)-NheI-F	AA AGCTAGCG CCATTTCAAATGATGATCG	Nhe I
9416(373)-XhoI-R	AA ACTCGAGC CATATTTATATTCGGCATTTTGG	Xho I
CG14687(5')NheI-F	TAG CTAGCC ATGATCCGACGTGGAGAGC	Nhe I
CG14687(5')SalI-R	ATA GTCGAC CGATGCTGATTCCGGTGAG	Sal I
CG30035-NheI-F	AA AGCTAGCC GAATCTTGAACCTCAGTGCC	Nhe I
CG30035-XhoI-R	AA ACTCGAGC CCACCCGAAAGTTGAATTG	Xho I
gol2.9-KpnI-F	AA AGGTACCC AATCTACTGAATCTAACGC	Kpn I
gol2.9-BglII-R	AAA AGATCTG AGGTCTACTACCTTTGC	Bgl II
ttk(e)-KpnI-F	AA AGGTACCG GAAACGGCGTCGTCG	Kpn I
ttk(e)-SacI-R	AA AGAGCTCA AACTTGGATTTTTCCAGTGTGG	Sac I
ttk(e)-SacI-F	AA AGAGCTCG GAAACGGCGTCGTCG	Sac I

Name	Sequence	Restriction site
ttk(e)-NheI-R	AAAGCTAGCAAACCTGGATTTTTCCAGTGTGG	Nhe I
ttk(e)-NheI-F	AAAGCTAGCGGAAACGGCGTCGTCG	Nhe I
ttk(e)-XhoI-R	AAACTCGAGAAACCTGGATTTTTCCAGTGTGG	Xho I
ttk(l)-NheI-F	AATGCTAGCTATTCAACTTAAAGTCGGTGCAG	Nhe I
ttk(l)-XhoI-R	AATCTCGAGTGATCACACGGCACGAAC	Xho I
ttk(l)-KpnI-F	AATGGTACCTATTCAACTTAAAGTCGGTGCAG	Kpn I
ttk(l)-SacI-R	AATGAGCTCTGATCACACGGCACGAAC	Sac I
ttk(l)-SacI-F	AATGAGCTCTATTCAACTTAAAGTCGGTGCAG	Sac I
ttk(l)-NheI-R	AATGCTAGCTGATCACACGGCACGAAC	Nhe I
sug-KpnI-F	TTTGGTACCTTCGCCTCTCATAATAATGCC	Kpn I
sug-NheI-R	AATGCTAGCTCCCATTTCCCATTTCCCATC	Nhe I
sug-NheI-F	TTTGCTAGCTTCGCCTCTCATAATAATGCC	Nhe I
sug-XhoI-R	AATCTCGAGTCCCATTTCCCATTTCCCATC	Xho I
sug-XhoI-F	TTTCTCGAGTTCGCCTCTCATAATAATGCC	Xho I
sug-BglII-R	AATAGATCTTCCCATTTCCCATTTCCCATC	Bgl II

4.1.4.2. Oligos for qPCR

Name	Sequence
blow-qPCR1-F	AAAGTTTCTGTTGATCTATCTCACACTAACTG
blow-qPCR1-R	AGCAAAGCAAAATTGAAGCCA
btub-RT1-F	GACAAAGCCATTATCTGGCAAAT
btub-RT1-R	CATCGCTGATCGCTTTACTTTTAC
QPCR-b3t-B-F-J82	TGCAGACGCCATGGGTAG
QPCR-b3t-B-R-J83	TGCGAGGAGAAGGAGCAGT
QPCR-b3t-C-F-J84	CGTCAAGTTCAAGTGCCAAAG
QPCR-b3t-C-R-J85	TGGCAACAGTCACCGAGATT

Name	Sequence
btub-qPCR4-F	CCATTCTGCTCTGCTCCGC
btub-qPCR4-R	GCTCCTGGGGAGAAATGCA
CG5080-qPCR1a-F	AGGGGGTTAGGGTTAGTGGC
CG5080-qPCR1a-R	ATTAATGGTCCGCAGCGAG
CG5080-RT3-F	GGGCCGATGTGGATTCTG
CG5080-RT3-R	CTCCGCGATGTGTGACATGT
CG9005-RT1-F	AATCCCCCTCACTTACCTTTCAA
CG9005-RT1-R	AAGCAAAGAATAATGGAATTTTAACAAA
CG9005-qPCR3-F	AGCCAGAACAGGACGAGCAC
CG9005-qPCR3-R	AGCGAATAAGTGCGTGTGTTCT
CG14687-RT3-F	CCTACGTCATTCCGACAAATCAC
CG14687-RT3-R	AGTGGCCAAGGCAATATGATTG
CG14687-RT4-F	TCCGGAAGGAAATCTTTACAATCT
CG14687-RT4-R	AATACAGTCATTCCGCAAATGTTC
CG14687-RT5-F	CCGAACCCAGGGTCAAGATA
CG14687-RT5-R	CAATTAATCTCTTATTGTTTGATGTTTGAA
CG14687-RT6-F	AAAAATAGTGATTCCCTGCGTGATG
CG14687-RT6-R	AGGGCTTAGCTCGTGTTGACA
gol-qPCR1-F	GCTGCATTACTTGCTTGTC
gol-qPCR1-R	AGCAAAATGCTGCCGGTG
gol-qPCR2-F	CTTCCACTTGCTAAGTAACAAG
gol-qPCR2-R	CCGCTTATAGAAATTAACCAG
pax-qPCR1-F	AAGAGCCCCACCACGTAGCT
pax-qPCR1-R	AAGCCAAAATGAAAAGCCACTC
pax-qPCR2-F	CAGAAAAGGCAGAAATGGGATC
pax-qPCR2-R	AGTGGGACGAAAGGTTAAAGAGTTT
sns-qPCR1-F	GCAACTCCGAAAGCGCACA

Name	Sequence
sns-qPCR1-R	CGAAAAGTTCTGTTTCAGTTGCAGG
sns-qPCR3-F	TATACGACTTCCACCCCCGG
sns-qPCR3-R	CCATCAACTTATACGGGCCA
sug-qPCR1-F	AAAAAATAGCAGCACCCATTGAA
sug-qPCR1-R	TCCGGCTGAAGCTCTATTTTATAC
sug-qPCR3-F	CGACTGTACCTCGGCTCGA
sug-qPCR3-R	CATAATCGGACCACAACTGCTC
sug-qPCR4-F	ATCTTATAGTGGCCTCTTTGTAGATTCTAGA
sug-qPCR4-R	TTTGCCTGAGAATGGCTAGTTCT
ttk-qPCRa-F	CGAAGCGCACGACTTTGG
ttk-qPCRa-R	CCATGGACGTGTGTGTTTTGC
ttk-qPCRb-F	CGATTAAGGCTTCCATTATCAGC
ttk-qPCRb-R	GGAAGGCCGTTATCTCTC
ttk-qPCRe-F	GACGATCCTCCCCTTTGAATAG
ttk-qPCRe-R	TCTGGTGCCCCGCTAAAAATAG

4.1.4.3. Other oligos

Name	Sequence
hsp70-BglII-F	ATTAGATCTGAGCGCCGGAGTATAAATAGAG
hsp70-HindIII-R	ATTAAGCTTCTGCAGATTGTTTAGCTTGTTTCAG
J207	CCATGGTGAGCAAGGGCG
J207	GTAATACGACTCACTATAGGGCCTTGTACAGCTCGTCCATG

4.1.5. Antibodies

Antibody	Dilution	Cat. nr.	Source
Rabbit α -GFP IgG (0.5mg/ml) (Immunohistochemistry)	1:300	TP401	Torrey Pines Biolabs
Donkey α -Rabbit IgG, biotin-coupled (Immunohistochemistry)	1:200		Jackson Immunoresearch
Anti-Dig-Peroxidase (Fluorescent insitus)		1207733	Roche
Anti-Fluor-Peroxidase (Fluorescent insitus)		1426346	Roche
Anti-Fluor- Alkaline Phosphatase (Colorimetric)		1426338	Roche
Anti-Dig- Alkaline Phosphatase (Colorimetric)		1093274	Roche

4.1.6. Plasmids

Name	Purpose	Source
pH-stinger	Generation of transgenic <i>Drosophila melanogaster</i> GFP-reporter lines	(Barolo et al., 2000)
pAc5.1/V5-hisB	Expression of TFs for <i>in vitro</i> luciferase assays	Invitrogen
pGL3-Promotor	Start vector for pGL3-hsp70	Promega
pGL3-hsp70	Cloning of enhancer sequences for luciferase assays or transcriptional regulation	This study
“copia”-Renilla	Renilla luciferase transfection control	Steve Cohen
pCRII-TOPO	Template for <i>in vitro</i> transcription reactions	Invitrogen
pUAST	Ectopic expression with GAL4-system,	Pernille Rørth

4.1.7. Software

Name	Purpose	Source
Vector NTI	Visualization of cloning projects, DNA sequence analysis	Invitrogen
Tm4	Microarray normalization and analysis	TIGR, USA
ImageJ	Image processing	NIH

4.1.8. Media, solutions and buffers

Complete SFM	500 ml SFM 45 ml 200mM L-Glutamine 5 ml Penicillin Streptomycin (100x)
LB ^{+Amp} –medium:	10 g Trypton Peptone 5 g Bacto-yeast extract 10 g NaCl ad 1 l with H ₂ O after autoclaving: ad 1 ml 1000x Ampicillin
LB ^{+Amp} –plates:	10 g Trypton Peptone 5 g Bacto-yeast extract 10 g NaCl 15 g Agar-Agar ad 1 l with H ₂ O after cooling off to 50°C: add 1 ml 1000x Ampicillin
SOC -medium:	5 g Bacto-yeast extract 20 g Bacto-Peptone 20 g Dextrose 10 mM NaCl 2,5 mM KCl 10 mM MgSO ₄ ad 1 l with H ₂ O
Standard fly medium:	1 l H ₂ O 12 g agar 80g corn powder 18 g dry yeast 22 g sirup 10 g soy powder 6.2 g propionic acid 80 g malt extract 2.4 g nipagin
1kb DNA ladder:	#N 3232 L (NEB) 1000µl of 500 µg/µl 1kb-ladder diluted to 1 µg/10µl in 700 µl 6x Loading Buffer (without xylene cyanol) and 3300 µl 1x TE-buffer used at 1 µg/10µl working stock

100bp DNA-ladder:	# N323L (NEB) 500 µl of 500 µg/µl 100bp DNA-ladder diluted to 1 µg/10 µl in 350 µl 6x Loading Buffer (without xylene cyanol) and 1650 µl 1x TE-buffer use: 0.5 µg/10 µl working stock
1000x Ampicillin:	100 mg/ml, sterile
20x PBS:	175.2 g NaCl 44.8 g KCl 46.6 g Na ₂ HPO ₄ x 12 H ₂ O 4.2 g KH ₂ PO ₄
50x TAE:	2 M Tris/glacial acetic acid, pH 7.7 5 mM EDTA in H ₂ O
6x Loading Dye:	30% glycerol 0.25% bromophenol blue 0.25% xylene cyanol
DAB Staining solution:	3,3' Diaminobenzidine (DAB) staining solution diluted 1:20 in 3% H ₂ O ₂
Fixing solution:	125 µl 16% formaldehyde (4% final) 375 µl PBS
Fix/Heptane:	500 µl Fixing solution 500 µl n-heptane
Methanol/heptane:	50% methanol 50% n-heptane
Methanol/PBT:	50% methanol 50% PBT
PBT:	1x PBS 0.1% Triton-X-100
PBTween	1x PBS 0.1% Tween-20
PBT/BSA:	PBT + 0.2% BSA
PBT/BSA/NGS:	PBT/BSA + 0.2% Normal Goat Serum (NGS)

Protease inhibitors:	1x Aprotinin 1x Leupeptin 1x Pepstatin 1x PMSF
Streptavidin/HRP:	A + B solutions (Vector Laboratories) 1:100 in PBT/BSA each; incubated 1h at r/t prior to use
TE-buffer:	10 mM Tris-HCl, pH 8.0 1 mM EDTA
2x Carbonation Buffer	120 mM Na ₂ CO ₃ , 80 mM NaHCO ₃ DEPC H ₂ O, pH 10.2
Hyb-A Buffer	50% Formamide 5x SSC pH 5.0 100 µg/ml salmon sperm 0.1% Tween 20 50 µl/ml Heparin
Hyb-B Buffer	50% Formamide 5x SSC pH 5.0

4.1.9. Fly lines

Genotype	Source
	(Duan et al., 2001)
$\frac{wt}{Y}; \frac{Mef2^{22,21}}{cyo,wz}; \frac{wt}{wt}; \frac{wt}{wt}$	(Bour et al., 1995)
$\frac{wt}{Y}; \frac{Mef2^{P544}}{cyo,wz}; \frac{wt}{wt}; \frac{wt}{wt}$	(Lilly et al., 1995)
$\frac{en - Gal4}{en - Gal4}$	(Brand and Perrimon, 1993)
$\frac{wt}{Y}; \frac{wt}{wt}; \frac{UAS - Mef2 - 3xHA}{UAS - Mef2 - 3xHA}; \frac{wt}{wt}$	(Sandmann et al., 2006b)
$\frac{wt}{Y}; \frac{UAS - lmd}{UAS - lmd}; \frac{wt}{wt}; \frac{wt}{wt}$	Previously published as UAS-glf (Furlong et al., 2001a)

4.2. Methods

4.2.1. Molecular Biology and Biochemistry

4.2.1.1. Cloning of constructs to generate transgenic *Drosophila melanogaster* reporter strains

To investigate the regulatory potential of genomic DNA regions transgenic *Drosophila melanogaster* reporter lines were generated. Evaluating conservation of non-coding sequences in other *Drosophila* species allowed further refinement of the enriched coordinates. Fragments within the following coordinates were cloned into the pH-stinger vector (Barolo et al., 2000) and germ-line transformed into *Drosophila melanogaster white*⁻ flies: chr2R:16,451,010-16,451,608 (*Act57B*), chr2R:3,096,924-3,097,695 (*blow*), chr2R:19,817,121-19,817,497 (*βTub60D*), chr3R:6,616,700-6,618,790 (*CG14687*), chr2R:7,181,666-7,183,332 (*CG30035*), chr2L:1,162,146-1,162,550 (*CG5080*), chr2R:14,886,256-14,886,651 (*CG9416*), chr2R:20,586,673-20,589,678 (*gol*), chr2R:8,441,630-8,442,972 (*sug*) chr3R:27,529,670-27,530,400 (*ttk*). (Coordinates based on *D. melanogaster* genome release 4.2.) For all constructs but *CG5080*'s regulatory region, at least two independent transgenic lines were obtained and assayed.

4.2.1.2. Cloning of constructs for *in vitro* luciferase assays

The direct activation of target enhancers by Mef2 and Lmd *in vitro* was tested by luciferase assays. After initial testing of the pGL3-Promotor vector (Promega), the expression from the sv40 promotor was found to be insufficient in Schneider 2 (S2) cells. The sv40 promotor was cut out (Bgl II / Hind III) and replaced with the hsp70 promoter from pH-Stinger (Bgl II / Hind III) increasing the activation in S2 cells. At the same time, the enhancers were trimerised in order to achieve higher activation.

Fragments within the following coordinates were amplified using Pfu DNA Polymerase (Stratagene) from genomic DNA and cloned into the pGL3-hsp70 vector: chr2R:16,451,010-16,451,608 (*Act57B*), chr2R:3,096,924-3,097,695 (*blow*), chr2R:19,817,121-19,817,497 (*β Tub60D*), chr3R:6,616,700-6,618,790 (*CG14687*), chr2R:7,181,666-7,183,332 (*CG30035*), chr2L:1,162,146-1,162,550 (*CG5080*), chr2R:14,886,256-14,886,651 (*CG9416*), chr2R:20,586,673-20,589,678 (*gol*), chr2R:8,441,630-8,442,972 (*sug*) chr3R:27,529,670-27,530,400 (*ttk*), (Coordinates based on *D. melanogaster* genome release 4.2.).

Mef2 and Lmd 3HA-epitope fusions in pUAST (Sandmann et al., 2006b) were digested (EcoRI / XbaI) and cloned into pAC-5.1-V5-hisB (EcoRI / XbaI).

4.2.2. Histological techniques

4.2.2.1. Colorimetric *In situ* hybridization

The following ESTs were used to generate digoxigenin or fluorescein-labeled probes: RE53159 (*β Tub60D*), LD04994 (*Act57B*), LD34147 (*CG5080*), LP02193 (*blow*), LD36528 (*sug*), RE74890 (*CG14687*), RE28322 (*CG9416*), GH20973 (*gol*), AT15089 (*twi*) and RE02607 (*wg*). The full-length *sns* cDNA was a kind gift from S. Abmayr.

Colorimetric *in situ* hybridizations were done using standard protocols as described previously (Furlong et al., 2001a). Briefly, probes were synthesized and labeled for 2.5 hours at 37 °C according to the following reaction:

Table I – Probe labeling reaction for *in situ* hybridization

Volume	Reagent
5 μ l	PCR product
2 μ l	Transcription Buffer
2 μ l	Dig or Fluo RNA Labeling Mix
1 μ l	RNAse inhibitors
1 μ l	RNA Polymerase
9 μ l	DEPC H ₂ O
20 μl	Total Volume

The DNA template in this reaction was then digested for 15 min at 37 °C with the addition of 2 µl RNase-free DNase I, and treated in Carbonation Buffer for 20 min at 65 °C. The probe was subsequently precipitated and re-suspended in 100 µl of Hyb-A buffer.

Embryos previously fixed in formaldehyde and stored in ethanol were transferred to methanol and then to PBTween by a stepwise decrease in methanol content. They were then post-fixed for 20 min in 4% formaldehyde in PBS, and then washed in PBTween. A Proteinase K digestion (8 µg/ml in PBS) was followed by a second post-fixation and wash cycle. The embryos were then transferred to Hyb-B buffer by a stepwise decrease in PBTween content and pre-hybridized in Hyb-A at 65 °C for at least 3.5 hrs. At this point the probe was heated up to 80 °C for 10 min, chilled on ice, added to the embryos at 1:50 (in Hyb-A) and hybridization was allowed to take place overnight at 65 °C.

The probe was washed off the embryos with Hyb-B (3x 30 min followed by 3x 1 hr washes), and the embryos were transferred to PBTween by a stepwise decrease in Hyb-B content. The embryos were then blocked with Western Blocking Reagent at 1:5 in PBTween (2x 30 min at RT) and the first antibody was incubated overnight at 1:2,000 in PBTween with Western Blocking Reagent.

The antibody was washed off with PBTween washes (6x 15 min at RT). The first TSA reaction was performed according to the manufacturer's instructions at 1:50 in amplification buffer for 5 min. This was immediately followed by PBTween washes (6x 20 min at RT). The embryos were then mounted in 80% glycerol. In the case of double in situ hybridizations (Section 4.2.2.2), the last washing steps were followed by a peroxide inactivation reaction with 3% H₂O₂ in PBTween (15 min at RT). After four 15 min washes with PBTween, the embryos were again blocked in Western Blocking reagent and the whole process repeated for the second antibody (with the exception of the peroxidase inactivation reaction).

4.2.2.2. Fluorescent *In situ* hybridization

Double fluorescent in situ hybridisations were done as described previously (Furlong et al., 2001a) (Section 4.2.2.1). Probes were synthesized as described above (Section 4.2.2.1). The probe for GFP was made by amplifying the eGFP sequence from the pH-Stinger (primers J207, J208). As a T7-polymerase site was included in one primer, the amplified DNA could be utilized directly in the probe-generation reaction. This probe was used for GFP mRNA-expression detection in transgenic animals placed in the mutant background of *lmd* and *Mef2*.

To minimize experimental differences, the embryo fixations and the in situ hybridizations were done in parallel and the confocal imaging was performed with identical laser and gain settings for each gene in the four genetic backgrounds.

4.2.2.3. Immunohistochemistry

GFP expression in transgenic animals was detected by immunohistochemistry with rabbit α -GFP antibody (Torrey Pines Biolabs) at a concentration of 1:300, according to standard protocols. Biotinylated secondary antibodies were used in combination with the Vector Elite ABC kit (Vector Laboratories).

4.2.3. Quantitative Real-Time Polymerase Chain Reaction (qPCR)

Primer pairs were designed flanking putative *Mef2* binding sites as well as a region of genomic DNA without putative *Mef2* sites or expression in the mesoderm to be used as a negative control (in the 5' region of the *oskar* gene). All of these primer pairs amplify a similar sized amplicon (50 bp) with similar CG content (50 bp amplicon (GC% 45-55). Reactions were as follows:

Table II - qPCR Reaction Mix

Volume	Reagent
2 μ l	ChIP or mock eluate
2.5 μ l	2.5 μ M primer A
2.5 μ l	2.5 μ M primer B
12.5 μ l	SYBR green PCR Master mix
5.5 μ l	Water
25 μl	Total Volume

For each primer pair, a standard curve was determined in duplicate using serial dilutions from ca. 40 ng/ml sheared genomic DNA (1:10 to 1:10.000 dilutions). The amplification reactions were performed and recorded on an ABI PRISM 7500 real-time PCR system (Applied Biosystems, Foster City, USA) using standard settings for absolute quantitation. Dissociation curves were recorded after each run to evaluate the amplification of uniform products. The results were converted into enrichment ratios by referring to the respective standard curve for each primer pair:

4.2.4. Cell culture and Luciferase assays

Schneider 2 cells (S2 cells) were sub-cultured in 96-well plates the day before transfection. A dense cell culture was diluted with Complete SFM medium to a concentration of 1.5×10^6 cells/ml. 100 μ l of this suspension (1.5×10^5 cells) were aliquoted into each well of a 96-well plate, and cultured for 24 hrs at 25 °C. The cells were then transfected with 0.5 ng of the “Copia-Renilla” transfection control vector, 50 ng of the enhancer-pGL3-hsp70 construct, and 1 to 10 ng of Lmd-pAc5.1/V5-hisB, Mef2-pAc5.1/V5-hisB, or both together. pAc5.1/V5-hisB was added as needed to ensure the total amount of DNA transfected in each well was the same (61.5 ng). Transfection was performed with Cellfectene Reagent

(Invitrogen) according to instructions by the supplier. The transfection mixture was removed after 24 hrs and the cells were allowed to recover for a further 24 hrs with fresh Complete SFM medium. Luminescence as a measure of enhancer activity was assessed using the Dual-Luciferase® Reporter Assay System (Promega). The cells were lysed in 20 µl Passive Lysis Buffer (PLB) and Firefly and *Renilla* luciferase activities were assessed sequentially using 50 µl of LARII and Stop & Glo buffer respectively. The luminescence was read using a VICTOR Light 1420 Luminescence Counter (PerkinElmer), and the reagents were injected automatically. The following program was used:

1. 50 µl of LARII injected
2. 1.6 s shaking (waiting time)
3. 5 s luminescence reading (Firefly luciferase)
4. 50 µl of Stop & Glo buffer injected
5. 1.6 s shaking (waiting time)
6. 5 s luminescence reading (*Renilla* luciferase)

Three independent wells were assayed for every condition. All Firefly luciferase luminescence values in Counts Per Second (CPS) were normalized to the corresponding *Renilla* Luciferase CPS values. All values were compared to the average result of the negative control (empty pAc5.1-pGL3-hsp70) which was set to 1. Therefore, all results indicate a fold change in enhancer activation/repression compared to the control, \pm Standard Error of the Mean (SEM).

4.2.5. ChIP-on-chip and Expression profiling

4.2.5.1. Chromatin Immunoprecipitation and DNA Amplification

Embryo collections and chromatin immunoprecipitations were performed as described previously (Sandmann et al., 2006b) (Sandmann et al., 2006a). Two antisera were raised against the amino terminus of Lmd and purified from *E. coli* by poly-His tag affinity purification. Four independent staged wild-type embryo populations were collected at 6-8 and 8-10 hrs after egg-laying and fixed with

formaldehyde. For each time point, chromatin from all four populations was precipitated with both antisera as well as the respective preimmunesera, leading to a total of 16 reactions (8 mock, 8 anti-Lmd) per time point. DNA amplification, labeling and hybridizations were performed as described previously (Sandmann et al., 2006b) (Sandmann et al., 2006a) and dye swaps were included to account for possible dye biases.

4.2.5.2. Expression Profiling of *lmd* Loss-of-Function Mutants

The assayed *lmd*^l (Duan et al., 2001) line was outcrossed to wild-type flies (Canton S) twice to remove any spurious mutants. Six one-hour embryo collections were assayed in an expression profiling timecourse (between 5 and 11 hours after egg-laying). At each time point, 4 independent populations of *lmd* mutant and stage-matched Canton S embryos were collected and aged. Homozygous mutants were selected with an automated embryo sorter (Furlong et al., 2001a) (Furlong et al., 2001b). The staging of all collections was verified by formaldehyde fixation of a small sample to ensure that wild-type and mutant embryos were tightly stage matched. Total RNA was extracted using Trizol (Invitrogen, Carlsbad, US), amplified, reverse-transcribed and labelled as described previously (Sandmann et al., 2006b).

4.2.5.3. Microarray data analysis

For expression profiling analysis, mutant and stage-matched control cDNA was hybridized directly against each other. Raw data was normalized using print-tip LOESS. Differentially expressed genes were identified using Significance analysis of microarrays (SAM) (Tusher VG, 2001). Genes with a $q < 1\%$ and a fold change > 1.6 ($\log_2 > 0.7$ or < -0.7) were considered to be differentially regulated. Immunoprecipitated DNA from Lmd-specific or mock precipitations was hybridized against a total genomic reference DNA sample. Sequences significantly enriched by the anti-Lmd-antibodies were identified by comparing rank products (Breitling R, 2004) and the false-discovery rate was estimated. Only fragments with an FDR $< 2\%$ and a fold enrichment > 1.5 ($\log_2 > 0.58$ or < -0.58) were considered to be significantly enriched (Appendix, 8.1, Table III).

Automatic assignment of ChIP-enriched fragments to target genes was performed as described previously (Sandmann et al., 2006b). The majority of regions co-occupied by Mef2 and Lmd was independently assigned to the same target genes using either *Mef2*-mutant or *lmd*-mutant expression profiling data. For a small number of regions, data from this study indicated a more likely target gene than had been assigned previously with Mef2 data alone (Sandmann et al., 2006b); in these cases, the updated target prediction was chosen for further analysis. A complete list of ChIP-enriched regions, expression profiling results and target assignments is available in the Appendix. All raw microarray data is available from ArrayExpress (Lmd ChIP (E-TABM-895) and *lmd* expression profiling (E-TABM-894). Lmd- and/or Mef2-bound regions and mutant expression data can be visualized at <http://furlonglab.embl.de/data/>.

5. Results

5.1. Analysis of *lmd* expression profiling and ChIP-on-chip data

The first step taken to understand the interaction in transcriptional regulation between *Mef2* and *lmd* was the identification of the direct target genes for each transcription factor. The approach used was twofold. Direct binding to genomic regions was assessed by Chromatin Immunoprecipitation (ChIP) followed by analysis on genomic tiling arrays (chip), a technique known as ChIP-on-chip. This technique reveals the genome location where each of the transcription factors bind *in vivo*, and this binding can then be allocated to specific genes. To complement this information, the direction of effect (activation/repression) was determined by performing expression profiling in the mutant backgrounds.

In brief, genes were considered direct targets when they were assigned binding by a transcription factor (by ChIP-on-chip) and their expression was affected in the mutant background of that same transcription factor.

All ChIP-on-chip and expression profiling experiments and data collection was done by Thomas Sandmann in the Furlong lab for both *lmd* and *Mef2*, and the data concerning *Mef2* has already been analyzed and published (Sandmann et al., 2006b).

5.1.1. Genomic regions bound by Lmd *in vivo*

ChIP-on-chip analysis provided an unbiased map of regions bound by Lmd *in vivo*. Lmd-bound DNA was precipitated from stage-matched embryos at two consecutive developmental time-points spanning most of the developmental stages during which *lmd* is expressed (stages 10-13) (Figure 10). For each time point, four independent chromatin immunoprecipitations were made, each using two different antisera raised against Lmd. Hence, eight independent experiments were performed per time-point, increasing the sensitivity and specificity of this approach. Potential

false targets that could arise from non-specific antibody binding were reduced, as genomic regions were considered bound only if they were significantly enriched with both antibodies

The immunoprecipitated DNA was analyzed on microarrays containing overlapping 3kb fragments tiling across ~50% of the *Drosophila* genome (Sandmann et al., 2006b).

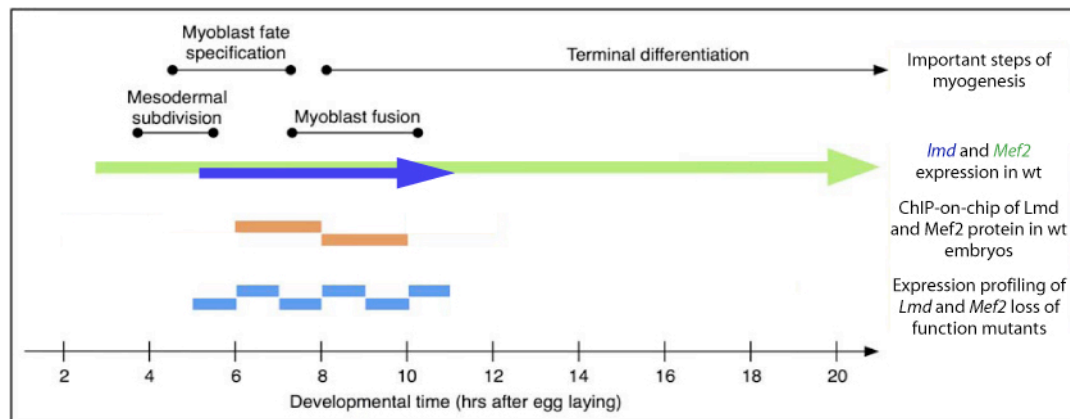


Figure 10 - Schematic overview of *lmd* and *Mef2* function during myogenesis and collected data-points.

Lmd and Mef2 genome binding was assayed at two consecutive 2 hr time-points (orange bars), covering the stages of myoblast specification and fusion, the time window when both transcription factors are simultaneously expressed. This information was complemented by expression profiling of *lmd* and *Mef2* mutant embryos at 4 one hr time points (blue bars). Adapted from (Sandmann et al., 2006b).

By using a stringent criteria of a combined fold cutoff (> 1.5 ($\log_2 > 0.58$ OR < -0.58)), and a False Discovery Rate (FDR) ($< 2\%$), Lmd binding was detected at 154 unique genomic regions (Appendix, 8.1, Table III). Comparing this set of bound sequences with data obtained previously for Mef2 at the same stages of development (fold cutoff > 1.6 , $q < 0.01$) (Sandmann et al., 2006b) (Sandmann et al., 2006b) shows that 106 out of 154 (68.8%) Lmd-bound sequences are also bound by Mef2 at stages 10-14 (Figure 12 A). The overlap of co-bound regulatory elements suggests an extensive co-regulation of target genes by these two transcription factors. This is, moreover, a conservative estimate of enhancer co-occupancy, as regions bound by one or both transcription factors just below the threshold will be missed due to the strict enrichment cutoffs used.

5.1.2. Known direct target genes are identified, underscoring the accuracy of the ChIP-on-chip results

Mef2 is at this time the only known direct target of *lmd*, with the binding occurring at the IE_{d5} enhancer (Duan et al., 2001). *sns*, the first gene identified with specific FCM expression, was shown to be genetically downstream of *lmd* in the SM (but not in the VM) (Duan et al., 2001) (Ruiz-Gomez et al., 2002) and is a very likely candidate *lmd* target gene. Interestingly, the expression of *blow* in the SM has also been shown to be initially restricted to FCMs (Schroter et al., 2006), making it a third likely candidate for regulation by Lmd.

ChIP-on-chip binding was indeed identified in the *Mef2* locus, and specifically in fragments covering the only identified Lmd binding region to date (IE_{d5} fragment) Figure 11 A). Lmd binding is also detected on a previously characterized (Stute, 2004) enhancer of *sns* (Figure 11 B), confirming that *sns* is a direct target of Lmd. *blow* is identified as a direct target gene of Lmd as well, and binding can be seen in an upstream region previously identified as an enhancer (Schroter et al., 2006) (Figure 11 C).

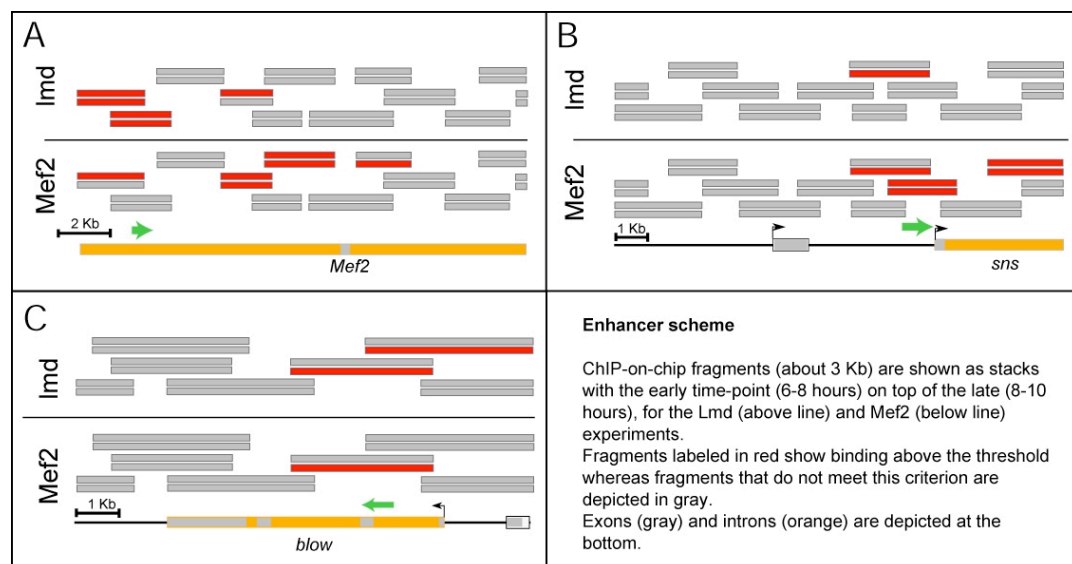


Figure 11 - Positive controls are recovered in the ChIP-on-chip data.

(A) The known IE_{d5} enhancer region is recovered in both the Lmd and Mef2 ChIP-on-chip binding data. This was the only known Lmd direct target gene, but both the *sns* (B) and *blow* (C) locus reveal the presence of Lmd and Mef2 binding showing that both genes are actually direct target genes of Lmd. ChIP-on-chip fragments (about 3 Kb) are shown as stacks with the early time-point (6-8 hours) on top of the late (8-10 hours), for the Lmd (above line) and Mef2 (below line) experiments. Fragments labeled in red show binding above the threshold whereas fragments that do not meet this criterion are depicted in gray. Exons (gray) and introns (orange) are depicted at the bottom. Green arrows illustrate enhancers cloned for this study.

Expression of the bHLH transcription factor *twist* persists longer in *lmd* loss-of-function mutants than in *wildtype* embryos and direct repression by *lmd* has been proposed to underlie this phenotype (Ruiz-Gomez et al., 2002). Although the genomic region containing the *twist* locus is extensively covered by the microarray, no significant Lmd-binding can be detected (data not shown). Even though low-level Lmd-binding to the *twist* region below the detection limit of the assay cannot be excluded, this result suggests an indirect regulatory effect instead.

The recovery of the known *Mef2* IE_{d5} enhancer as well as binding close to the suspected targets *sns* and *blow* underscores the sensitivity of the ChIP-on-chip results. Moreover, a number of Lmd-bound regions overlap additional previously characterized regulatory regions, including enhancers of *βTub60D* (Hinz et al., 1992), *Act57B* (Kelly et al., 2002), *CG14687* and *CG9416* (Sandmann et al., 2006b).

5.1.3. Defining direct targets from ChIP-bound regions

Moving from directly bound genomic regions to the actual implicated genes is often a challenge, as regulatory regions in *Drosophila* can be located at varying positions and distances relative to the target gene (section 2.1). Therefore, a functional relationship cannot be simply deduced from the proximity of a transcription factor binding site to a gene locus. As a starting point, the expression of the target gene should be dependent on the presence of the transcription factor *in vivo*, but additional information must also be taken into account.

Expression profiling data for both *lmd* and *Mef2* was obtained by comparing transcription in *wt* and mutant embryos at six consecutive one-hour windows of development (Figure 10, (Sandmann et al., 2006b)). For the *lmd* dataset, a combined stringent cut off of fold change (> 1.6 ($\log_2 > 0.68$ OR < -0.68) and FDR ($q < 0.01$) yielded 640 genes with significant gene expression differences between *wt* and *lmd* mutant embryos, in one or more of the six consecutive one-hour windows of the developmental time-course (Appendix, 8.2, Table IV). This data was combined with the ChIP-on-chip results for Lmd as well as supporting information using an automated scoring approach described earlier (Sandmann et al., 2006b), yielding a high-confidence list of 74 direct Lmd target genes (Appendix, 8.3, Table V).

5.1.4. Extensive co-regulation of target genes by *lmd* and *Mef2* via common enhancers

An immediate observation when comparing the direct target genes for *lmd* with the ones previously described for *Mef2* is that most of the genes directly regulated by *lmd* are also direct targets of *Mef2* (59/74, 79.7%) (Figure 10 B). This includes genes involved in myoblast fusion, as *sns* and *blow* as well as structural genes as *Act57B*, *Act87E* or *β Tub60D*. Looking at the data from the perspective of the *Mef2* direct targets, it is obvious that the number of *Mef2* targets co-regulated by *lmd* is only a smaller fraction of the total number of *Mef2* target genes (59/203, 29.1%). This is in accordance to what could be expected considering the much broader spatio-temporal expression *Mef2*: the tight group of *lmd* co-regulated genes can be seen as a defined activity of *Mef2* during the more restricted spatio-temporal expression of *lmd*, namely in FCMs between stages 10 and 14.

This stringent set of directly co-regulated genes provides an opportunity to examine the details of how input from the same two transcription factors can be differently integrated at enhancers both *in vivo* and *in vitro*.

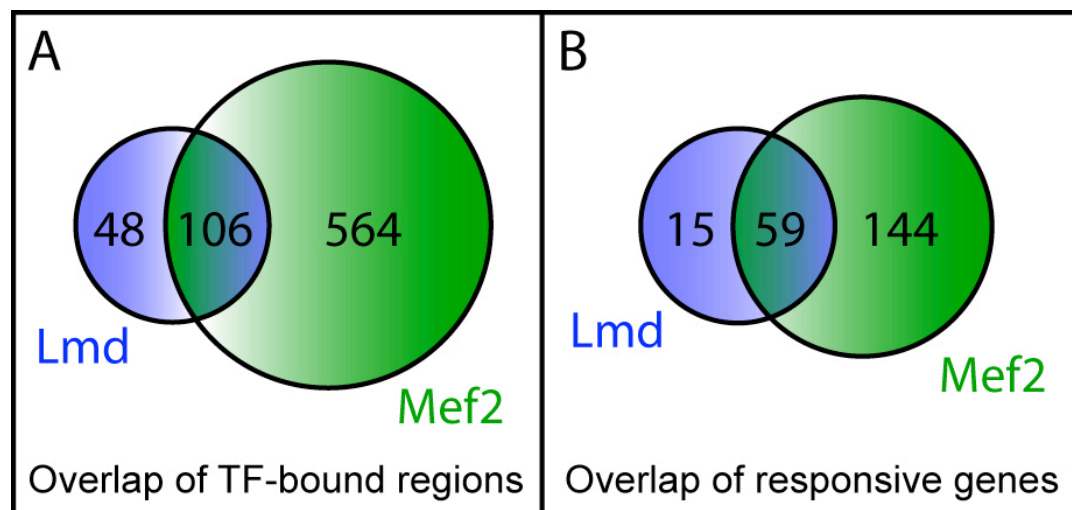


Figure 12 - Overlap between fragments bound by Lmd and Mef2, as well as direct target genes of both TFs.

(A) Venn diagram representing the number of fragments bound by Lmd (154) and Mef2 (670). 106 fragments (68.8 %) are bound by both Lmd and Mef2 at the same time-points. (B) When bound fragments are allocated to specific genes it becomes apparent that a great fraction of *lmd* target genes (57/74, 79.7 %) are also targets of *Mef2*, indicating a high level of co-regulation by *Mef2*.

5.1.5. Lmd and Mef2 CRM occupancy has different effects on target gene expression

A list of shared direct target genes of these two transcription factors raises the important question: what is the end result of this co-regulation? The expression profiling data begins to address this by showing the overall transcriptional response to loss of either transcription factor.

A comparison between the expression profiling data obtained with *lmd* or *Mef2* mutant embryos using K-means clustering revealed seemingly distinct classes of direct target genes. A first group of genes is down-regulated in both *lmd* and *Mef2* mutants (compared to their wildtype controls) and includes e.g. the structural muscle proteins *Act57B*, *Act87E* and *βTub60D* (Figure 13, Cluster I). This could be seen as the expected or default behavior, assuming Lmd is an activator of gene expression (as seems to be the case with Lmd’s regulation of *sns*) and given the fact that *Mef2* is a transcriptional activator. On the other hand, the expression of *Mef2* is also strongly

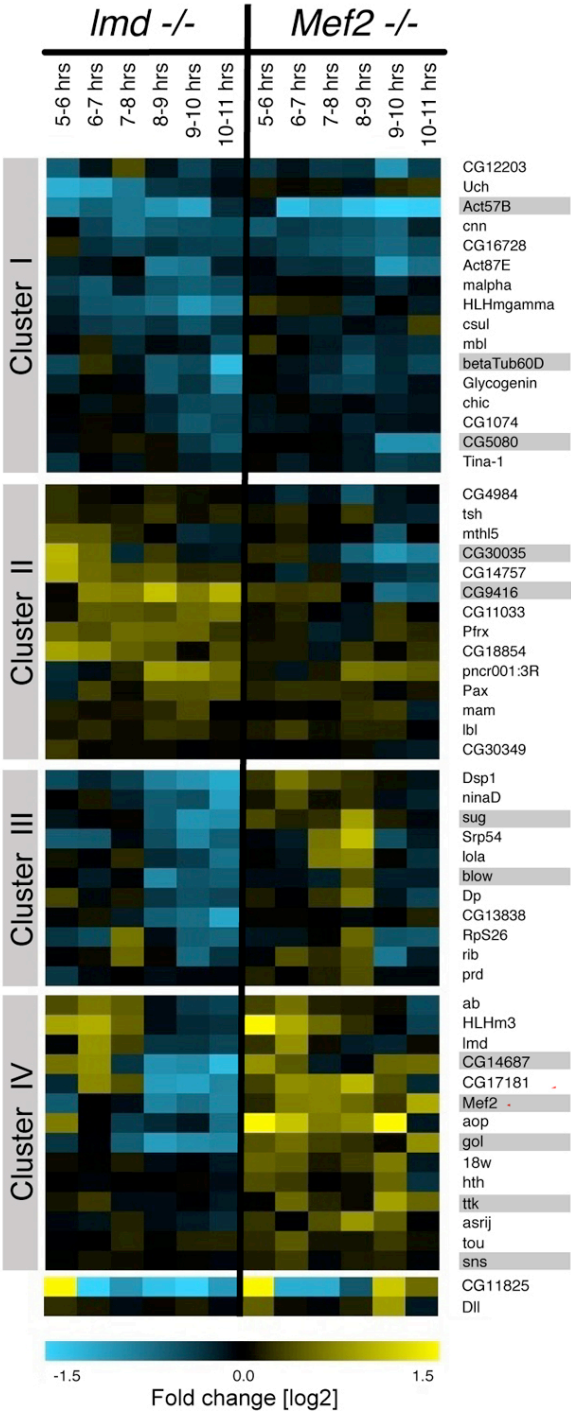


Figure 13 - k-means clustering of *lmd* and *Mef2* expression data.

Differential gene expression in *lmd* and *Mef2* loss-of-function mutants: differences in expression between mutant and wt embryos were recorded in a timecourse for *lmd* (left) or *Mef2* (right) mutant embryos.

reduced in *lmd* mutant embryos. Therefore, downregulated genes in the *lmd* mutant condition might be dependent on activation by both transcription factors or even on *Mef2* alone via activation by *lmd*.

Surprisingly though, the majority of direct target genes respond differently in the two mutant backgrounds, despite occupying a shared enhancer. Indeed, a second group of genes including *blown fuse (blow)*, *goliath (gol)* and *tramtrack (ttk)*, show reduced or unchanged levels of expression in the *lmd* mutant, while having increased expression in the *Mef2* mutant background. This unexpected result could indicate a possible (most likely indirect) repressive effect of *Mef2* on these genes.

Finally, a group of genes including *CG9416* and *CG30035* are downregulated in the *Mef2* mutants but upregulated in the *lmd* mutant background. This suggests either direct repression by *lmd*, or an indirect regulatory effect instead.

In conclusion, the overall expression of common target genes as assessed by expression profiling yields four seemingly distinct clusters of genes. It should be noted that these are most likely not strict classes, but rather reflect an overall readout of distinct individual behaviors that must be studied in finer detail.

5.2. *lmd* and *Mef2* regulate target genes *in vivo* in a synergistic or antagonistic manner

A complementary method to examine the regulatory connection between *lmd* and *Mef2* and their targets is to ask if these transcription factors are sufficient to drive the target gene expression *in vivo*. This was tested by ectopically expressing Lmd and Mef2 in the ectoderm under the control of the *engrailed*-Gal4 driver (Brand and Perrimon, 1993), and assaying target gene activation by colorimetric *in situ* hybridization (Figure 14). *lmd* was previously shown to activate *Mef2* in the CNS, but not in the remainder of the ectoderm (Furlong et al., 2001a) (Ruiz-Gomez et al., 2002) (Duan and Nguyen, 2006). This allowed the direct contribution of *lmd* to be assayed independently from *Mef2*. In addition, the factors were also expressed in combination, thus allowing the assessment of their combinatorial input.

Double fluorescent *in situ* hybridization (FISH) was also performed using the same conditions (Figure 15), with *wingless* (*wg*) as the second hybridization. The *engrailed*-driven ectopic expression was then easily scored adjacent to the *wingless* domain.

Several different modes of interaction between Lmd and Mef2 were observed in these experiments. In this setting, Lmd is sufficient to activate the transcription of *CG14687* (Figure 14 & Figure 15 G'), whereas Mef2 alone is not (Figure 14 & Figure 15 G''). However, when the two factors are expressed simultaneously there is an increase in the expression of these genes, indicating a positive interaction between Mef2 and Lmd. Conversely, *Act57B* and *βTub60D* are activated by Mef2 (Figure 14 & Figure 15 A'', B'') but not Lmd alone (Figure 14 & Figure 15 A', B'), and again an increase of expression can be seen when the two factors are expressed together (Figure 14 & Figure 15 A''', B''').

CG5080, *blow*, *sug* and *sns* represent an even stronger argument for a synergistic effect between these transcription factors. Under these conditions neither Lmd (Figure 14 & Figure 15 C', D', E', F') nor Mef2 (Figure 14 & Figure 15 C'', D'', E'', F'') alone is sufficient to drive ectopic expression of these genes, while their combination leads to clear expression in the engrailed domain (Figure 14 &

Figure 15 C''', D''', E''', F'''). Interestingly, ubiquitous overexpression of Mef2 using a *daughterless*-Gal4 driver has been reported to ectopically activate *CG5080* in the head mesoderm (Elgar et al., 2008), adding further evidence to a role for Mef2 as a regulator of this locus and hinting at the presence of other tissue-specific co-activators in other parts of the developing embryo.

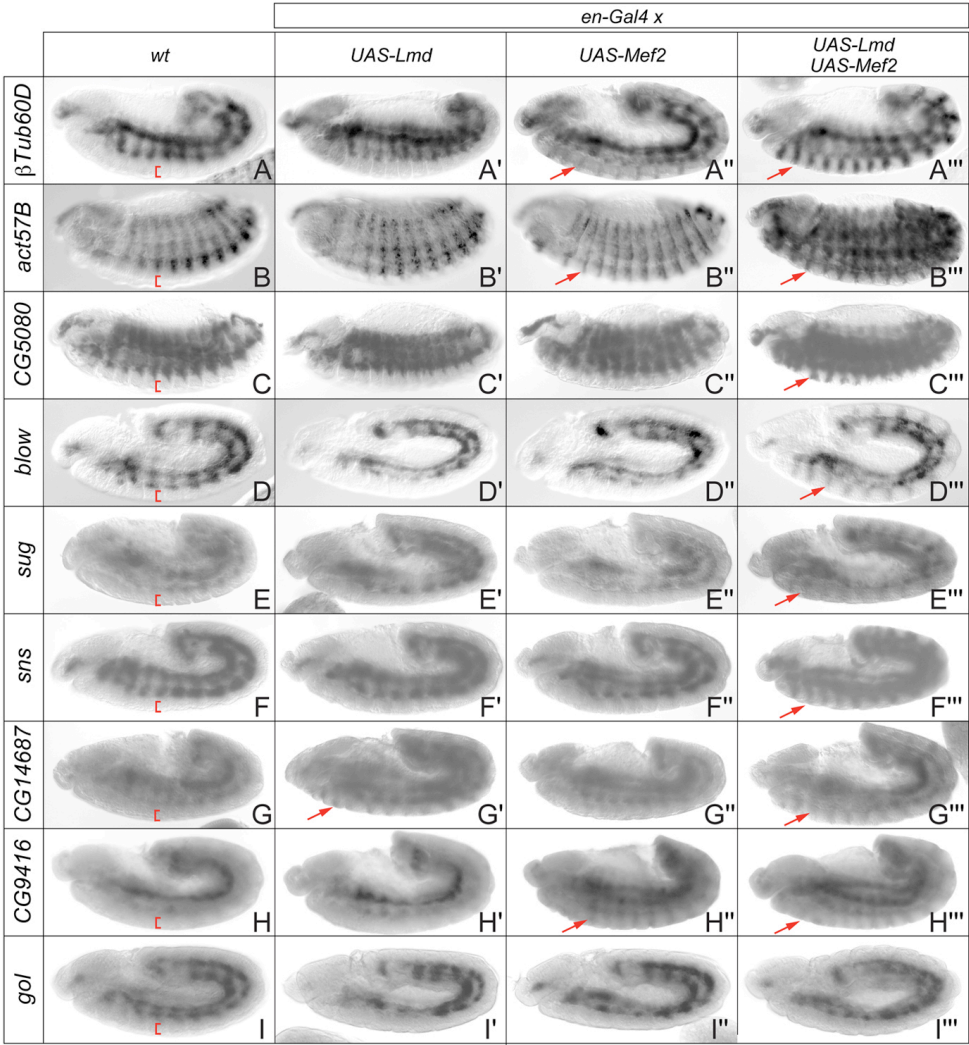


Figure 14 - Ectopic Expression detected by colorimetric *in situ* hybridization.

Lmd and Mef2 were expressed via the UAS/Gal4 system using *engrailed*-Gal4 as a driver. Ectopic gene expression in the ectoderm (red arrows) was detected by in situ hybridization. Expression driven by Lmd (prime) and Mef2 (double) prime can be compared with the level of expression obtained by expressing both transcription factors simultaneously (triple prime). Red brackets in the wildtype column point up to a section of the ectoderm devoid of expression for comparison. Most genes are ectopically expressed in the ectoderm by either Lmd or Mef2. When expression is forced simultaneously by both Lmd and Mef2 the expression seems often stronger (A''', B''', C''', D''', E''', F''', G'''). Interestingly, in the case of CG9416, co-expression of Lmd (H''') seems to repress activation by Mef2 (H'').

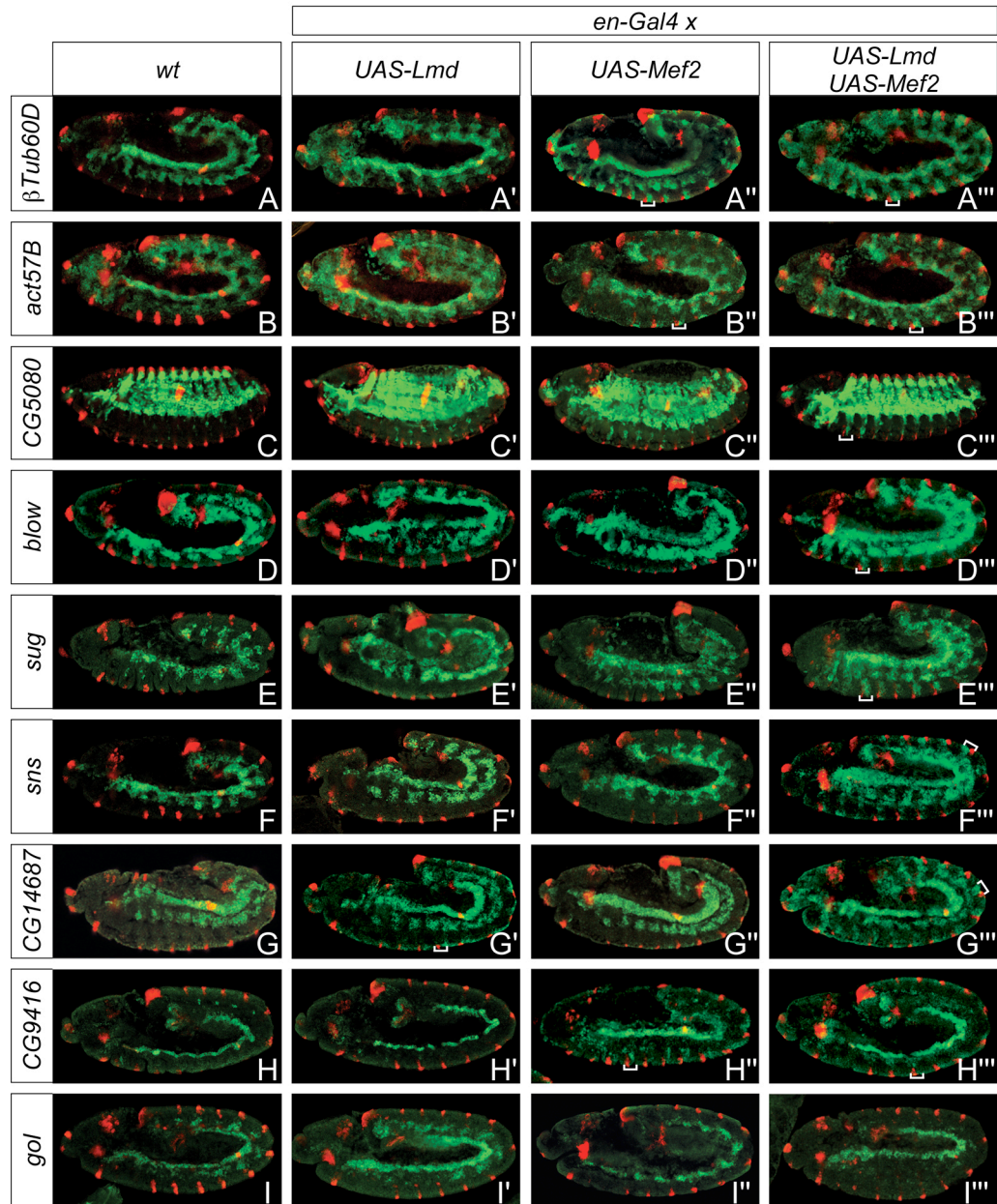


Figure 15 - Ectopic Expression detected by fluorescent *in situ* hybridization.

Lmd and Mef2 were expressed via the UAS/Gal4 system using *engrailed*-Gal4 as a driver, detected by double fluorescent *in situ* hybridization. Ectopic gene expression in the ectoderm (green channel) is shown together (within white brackets) with adjacent wingless expression (red channel). Expression driven by Lmd (prime) and Mef2 (double) prime can be compared with the level of expression obtained by expressing both transcription factors simultaneously (triple prime).

Loss-of-function expression profiling data revealed a number of genes that appear to be upregulated in the absence of Lmd (Figure 13, Cluster II). This is an intriguing observation that points to the possibility that some genes might actually be directly repressed by Lmd. One of these genes, *CG9416*, was selected to test

this hypothesis. Mef2 is sufficient to drive the expression of *CG9416* in the *engrailed* domain (Figure 14 & Figure 15 H'') whereas no such expression can be seen with Lmd alone (Figure 14 & Figure 15 H'). Interestingly, compared to the activation by Mef2 alone, there is a reduction of expression when both transcription factors are used together (Figure 14 & Figure 15 H'''), indicating an inhibitory effect of Lmd on Mef2 driven activation. Finally in the single case of the gene *gol* neither Lmd nor Mef2, alone or in conjunction, were able to ectopically drive expression in the ectoderm.

In summary, these results reveal the complexity of regulation of these shared target genes. All of the genes with the exception of *gol* were ectopically activated in the ectoderm by either Lmd or Mef2 alone, with a synergistic effect being the most common result of the combination of both factors, which indicates extensive co-regulation. However, there is considerable flexibility in how information is integrated at each individual locus, with one factor or the other being predominant for ectopic expression. Furthermore, *CG9416* represents an interesting case of activation by Mef2 and repression by Lmd on a common locus.

5.3. Delimiting enhancers from ChIP bound regions for *in vivo* and *in vitro* studies

Individual enhancer regions in *Drosophila* typically range from 0.5 to 1 kb in size. However, the ChIP-on-chip resolution was limited by the size of the spotted genomic fragments (≈ 3 Kb) and frequently one predicted enhancer spanned different overlapping fragments, which led to combined fragments of up to 5 Kb in length. To better understand the complex direct regulation by *Mef2* and *lmd*, it was crucial to analyze the behavior of the actual shared enhancers. As the ChIP fragments could theoretically encompass two separate enhancers, the co-bound regions were further narrowed down. Briefly, as the chromatin immunoprecipitated regions were in the size range of 500 bp, it could be assessed whether Lmd and Mef2 co-bind within a 500 bp window. Real time PCR primers were designed flanking Mef2 sites within Mef2-bound regions. These primers were then used to amplify Mef2 bound regions from the Lmd immunoprecipitated DNA. If both transcription factors are binding within a 500 bp window, then the Mef2 sites should be present within the Lmd immunoprecipitated regions, leading to the generation of a successful PCR product (Figure 16). The refined enhancer regions were then used both for *in vitro* and *in vivo* studies in order to allow for a direct comparison between all results.

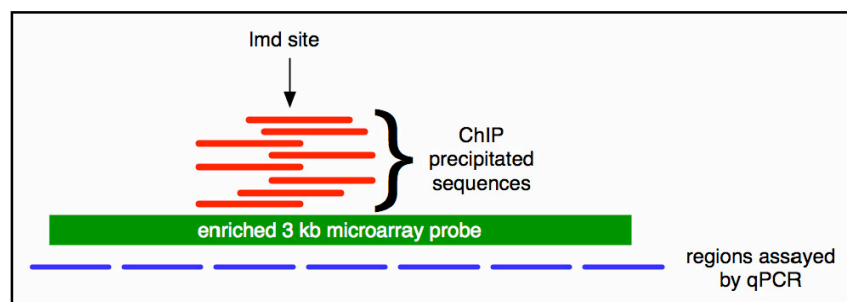


Figure 16 - Enhancers were further refined by qPCR.

ChIP-on-chip resolution is limited by the relatively large 3 Kb spotted microarray probes. ChIP precipitated sequences, at around 500 bp are however much smaller. Once a region was identified by ChIP-on-chip, it was assayed by qPCR, with probes scanning the length of the region, and signal detected from the ChIP fragments.

5.3.1. Scanning the sequences with a Mef2 PWM reveals the presence of several putative Mef2 binding sites

First, the bound regions were scanned for putative Mef2 binding sites using a Position Weight Matrix (PWM) generated from known Mef2 sites by Michal Karzynski in the Furlong lab. It would have been instructive to cross this data with the location of putative Lmd sites, but unfortunately there is no consensus site available at the moment. Lmd has been shown to bind to a 50 bp fragment - IEd5[C/D]* by an Electrophoretic Mobility Binding Assay (EMSA) (Duan et al., 2001) - but a refined binding site has not been identified

The Mef2-binding sites were also ranked according to structure-based estimations of the affinity of each site (computed by Luis Serrano) to reduce false positives and only sites with high affinity were considered.

5.3.2. Conservation of sites in other *Drosophila* species helps to reduce false-positives

A useful method to reduce false-positives, therefore helping to narrow down fragments, is to look for conservation of putative binding sites in related species. The putative Mef2 binding sites and surrounding regions were analyzed using the UCSC Genome browser, comparing with the six closest sequenced *Drosophila* species (looking as far down as *Drosophila pseudoobscura*) for conservation of sequence.

While this approach has yielded significant results when analyzing vertebrate genomes, it poses a challenge in *Drosophila melanogaster* due to small genome size of the species. Smaller genomes contain less non-coding DNA, and so generally a larger fraction of this DNA is functional; about 5% of human non-coding DNA appears to be under evolutionary constraint compared to about 50% in *D. melanogaster* (Peterson et al., 2009). This massive conservation in non-coding DNA means it is more difficult to find stretches of unconserved DNA therefore obscuring the boundaries between functional elements.

5.3.3. qPCR shows enrichment of Lmd Chromatin Immunoprecipitates in the vicinity of Mef2 sites

Lmd sites are expected to be in the vicinity of the Mef2 sites in co-regulated fragments, so when more than one conserved Mef2 site was present within a large conserved region (see previous section) a supplemental approach was used to discern between them. Quantitative real-time polymerase chain reaction (qPCR) was performed on Lmd ChIP samples using primers designed to flank either side of conserved Mef2 sites (Figure 17). As ChIP fragments are around 500 bp long, this allowed confirming Lmd binding in the vicinity of conserved Mef2 sites (Figure 16) and thereby delimited the fragments to a size that is reasonable to use for *in vitro* studies.

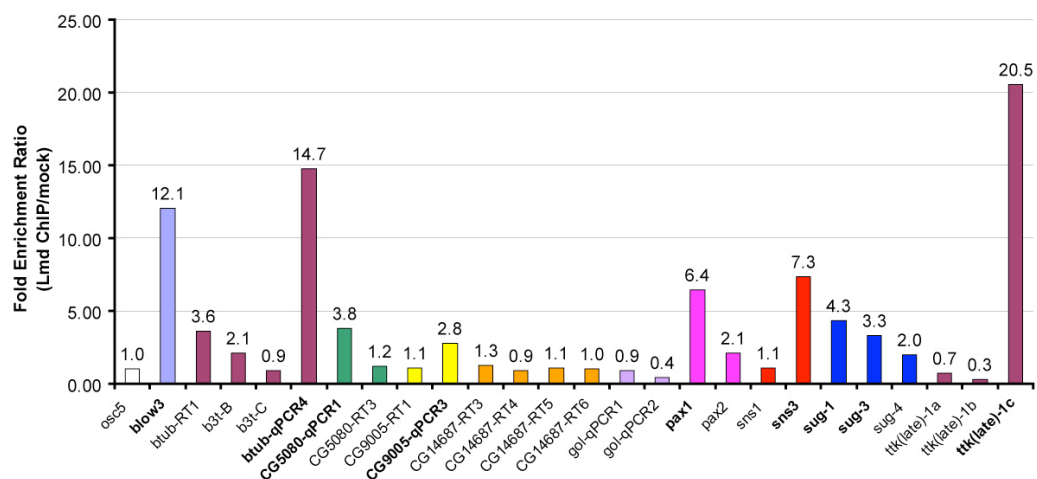


Figure 17 - Quantitative PCR results show enrichment of Lmd binding in the vicinity of different Mef2 binding sites.

Occasionally, several good quality Mef2 sites present in large bound region could not be discerned by either energy of affinity or conservation in related species. In these cases, Lmd binding on top of different Mef2 sites was assayed by qPCR, under the rationale that Lmd should bind in the proximity of the functional Mef2 site on co-regulated enhancers. Examples are shown with results for sites within the same fragment depicted in the same colour and selected Mef2 sites highlighted in bold. Occasionally, as in the case of *CG14687* and *gol*, it was not technically possible to discern between sites, and therefore the whole fragment was kept.

5.4. Characterization of novel enhancers

The newly defined enhancers were cloned in front of a minimal promoter and a GFP reporter, and transgenic lines created to analyze the expression driven by these enhancers *in vivo*. This analysis demonstrated that 9 out of 10 of novel enhancers lead to expression in the muscle. The cloned fragments for *Act57B*, *CG9416*, and *CG14687* correspond to previously characterized *Mef2* enhancers that were further refined. As a good example, the enhancer for the gene *CG5080* was reduced to half of its previously defined size. Among the novel enhancers further characterized in this study are new enhancers for the genes *tramtrack (ttk)*, *blown fuse (blow)*, *goliath (gol)* and *sugarbabe (sug)*.

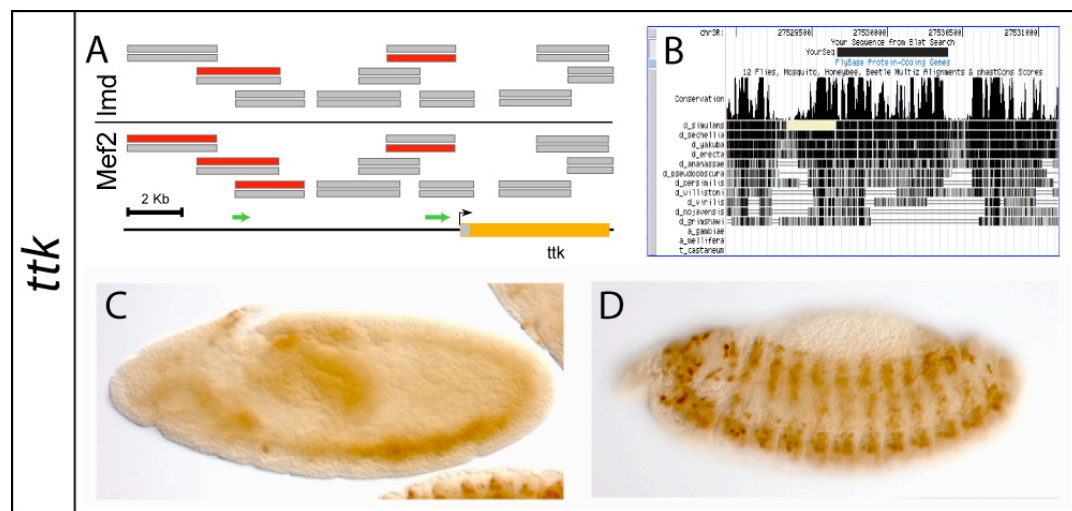


Figure 18 - Novel *tramtrack (ttk)* early and late enhancers.

(A) Lmd and Mef2 bind coherently to two different regions upstream of the *ttk* locus. There is early binding to a region 9 kb upstream of the gene, as well as late binding immediately upstream of the transcriptional start site. ChIP-on-chip fragments (about 3 Kb) are shown as stacks with the early time-point (6-8 hours) on top of the late (8-10 hours), for the Lmd (above line) and Mef2 (below line) experiments. Fragments labeled in red show binding above the threshold whereas fragments that do not meet this criterion are depicted in gray. Exons (gray) and introns (orange) are depicted at the bottom. (B) Cloned *ttk*(early) enhancer (top black box, “YourSeq”) showing conservation in various species, visualized using the UCSC browser. (C) Stage 10 embryo showing the beginning of *ttk* (early) expression. The expression continues throughout embryogenesis and can be seen in the somatic muscle at stage 13 (D). The late fragment also drove expression specifically in muscle (not shown).

ChIP-on-chip binding is detected in two regions of the *ttk* genomic locus, with the peculiarity that one region immediately upstream of *ttk* shows binding by both Lmd and Mef2 at the early (6-8 hours) time-points whereas another region

further upstream is bound only at the late (8-10) time-points (Figure 18 A). This would suggest that two different enhancers are regulated by both *lmd* and *Mef2* at different stages of development. Both enhancers were cloned and drive expression in the muscle. The *ttk* enhancer bound in the early time-points [*ttk(early)*] was used throughout this study. It was restricted to 0.7 kb according to the previously defined criteria (Section 5.3) including conservation with other *Drosophila* species (Figure 18 B). The enhancer is expressed from stage 10 (Figure 18 C) to the end of embryogenesis, and is specific to mesoderm and muscle cells (Figure 18 D).

An enhancer for the gene *blow* was also cloned, that partially overlaps a previously identified enhancer (Schroter et al., 2006) from the first intron of the gene.

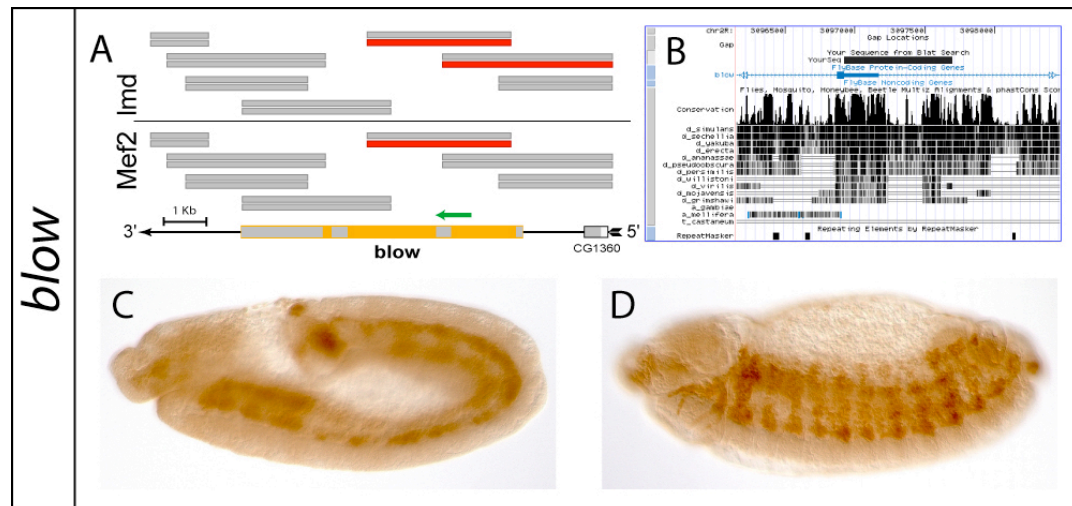


Figure 19 - *blown fuse (blow)* enhancer

(A) Lmd and Mef2 bind at the late time-point to the same fragment spanning the first and second introns of *blow*. ChIP-on-chip fragments (about 3 Kb) are shown as stacks with the early time-point (6-8 hours) on top of the late (8-10 hours), for the Lmd (above line) and Mef2 (below line) experiments. Fragments labeled in red show binding above the threshold whereas fragments that do not meet this criterion are depicted in gray. Exons (gray) and introns (orange) are depicted at the bottom. (B) The *blow* enhancer to be cloned (top black box, “YourSeq”) was selected from the first intron, based on conservation in various species visualized using the UCSC browser. (C) Stage 11 embryo showing *blow* enhancer expression in both the somatopleura and splanchnopleura. (D) Later expression in the somatic muscle at stage 13-14.

The gene *goliath (gol)* is representative of the difficulties of defining the borders of an enhancer for cloning. Both Lmd and Mef2 bind at both time points to the same fragment (Figure 20 A). However, only two Mef2 sites can be identified in the fragment. qPCR analysis does not show enrichment for Lmd at either site

(Figure 17), and the whole region is overall poorly conserved (Figure 20 B). Nevertheless, taking the full 3 Kb region as an unrefined enhancer, the reporter line shows specific expression in the muscle between stages 11 (Figure 20 C) and 14 (Figure 20 D).

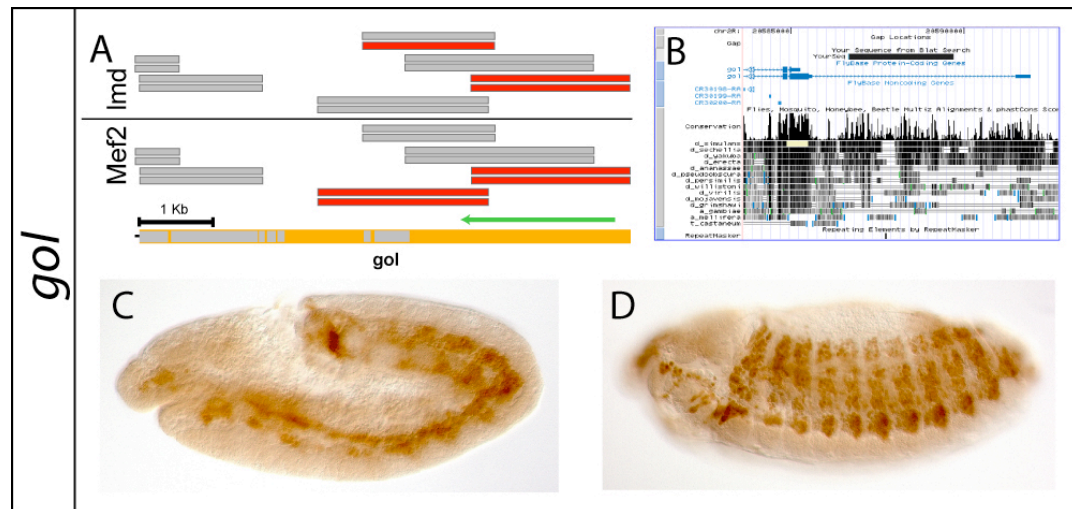


Figure 20 – Novel *goliath* (*gol*) enhancer.

(A) Lmd and Mef2 bind to the same fragment in the first intron of *gol* in both the early and late time-points. (B) In this case there was minimum conservation as can be seen using the UCSC browser, and therefore, the whole 3 Kb fragment was cloned (top black box, “YourSeq”). (C) Stage 11 embryo showing *gol* expression in both the somatopleura and splanchnopleura. (D) Later expression in the somatic muscle at stage 13-14.

A *Mef2*-responsive enhancer for *CG5080* was identified previously (Sandmann et al., 2006b). The enhancer was refined based on a positive enrichment for Lmd near the *Mef2* site on the 3', but not on the 5', section of the first intron (Figure 17, *CG5080*), which is in line with the greater conservation in the 3' region of the enhancer (Figure 21 B).

Other enhancers previously identified are shown in Figure 22. In every case, Lmd and *Mef2* bind to fragments covering the enhancer at the same time-points, with *CG14687* showing binding at different time-points (Figure 22 D) but with the corresponding fragments at both time-points excluded just below the strict thresholds.

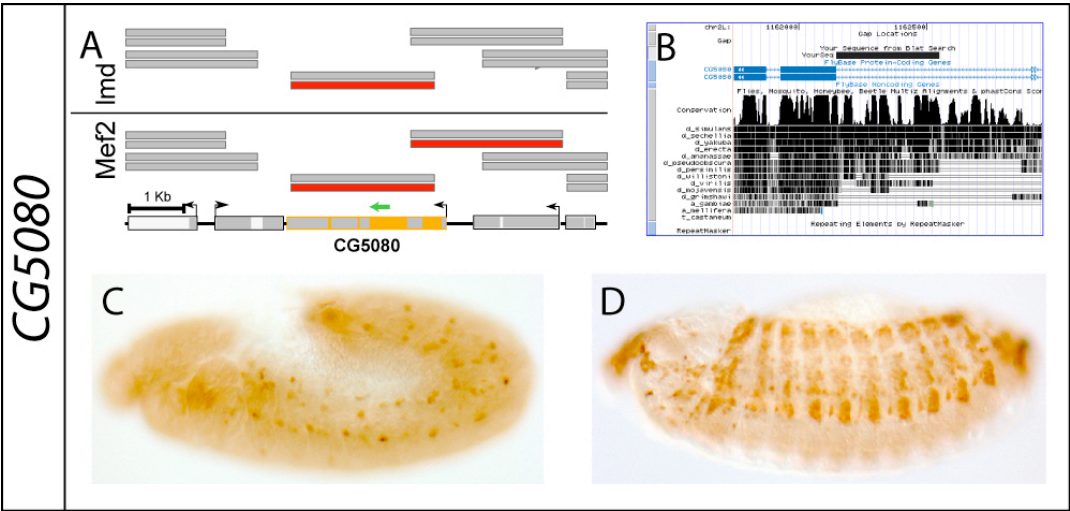


Figure 21 - Refined CG5080 enhancer.

A) Lmd and Mef2 bind to the same fragment in the first intron of *CG5080* the late time-points (B) Conservation down to *Drosophila pseudoobscura* is larger in the 3' half of the first intron, and Lmd enrichment by qPCR was also detected in that 3' fragment, but not in the 5' fragment (Figure 14) (top black box, "YourSeq"). (C) Stage 11 embryo showing *CG5080* expression at stage 11. (D) Later expression in the somatic muscle at stage 13-14.

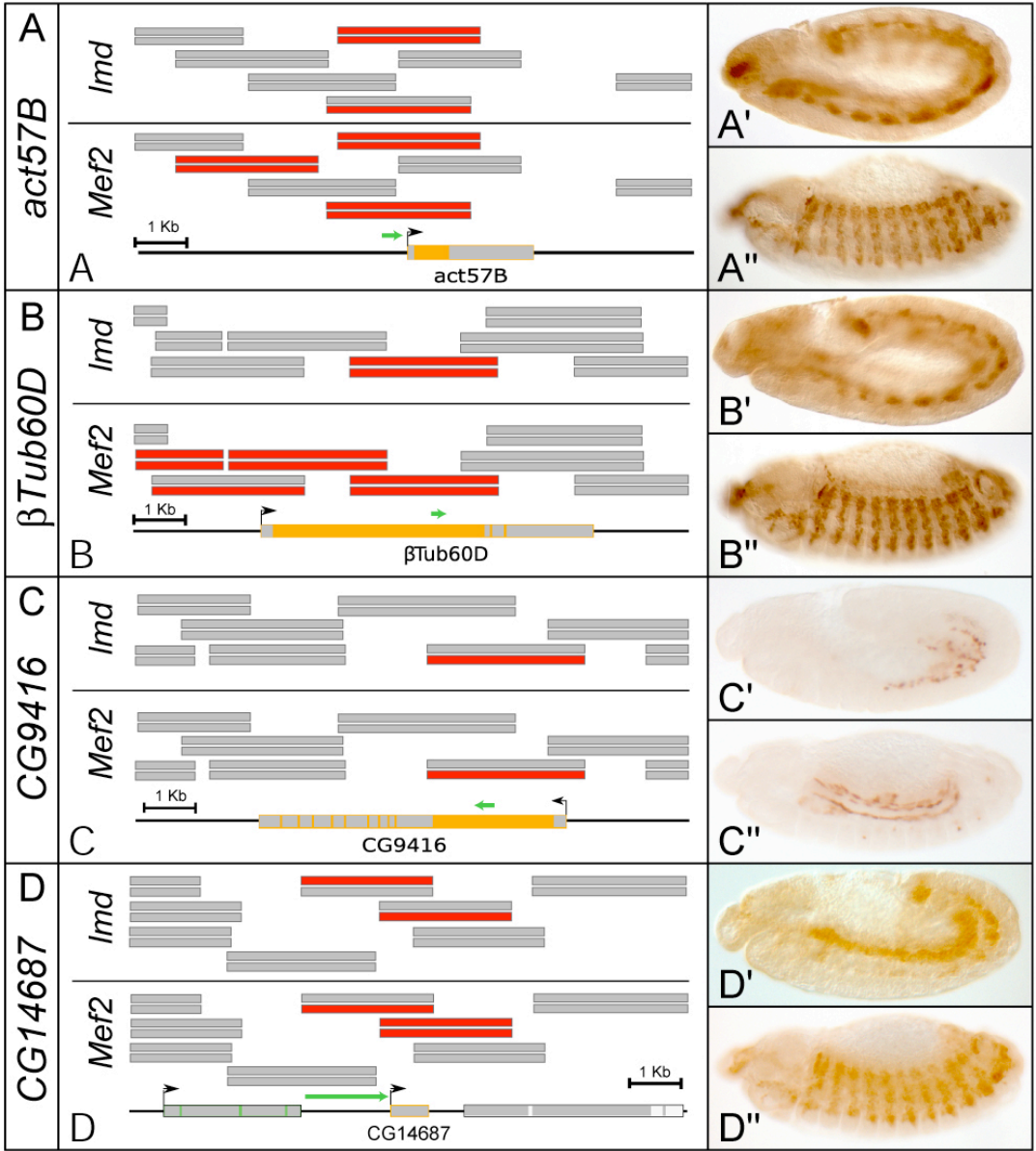


Figure 22 - Reporter lines previously characterized or refined in this study.

(A-D) ChIP-on-chip fragments (about 3 Kb) are shown as stacks with the early time-point (6-8 hours) on top of the late (8-10 hours), for the Lmd (above line) and Mef2 (below line) experiments. Fragments labeled in red show binding above the threshold whereas fragments that do not meet this criterion are depicted in gray. Exons (gray) and introns (orange) are depicted at the bottom. Green arrows illustrate the cloned enhancers. (A'-D'') GFP reporter expression driven by the DNA fragment depicted in green in panels (A-D) at two stages of development.

5.5. Loss of *lmd* and *Mef2* differentially affects reporter activity *in vivo*

The GFP reporter lines created in this study were used to assess the contribution of *lmd* and *Mef2* to the activity of these enhancers *in vivo*. Six of these lines were placed in the background of two characterized loss-of-function alleles for these transcription factors; *lmd*^l and *Mef2*^{22.21}. It would have been interesting to include a condition of loss-of-function of both transcription factors in this analysis. Unfortunately, every effort to create a *lmd-Mef2* double mutant failed, which in itself provides further evidence of the interactive nature of these two transcription factors.

The GFP expression was detected by Fluorescent *In Situ* Hybridization (FISH). Homozygous mutant embryos for *lmd* were identified by FISH for *twist*, based on the fact that *lmd* mutants maintain broad *twist* expression beyond stages 11-12, in contrast to the *wildtype* situation (Ruiz-Gomez et al., 2002). *Mef2* heterozygous mutant embryos were identified by the *lacZ* expression pattern of the *engrailed-lacZ* balancer chromosome; the absence of which being an indicator for the homozygous mutant embryos.

The expression of the *βTub60D* gene has already been intensively studied and shown to be controlled by several independent *cis*-regulatory modules (Hinz et al., 1992) (Damm et al., 1998) (Kremser et al., 1999). One of these enhancers, upstream to the *βTub60D* locus requires *Mef2* for full activation (Damm et al., 1998). In contrast, the intronic *βTub60D* enhancer used in this study shows strongly reduced expression in *lmd* mutants (Figure 23 A, B), but appears unaffected in *Mef2* mutant embryos (Figure 24 A, B). The reduction in expression of the *βTub60D* gene in *Mef2* mutant embryos detected by expression profiling (Figure 13) therefore reflects the combined activity of at least two enhancers: one strongly responsive to *Mef2* levels and a second one dependent on *Lmd* (but not *Mef2*) for activation.

Expression profiling shows a strong reduction in *Act57B* expression in both *lmd* and *Mef2* mutants (Figure 13). The *Act57B* enhancer shows a clearly reduced expression in *Mef2* mutant embryos (Figure 23 C, D), in accordance with what has

been reported previously (Kelly et al., 2002). This expression is completely abolished in *lmd* mutant embryos (Figure 24 C, D) confirming the role of *lmd* in the activation of *Act57B*.

The *CG5080* enhancer shows reduction of expression in the *Mef2* mutant background (Figure 24 E, F), but is only mildly affected by the lack of *lmd* (Figure 23 E, F). *CG5080* is also downregulated by both *lmd* and *Mef2* mutants according to the expression profiling data (Figure 13) but this particular enhancer seems to be affected more predominantly by *Mef2*.

In contrast, reporter expression in the somatic muscle driven by the *blow* enhancer is completely abolished in both *lmd* (Figure 23 G, H) and *Mef2* mutant embryos (Figure 24 G, H). Additional expression in the hindgut persists in both genetic backgrounds, pointing towards additional, tissue-specific input at this enhancer.

The *CG14687* enhancer is activated in both somatic and visceral muscle in *wildtype* embryos (Figure 23 I, J, Figure 24 I, J). Expression in somatic muscle requires *lmd* (Figure 23 J), but is unaffected in *Mef2* mutant embryos (Figure 24 J). Interestingly, expression in the visceral muscle is independent of both *lmd* and *Mef2* expression (Figure 23 J, Figure 24, J), implicating additional factors in the activation of this enhancer specifically in this tissue. Both the homeodomain transcription factor *bagpipe* (*bap*) and the fork head domain transcription factor *binou* (*bin*) are recruited to this enhancer *in vivo* (Jakobsen et al., 2007) and most likely activate gene expression in this tissue.

Finally, the expression of the *gol* enhancer is clearly dependent on *lmd* activity (Figure 23 K, L), but remains unaffected on a *Mef2* mutant embryo (Figure 24 K, L).

In summary, all six muscle enhancers examined show reduced activity in one or both mutant conditions, demonstrating that the *in vivo* occupancy of these modules by *Mef2* and *Lmd* has regulatory function. *lmd* mutants generally display a stronger reduction in enhancer activity than *Mef2* mutant embryos. As the expression of *Mef2* is dependent on *lmd*, there is a stronger reduction in enhancer activity in this genetic background, which reflects and underscores the combinatorial regulation of these enhancers by both transcription factors.

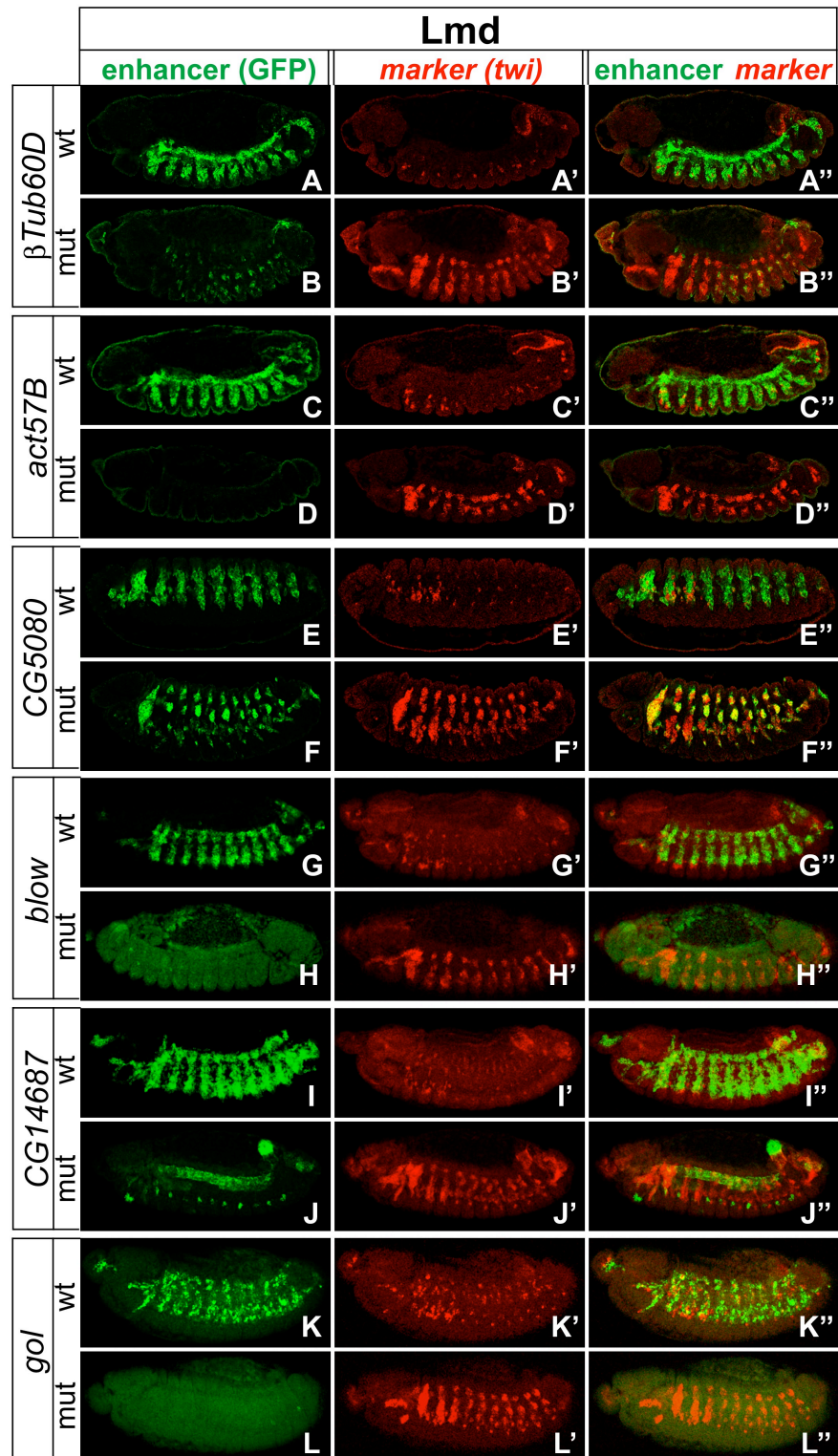


Figure 23 - *lmd* and *Mef2* are differentially required for enhancer activity *in vivo*.

In situ hybridization of GFP-reporter mRNA in a wt condition (embryos heterozygous for *lmd*¹) or mutant condition (homozygous *lmd*¹ mutant embryos). The same embryos were labeled by *in situ* hybridization for *twist* mRNA (prime) and shown with an overlay of both signals (double prime). Homozygous *lmd* embryos are recognized by the persistent broad *twist* expression after stages 11-12 (Ruiz-Gomez et al., 2002), whereas heterozygous embryos display a normal *twist* down regulation.

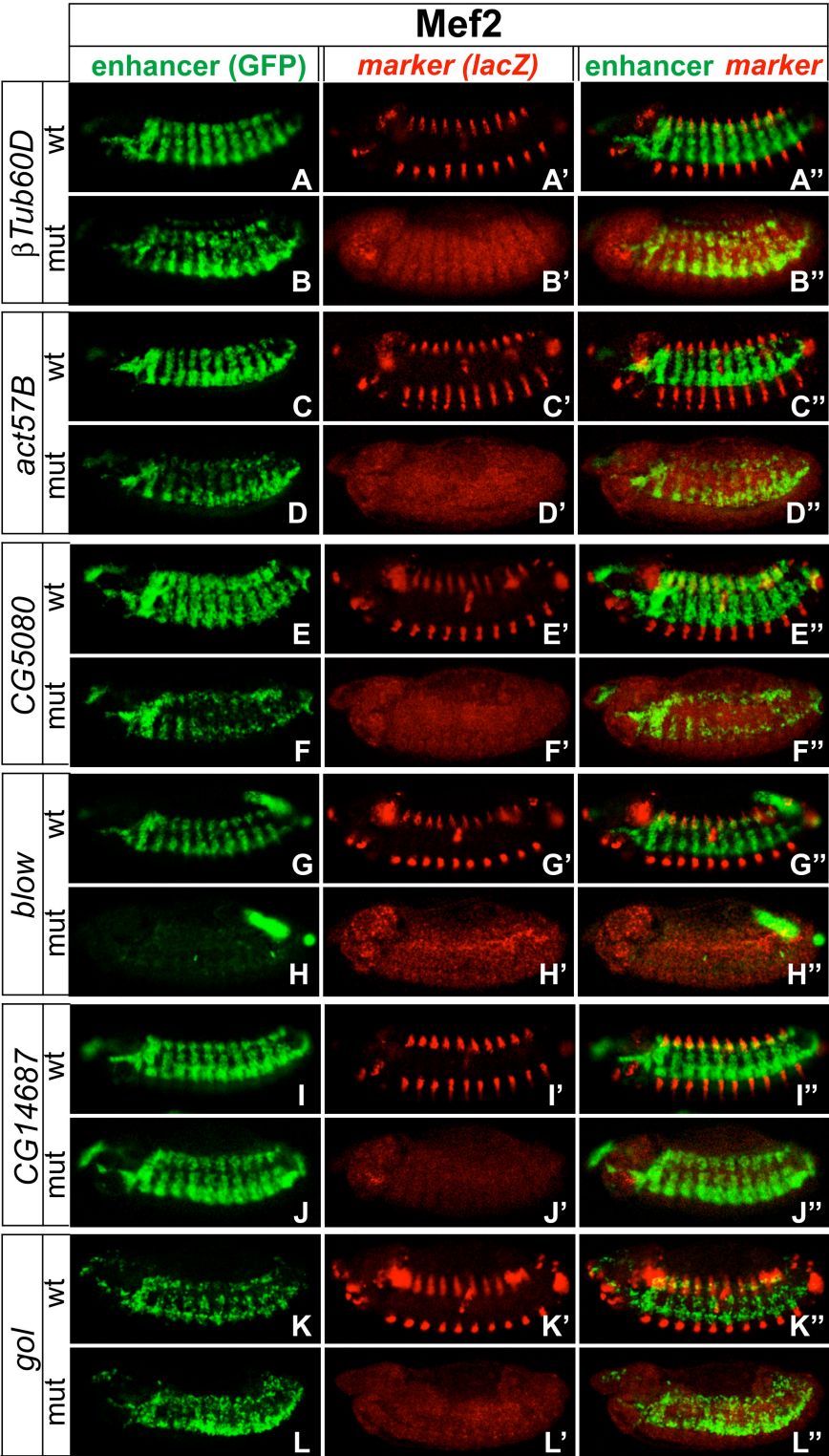


Figure 24 - *lmd* and *Mef2* are differentially required for enhancer activity *in vivo*.

In situ hybridization of GFP-reporter mRNA in a wt condition (embryos heterozygous for *Mef2*^{22,21}) or mutant condition (homozygous *Mef2*^{22,21} mutant embryos). The same embryos were labeled by *in situ* hybridization for *lacZ* (balancer chromosome) mRNA (prime) and shown with an overlay of both signals (double prime).

5.6. *lmd* co-regulates enhancers with *Mef2* in a cooperative, additive or inhibitory manner

The complex regulation of different genes by *lmd* and *Mef2* required an analysis aimed at understanding the interplay between these transcription factors regulation at the level of individual enhancers. The enhancers were analyzed *in vitro* by luciferase assays, providing a quantitative response to increments in the activity of Lmd and Mef2 on these individual enhancers.

Drosophila Schneider 2 (S2) cells were chosen, due to the extensive knowledge available on this cell line, and to the fact that they do not express any endogenous *lmd* or *Mef2* (Sims et al., 2006). Lmd and Mef2 were sub-cloned from HA-tagged versions created from full-length ESTs (LD47926 and GH24154, respectively), and placed in the pAc5.1/V5-hisB vector (Invitrogen). The enhancers were sub-cloned into an expression vector, upstream of a minimal promoter and the firefly luciferase gene. After initial tests using the pGL3 vector (Promega) revealed a signal level too close to background noise, the sv40 promoter was replaced with a hsp70 minimal promotor from pH-Stinger (Barolo et al., 2000), resulting in a satisfactory signal level. Some enhancers were still trimerized in order to obtain a more robust signal. A copia-Renilla luciferase vector was used as a transfection control, and the normalized values were calculated as the fold increase over the negative control (empty pAc5.1/V5-hisB vector) \pm Standard Error of the Mean (SEM).

5.6.1. *lmd* can act as a transcriptional repressor

One of the most intriguing questions raised by both the expression profiling and ectopic expression data was whether *lmd* could act directly as a transcriptional repressor. Evidence for this role came from the set of genes whose overall expression seemed to be enhanced in *lmd* mutants (Figure 13). *CG9416* and *CG30035* were selected as examples from this set of genes, with the former already showing additional evidence of repression by Lmd, namely repression of Mef2-driven ectopic expression (Figure 14 & Figure 15 H", H").

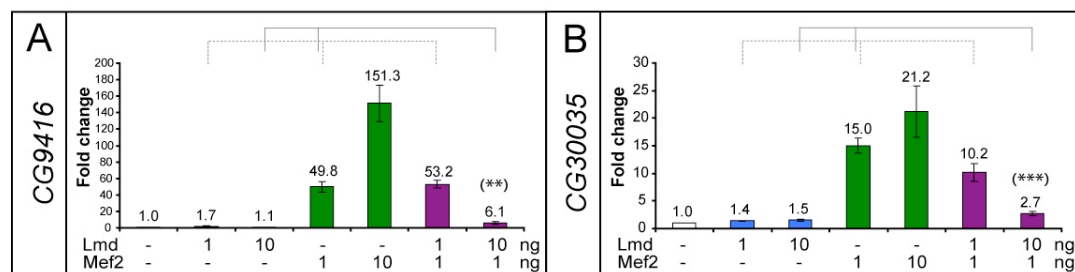


Figure 25 - Lmd can repress expression activated by Mef2 *in vitro*.

Cells were co-transfected with expression plasmids for *Renilla* luciferase (transfection control), Firefly luciferase reporter constructs for *CG9416* (A) or *CG30035* (B) and different concentrations of expression plasmids encoding Lmd or Mef2 (as shown). (A) *CG9416* expression does not change when transfecting 1 or 10 ng of Lmd (blue bars), while the enhancer responds dramatically to increasing amounts of Mef2 (green bars). There is no detectable effect when combining (purple bars) activation by 1 ng of Mef2 with 1 ng of Lmd (dotted line), but the effect is pronounced with 10 ng of Lmd (solid line): activation by Mef2 is repressed from 49.8 to 6.1 fold. (B) The *CG30035* enhancer responds in a similar fashion: repression by Lmd is visible by the suppression of Mef2-driven activation (1 ng) from 15.0 fold to 10.2 (dotted line) or 2.7 fold (solid line). Values represent fold change \pm SEM, n=3. Student's t-test (unpaired, two-tailed), (*) p<0.05, (**) p<0.01, (***) p<0.001).

The *CG9416* enhancer showed no significant change in expression when transfected with either 1 or 10 ng of Lmd alone (Figure 25 A, blue bars). The design of this system produces a diminutive plateau of expression due to the hsp70 minimal promoter, and for this reason it is very difficult to observe any reduction in this level on any condition. On the other hand, the enhancer responded steadily to increasing levels of Mef2: 49.8 fold with 1 ng and 151.3 fold in response to a 10 ng transfection of Mef2 cDNA (green bars). The strong activation of about 50 fold in response to 1 ng of Mef2 was used to access the effect of Lmd interacting with

the ability of Mef2 to activate this enhancer (purple bars). A co-transfection of 1 ng of Lmd was not enough to change this activation (dotted line), but the co-transfection of 10 ng of Lmd resulted in a pronounced decrease of Mef2 activity from 49.8 to 6.1 fold (solid bracket). This represents the first direct evidence that Lmd can directly repress Mef2-mediated activation on common enhancers.

The *CG30035* enhancer was cloned to provide a second example to study repression by *lmd*. As in the case of *CG9416*, Lmd alone was not able to significantly alter the activity of this enhancer (Figure 25 B, blue bars), while Mef2 was able to activate transcription (green bars). In this case, co-transfection of even 1 ng of Lmd (purple bars) led to a decrease in the activity of 1 ng Mef2 (dotted bracket), confirming a significant repression from 15.0 to 2.7 fold.

It is very significant that from more than a dozen enhancers tested by this assay only the two genes suspected of being repressed by Lmd actually showed this behavior. A number of other genes (*gol*, *ttk*, *CG14687*) show a slight up-regulation in *Mef2* mutant embryos according to the expression profiling data (Figure 13) and were tested correspondingly to check whether Mef2 could act as a direct repressor in a way similar to Lmd. However, Mef2 could not repress activation mediated by *lmd* under any experimental condition (data not shown).

In summary, these are the first examples of direct repression by Lmd, and the overall upregulation of a group of genes in the *Mef2* mutant background is most likely the result of indirect repression via *Mef2*.

5.6.2. *lmd* and *Mef2* can act additively to activate target genes

Most of the genes tested were ectopically expressed by either Lmd or Mef2, with a stronger activation often resulting from the combined action of both transcription factors (Figure 14 & Figure 15). The cloned enhancers were similarly shown to depend on a different level of one or both transcription factors for their *in vivo* expression (Figure 23, Figure 24). Nevertheless, the question of whether this activation is simply additive or cooperative cannot be answered by *in situ* hybridization. We therefore addressed this question *in vitro* using the quantitative nature of the luciferase assays.

The *CG14687* enhancer (Figure 26 A) could be activated to modest levels by increasing amounts of both Lmd (blue bars) and Mef2 (green bars). When

different amounts of Lmd were co-transfected with 1 ng of Mef2 (purple bars), the resulting activation was simply a sum of the activation of each transcription factor by itself. For instance, a 2.4 fold activation by 1 ng of Mef2 is supplemented by a 3.6 fold activation by 10 ng of Lmd, leading to an additive result of a 5.0 fold activation (solid bracket). A similar situation was seen for *gol* (Figure 26 C), even

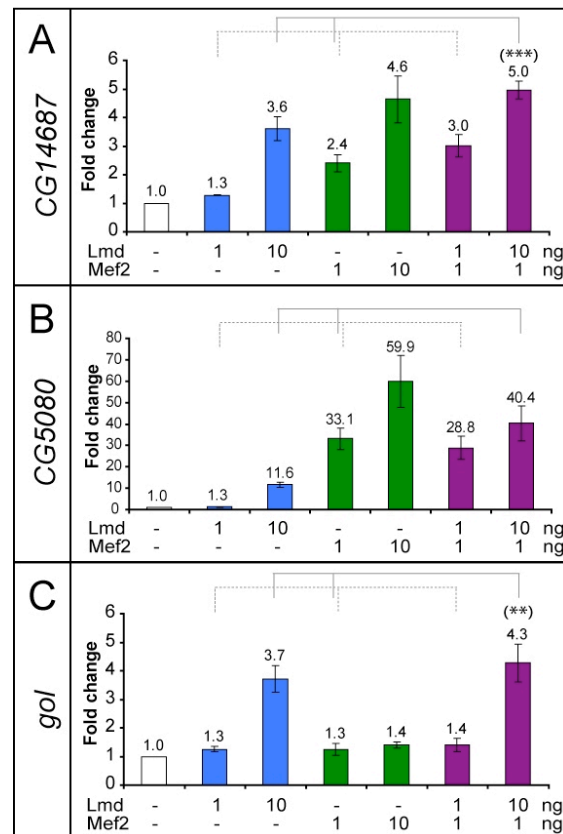


Figure 26 - Additive activation of targets *in vitro* between Lmd and Mef2.

Cells were co-transfected with expression plasmids for *Renilla* luciferase (transfection control), Firefly luciferase reporter constructs for *CG14687* (A), *CG5080* (B) or *gol* (C) and different concentrations of expression plasmids encoding Lmd or Mef2 (as shown). In all cases, there is an additive increase in the activation obtained from each transcription factor separately. Values represent fold change \pm SEM, n=4. Student's t-test (unpaired, two-tailed), (*) p<0.05, (**) p<0.01, (***) p<0.001).

though the very modest levels of activation render some of the comparisons less significant.

CG5080 (Figure 26 B) is another case of additive interaction between Lmd and Mef2. In this case, a strong activation of around 30 fold was observed in response to 1 ng of Mef2, which increased to ~40 fold when co-transfected with 10 ng of Lmd (which by itself induces a 10 fold activation of expression).

This additive behaviour suggests that Lmd and Mef2 exert their function independently from each other, possibly at remote binding sites and without physical interaction between the transcription factors.

5.6.3. Lmd and Mef2 can act cooperatively to activate target genes

When studying transcription factors with such an extensive overlap in their target genes and associated enhancers (79.7 % of the targets of *lmd* are also *Mef2* targets) and looking at the strong interaction between them observed for example on the ectopic expression of *blow* and β *Tub60D* (Figure 14 & Figure 15), one can suspect instances of a more complex cooperative interaction at some enhancers.

For example, the *ttk* enhancer (Figure 27 A) is extremely responsive to Lmd (blue bars) and modestly responsive to Mef2 (green bars). Interestingly, when co-transfecting 1 ng of Mef2 and 10 ng of Lmd (purple bars), the resulting 31.1 fold activation is clearly greater than the sum of the individual (1.7 & 8.9 fold) activations (solid line), indicating a strong cooperative interaction between Lmd and Mef2. This

cooperative effect is seen at still lower levels of transcription in the case of the *blow* enhancer (Figure 27 B). Even the low concentration of 1 ng of Lmd, insignificant on its own (blue bars) can boost the activation of 1 ng of Mef2 (green bar) from 2.8 fold to 8.4 fold when co-transfected (dotted bracket). This effect is

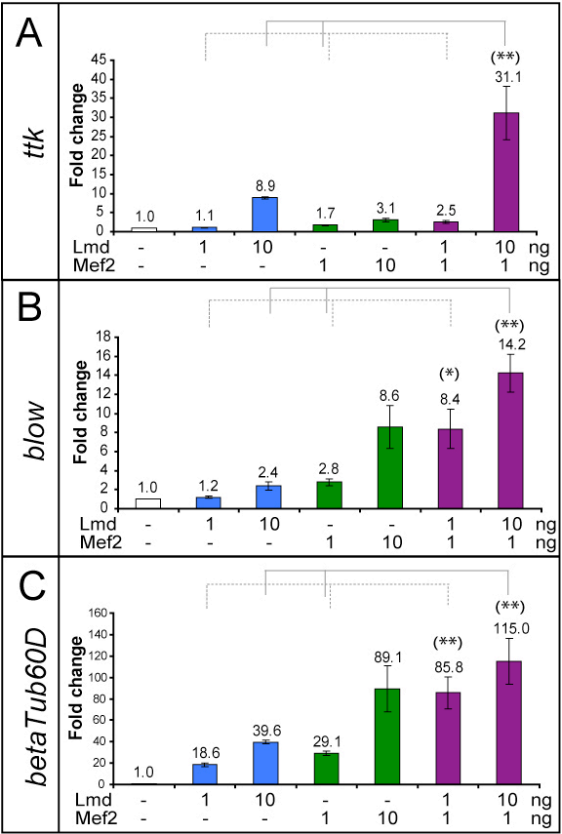


Figure 27 - Cooperative response.

Cells were co-transfected with expression plasmids for *Renilla* luciferase (transfection control), Firefly luciferase reporter constructs for *ttk* (A), *blow* (B) or β *Tub60D* (C) and different concentrations of expression plasmids encoding Lmd or Mef2 (as shown). In all cases, the enhancer activation by the addition of both Lmd (blue bars) and Mef2 (green bars) together is greater than the combined sum of affects of both transcription factors added separately (purple bars, dotted and full lines), indicating a cooperative effect between Lmd and Mef2. Values represent fold change \pm SEM, n=4 Student's t-test (unpaired, two-tailed), (*) p<0.05, (**) p<0.01, (***) p<0.001).

re-confirmed with 10 ng of Lmd (going from ~2.5 fold with each transcription factor separately to 14.2 fold when both are combined, solid bracket). The same robust effect can be seen with the *βTub60D* enhancer (Figure 27 C).

Overall, *lmd* and *Mef2* activate common enhancers either additively or cooperatively. This behaviour is expected to be dependent on the particular enhancer architecture. Unfortunately, the absence of a Lmd consensus binding site makes it difficult to test this hypothesis. Interestingly, *lmd* is also capable of acting as a repressor of *Mef2* mediated activation.

6. Discussion

The development of multicellular organisms involves the harmonious development of different tissues. Diverse tissues are made from specific cell types that reflect the coordinated activation and repression of particular genes. Traditional genetic studies have revealed key regulators of many processes, including transcription factors involved in myogenesis, such as *Mef2* and *lmd*. It is clear that unveiling the catalog of genes regulated by essential transcription factors is key to understand development, but there is a further layer of complexity. To achieve a molecular understanding of the regulatory networks controlling cellular decision-making, it is essential to understand how inputs from different regulators are being integrated at the level of shared enhancers. It is this interaction of TFs that ultimately gives rise to the defined patterns of gene expression that shape development.

6.1. A systematic genomic approach identifies direct target genes of *lmd*

This study has used a genomic approach to systematically identify the direct target genes of *lmd*, an important myogenic regulator, of which only one direct target was previously known. As expected, the list of newly identified direct targets includes genes involved in myoblast fusion, such as *sns* and *blow*, and also structural genes such as *Act57B*, *Act87E* or *β Tub60D*, suggesting a more prominent role of *lmd* in differentiation than was previously thought. Even more interestingly, comparing this list with the one previously generated for *Mef2* shows that *lmd* regulates the majority of its targets in conjunction with *Mef2*. While in a few instances (e.g. *ladybird-early*, *PAK-kinase* or *short stop*, data not shown) the two transcription factors target the same locus through different enhancers, the majority of targets were regulated via common enhancers. Moreover, analyzing the two different time points used for the ChIP-on-chip experiments shows a frequent

correlation in the timing of transcription factor binding. The *tramtrack* locus, for instance, contains both an exclusively early-bound and an exclusively late-bound enhancer. The early enhancer, used extensively for this study, is bound by both factors at stages 10-11 (6-8 h) but not later (Figure 18 A), whereas a second enhancer is bound at stages 12-13 (8-10 h) but not earlier. Additionally, the *blow* (Figure 19 A) and *CG5080* (Figure 21 A) enhancers are co-bound at stages 12-13 (8-10 h) but not earlier.

6.2. The integration of diverse techniques provides information from different perspectives

Using a diverse range of methods to approach the same problem from different perspectives is one of the hallmarks of scientific endeavor. The rationale is that any particular technique is prone to some degree of error and artifacts, and one can be better assured of the validity of an observation by combining data taken from different viewpoints. However, different techniques do read out different aspects of the problem under study and some degree of interpreting is required to assemble the whole picture.

This study was initiated with ChIP-on-chip, providing a genome-wide overview of the occupancy of two TFs that bind to common genomic regions. While this technique highlights sites bound *in vivo*, it provides no indication of the identity of the targeted gene or on the change in its transcriptional state as a result of the transcription factor's occupancy. The binding data had to be integrated with expression profiling in mutant backgrounds of the same TFs, to obtain a stringent list of direct targets and respective transcriptional effects. Analysis of the behavior of the direct target genes led to the identification of distinct modes of regulation by the TFs, and at this point, examples representing these modes of behavior were selected for further study. The TFs were tested for their ability to ectopically express their target genes in the ectoderm. A positive result in this experiment shows that a factor is sufficient to activate gene expression, yet a negative result is more difficult to interpret, taking into account the possibility of differences in chromatin structure or the absence of required co-factors in the ectopic location,

and even the general artifacts resulting from associations of proteins not normally expressed together. Considering the additional complexity of having different independent enhancers with different modes of regulation in the same locus (e.g. *βTub60D*, *ttk*), the study moved to the characterization of individual responsive enhancers. These enhancers were assessed both *in vivo*, comparing the expression of transgenic reporters in a wildtype and mutant background, and *in vitro* with the expression of reporters driven by the TFs in cell culture. Overall, it is expected that some discrepancies might arise from the use of such diverse techniques, but some results that do not appear immediately obvious are in many cases extremely indicative.

6.3. Combinatorial binding on shared enhancers leads to additive, cooperative or repressive effects

Act57B is ectopically expressed in the ectoderm by *Mef2* (Figure 14 Figure 15 B"), but not by *lmd* alone (Figure 14 Figure 15 B'). On the other hand, reporter expression is only slightly reduced in *Mef2* mutants (Figure 24 D), while being completely lost in *lmd* mutants (Figure 23 D), which also have significant lower levels of *Mef2*. A recent study showed that the initiation of *Act57B* expression at stage 11 requires *Mef2*. However, this expression could not be prematurely initiated by artificially increasing the levels of *Mef2* at this early stage (Elgar et al., 2008). These results can be better understood taking into account that the combined action of *Lmd* and *Mef2* is required for expression at this stage. Therefore, the presence of *Mef2* alone is not sufficient to activate transcription, while being capable of maintaining the expression of *Act57B* at later stages.

A good example of an additive interaction between *lmd* and *Mef2* is the gene *CG5080*. The expression of this gene is downregulated in both mutants (Figure 13, Cluster I), but the individual contribution of each TF to the activation is difficult to discern. The fact that none of the TFs is sufficient to ectopically express the gene (Figure 14 & Figure 15, C', C'), while their combined action is (Figure 14 & Figure 15, C""), indicates that neither factor is predominant over the other in activating the gene. The fact that there is a single regulatory region in the locus

where the two factors co-bind (Figure 21 A) means that there is probably only one enhancer where the factors can interact, and simplifies the integration of information from this enhancer to the basal promoter of the gene. Indeed, the transgenic reporter line is similarly affected, but not abrogated, in both mutant backgrounds (Figure 23 F and Figure 24 F), and the quantitative *in vitro* data shows a simple additive effect in the activation of the enhancer by *lmd* and *Mef2*. In conclusion, *lmd* and *Mef2* bind to the same enhancer and activate *CG5080* in a non-cooperative way. Their individual contributions, which separately are not sufficient to ectopically express the gene, is uncovered in the respective mutant backgrounds as a decrease in the expression of the reporter.

The *blow* enhancer, on the other hand, is a good example of cooperative activation by *lmd* and *Mef2*. Expression profiling shows a mild reduction of expression in *Mef2* mutants in the late time points (Figure 13) that is markedly more substantial in *lmd* mutants (in which *Mef2* levels are also compromised). It is also clear that neither Lmd (Figure 14 & Figure 15 C') nor Mef2 (Figure 14 & Figure 15 C'') are sufficient to ectopically express *blow* in the ectoderm, unless their activity is combined (Figure 14 & Figure 15 C'''). The enhancer requires both Lmd (Figure 23 H) and Mef2 (Figure 24 H) for expression, and is activated co-operatively by the two factors *in vitro* (Figure 27 B). Altogether, this cooperative activation of *blow* can be seen as a classic “AND gate” condition, where absence of, or low input from, either TF compromises activation. Only when there is robust input and co-operation from both TFs is the full activation achieved.

6.4. *lmd* as a transcriptional repressor

The ability of *lmd* to directly repress genes activated by *Mef2* is one of the most intriguing aspects of the co-regulation between the two transcription factors. A substantial portion of co-regulated genes is dependent on *Mef2* for overall activation, but seems to be repressed by *lmd* (Figure 13, Cluster II). *CG9416*, one of the genes previously identified as a *Mef2* target (Sandmann et al., 2006b) was immediately selected to further investigate this behavior, and has indeed confirmed, by every method used, the repressive potential of *lmd*. First, whilst

Mef2 is capable of driving ectopic expression of *CG9416* in the ectoderm, co-expression of *lmd* leads to a reduction in these expression levels (Figure 14 & Figure 15 C-C"). Directly analyzing the enhancer confirms the repression and provides a quantitative readout of this effect. Simultaneous transfection of *lmd* represses the *CG9416* enhancer, reversing the activation by *Mef2* to almost basal levels in a concentration dependent manner (Figure 25 A). To confirm this effect, the group of genes with the same overall expression change was re-visited, and a second example, *CG30035*, was selected for analysis. The size of the enhancer was refined and prompt *in vitro* analysis revealed a quantitative behavior mirroring that observed for *CG9416*: *Lmd* again inhibits activation by *Mef2* in a concentration dependent manner (Figure 25 B). A second independent example of this restricted behavior confirms the ability of *lmd* to act as a transcriptional repressor, and opens up multiple questions regarding the mechanism of this behavior.

Lmd is a member of the Gli superfamily of transcription factors (Section 2.6.3), known to act both as activators and repressors of transcription: the full protein activates transcription but can be proteolytically cleaved into a repressor form. While it is immediately tempting to envision such a mechanism of action for *Lmd* as well, there are some issues to consider beforehand. First, it should be noted that *Lmd* is quite a distant member of this family, and that *Ci* is the true *Drosophila* ortholog of the vertebrate Gli proteins. The homology observed between *Lmd* and other Gli superfamily members does not extend beyond the Zn-finger domain, and in particular fingers 3-5 (Duan et al., 2001). Importantly, the remainder of the protein contains a number of regulated motifs that affect *Lmd*'s subcellular localization and function, features that could be relevant in distinguishing *Lmd* from other Gli superfamily members. To complicate things further, it has not been possible to detect a cleaved form of *Lmd* to date (Duan and Nguyen, 2006).

This study demonstrates that *Lmd* can act as both an activator and a repressor in the same tissues at the same stage of development. Gli superfamily members, in contrast, respond to external signaling (Hedgehog) by switching from repression to activation in the whole cell. This switch mechanism, and for the same

reason any of the general modifications in protein function described for Lmd (Duan and Nguyen, 2006) are difficult to reconcile with the dual function of Lmd at different *loci* within the same cells and tissues, as is any mechanism of binding to Mef2 and sequestering the protein in the cytoplasm.

There are other examples of a transcription factor with the dual function of activation and repression, acting in a sequence-dependent manner in the same cells. One example is *lozenge (lz)*, a member of the Runx family of transcriptional regulators (Canon and Banerjee, 2003). Lz is an activator that can also repress expression by binding regulatory sequences and recruiting the general repressor Groucho. However, unlike Harry-family proteins that bind Groucho in a stable manner through the conserved tetrapeptide motif WRPW (Jimenez et al., 1997), the interaction between Lz and Groucho is mediated through the Runx-family motif WRPY (Canon and Banerjee, 2003). This later interaction is unstable, and requires the binding of the extra adaptor Cut to stabilize repression. Cut binds to DNA sequences adjacent to the Lz binding sites, and directly binds Groucho and Lz, stabilizing the complex. In this system, *lz* acts as an activator that can also directly repress expression on enhancers that are co-bound by a cofactor (Cut), by recruiting a general repressor (Groucho) (Canon and Banerjee, 2003). It should be noted, that this interesting model could only be elucidated by analyzing the genomic sequences in the vicinity of consensus Runx binding sites.

In the case of Lmd however, and given the fact that no consensus Lmd binding site has been identified, a more general hypothesis must be considered. Lmd could exert a dominant inhibitory influence over a transcriptional activator, either by locally quenching the activity of Mef2 or through direct repression of the locus, similar to transcriptional repressors described in other developmental networks (Gray et al., 1995), (Gray and Levine, 1996). In any case, the identification of a consensus Lmd binding site would allow to further distinguish between the different possibilities by allowing the analysis of the surrounding sequence, and the relative distance and position to the Mef2 site.

7. Conclusions

In summary, this study has revealed a large number of novel direct targets of *lmd*, a vast majority of which are co-regulated by *Mef2*. One of the very first observations regarding the activity of *lmd* was that it was an activator of *Mef2*. However, the severe *lmd* muscle phenotype is not due merely to the lack of *Mef2*, as reintroducing *Mef2* in a *lmd* background is not sufficient to rescue muscle differentiation (Ruiz-Gomez et al., 2002). The data provided in this study provides a molecular understanding for why this is the case: *lmd* modulates the activity of *Mef2* in a context-dependent fashion, allowing for additive, cooperative or repressive interactions in the same cells. Thereby both factors must act concomitantly on common enhancers to regulate the developmental program in muscle at these stages of development. The mechanism of how their input is integrated to finally give rise to either additive or cooperative activation, or even antagonistic behavior, remains to be elucidated.

8. Appendix

8.1. Non-Overlapping regions bound by Lmd

Table III - Non-overlapping regions obtained by merging all significantly enriched sequences.

Genome coordinates refer to *Drosophila melanogaster* genome ver. 5

Merged enriched sequence ID(s)	Chrom.	Start	End	Total length
D880_3_h7	X	13476129	13479662	3533
D906_1_c1/D906_1_d1/D906_1_e8	X	15164266	15169328	5062
D1191_4_f11	X	15692317	15695702	3385
D893_5_g2	X	16166237	16169372	3135
D904_3_d7/D904_2_a11	X	19323264	19328069	4805
D905_4_d2/D905_2_g8	X	19509152	19515045	5893
D843_2_e8/D275_1_g8/D843_2_b4	2L	592328	597682	5354
D845_1_g4	2L	1160403	1163603	3200
D847_2_c5	2L	2169778	2172949	3171
D847_1_g12/D847_1_h11/D847_1_g4/D847_1_g8	2L	2207469	2214721	7252
D1012_2_h1	2L	2750582	2753348	2766
D1012_2_h3	2L	2830271	2833602	3331
D1093_4_g9	2L	3409648	3412719	3071
D263_1_b6	2L	3802652	3805184	2532
D1088_5_f2/D1088_4_f1	2L	4994370	4999527	5157
D118_3_h5/D118_3_d7/D118_3_f8	2L	5976548	5983317	6769
D195_5_h9	2L	6868357	6871835	3478
D605_6_h3	2L	8104070	8106816	2746
D1018_1_g1	2L	8947934	8951093	3159
D1019_4_e5	2L	9160647	9163256	2609
D336_1_h12/D336_1_h7	2L	9173444	9178048	4604
D1019_4_b1	2L	9194603	9198375	3772
D574_1_e5	2L	9565732	9568940	3208
D571_4_f10	2L	9781599	9785424	3825
D1020_5_e1	2L	9918493	9922181	3688
D569_2_g9/D569_6_e10	2L	10964012	10970684	6672
D307_1_a9/D307_3_a1	2L	11224674	11230482	5808
D330_4_e3/D330_4_f9	2L	11804678	11808736	4058
D1137_1_a10	2L	12083640	12086257	2617
D865_1_b10/D865_1_f1	2L	12482373	12485903	3530
D539_1_f7	2L	18078231	18081716	3485
D327_5_f8/D327_2_e2	2L	18137047	18142291	5244
D543_1_h9	2L	18439322	18442346	3024
D1035_1_c8	2L	19057828	19061395	3567
D421_5_c1	2L	19130459	19133927	3468

Merged enriched sequence ID(s)	Chrom.	Start	End	Total length
D421_4_d1/D421_2_f12	2L	19152627	19156593	3966
D534_2_h2	2L	19419631	19423076	3445
D537_3_c3/D537_4_a6	2L	20461320	20467620	6300
D537_3_e1	2L	20472546	20475451	2905
D529_2_e9	2L	20806912	20809941	3029
D532_6_a11	2L	21815979	21819371	3392
D532_9_b3	2L	21884985	21887676	2691
D533_2_d4/D1171_1_e9/D533_4_h9	2L	22006608	22015305	8697
D1043_1_c5	2R	1591809	1594556	2747
D1043_1_c4	2R	1629542	1632607	3065
D916_1_f3	2R	1663764	1666633	2869
D916_1_a8	2R	1742648	1745613	2965
D1144_1_d7	2R	2084464	2087669	3205
D620_2_f3/D620_2_f12	2R	2110150	2114114	3964
D921_2_g11	2R	3095224	3098606	3382
D578_7_d12	2R	3685720	3689195	3475
D580_4_f8/D580_7_h8	2R	4157328	4162837	5509
D581_6_d6	2R	4306593	4310326	3733
D582_1_f1	2R	4374401	4377431	3030
D582_1_h8	2R	4424062	4426759	2697
D585_6_e2	2R	4914169	4916610	2441
D443_3_e5/D443_3_e12	2R	5057907	5061560	3653
D600_2_e4/D599_4_h8	2R	5440854	5445049	4195
D601_1_f1	2R	5611885	5614537	2652
D627_1_b10	2R	5932678	5935578	2900
D1049_1_g2	2R	6050432	6053440	3008
D1049_2_g4	2R	6129963	6133493	3530
D628_2_c12	2R	6153065	6156237	3172
D1050_1_c5	2R	6322303	6326142	3839
D590_8_a7/D1156_2_f7/D590_4_d7	2R	7119133	7124324	5191
D590_8_g4	2R	7145035	7147706	2671
D590_5_a10	2R	7151675	7154633	2958
D1156_2_e7	2R	7180865	7183742	2877
D595_6_a8	2R	7967900	7970685	2785
D595_8_e1/D595_6_h7	2R	8101694	8106719	5025
D412_2_c7	2R	8275771	8278491	2720
D587_1_h10	2R	8440520	8444253	3733
D587_1_e8	2R	8531476	8534265	2789
D413_3_a11	2R	8738267	8741827	3560
D474_9_b8	2R	8962362	8966136	3774
D598_2_h3	2R	9078814	9082044	3230
D598_2_e8	2R	9099446	9102059	2613
D598_2_d6	2R	9169498	9172117	2619
D448_1_e11	2R	9366097	9369853	3756
D615_1_e2	2R	9389527	9392879	3352
D616_1_g12	2R	9556940	9560149	3209
D1052_8_g3	2R	10476910	10480184	3274
D933_1_g7	2R	11779450	11782030	2580
D933_1_c3	2R	11819843	11822615	2772
D435_15_b11	2R	12778247	12781477	3230
D665_1_a7/D665_1_h10	2R	13229524	13233678	4154
D937_5_b12	2R	13869627	13872893	3266

Merged enriched sequence ID(s)	Chrom.	Start	End	Total length
D939_1_a4	2R	14786294	14789208	2914
D940_1_e12	2R	14885388	14888474	3086
D178_3_a2	2R	15144361	15147969	3608
D179_3_f12/D943_1_d9	2R	15617913	15622538	4625
D943_1_a3	2R	15625121	15627887	2766
D1055_2_d6/D651_2_b4	2R	16450050	16453029	2979
D651_2_f7	2R	16503763	16506941	3178
D946_1_d5	2R	16707679	16710441	2762
D186_3_f2	2R	17010236	17013344	3108
D436_13_h7	2R	17890438	17894406	3968
D950_1_d11	2R	18017428	18020445	3017
D950_1_a3	2R	18076379	18079830	3451
D953_2_c2	2R	18398794	18401401	2607
D635_2_c2	2R	19173661	19176660	2999
D956_1_a5	2R	19815670	19818422	2752
D432_4_d12/D432_3_c5	2R	20320270	20323642	3372
D431_1_c3	2R	20449921	20452927	3006
D642_1_h2	2R	20586696	20589629	2933
CG17181-2-PCR/CG17181-1-PCR	3L	572793	576793	4000
D1081_6_g4	3R	143200	146222	3022
D965_3_e1	3R	183867	187506	3639
D653_1_b5	3R	256888	259616	2728
D653_2_b11/D653_1_c9	3R	277161	281688	4527
D670_7_e7	3R	1089484	1091992	2508
D672_1_h11	3R	1496776	1499733	2957
D1184_3_h4	3R	2173688	2177210	3522
D967_4_a7	3R	4879804	4883201	3397
D834_5_e2	3R	5356583	5360429	3846
D711_1_e12	3R	6421273	6424345	3072
D972_2_c9/D973_1_b10	3R	6616897	6621015	4118
D972_2_e12/D972_1_e3	3R	6650983	6655300	4317
D679_1_d12	3R	7177783	7180510	2727
D696_2_a11	3R	7677016	7679506	2490
D709_3_a8	3R	7711419	7714844	3425
D696_1_c10	3R	7744998	7747298	2300
D696_2_f2	3R	7783916	7786716	2800
D976_5_g10	3R	8104679	8107804	3125
D979_1_g5/D979_2_b8	3R	9252216	9255920	3704
D688_5_b4	3R	9637723	9640933	3210
D689_1_f8	3R	9808951	9811856	2905
D1195_1_e6	3R	10239057	10241865	2808
D705_2_e2/D705_1_d4	3R	11110216	11115624	5408
D700_2_c12	3R	11731656	11735569	3913
D700_1_b11	3R	11862544	11864667	2123
D987_2_f7	3R	14517987	14520669	2682
D728_2_h9	3R	14674329	14676644	2315
D732_1_b8	3R	15659891	15662868	2977
D992_2_a9	3R	16079123	16082431	3308
D743_2_h9	3R	17113053	17115780	2727
D1189_1_g6/D1189_1_f4/D1189_1_c3	3R	17258156	17262118	3962
D747_1_a6	3R	17430823	17433563	2740

Merged enriched sequence ID(s)	Chrom.	Start	End	Total length
D751_4_f11	3R	18192657	18195579	2922
D757_1_a2	3R	18861125	18863639	2514
D757_1_b10	3R	18867662	18870482	2820
D767_1_d11	3R	21008759	21011340	2581
D773_1_f7	3R	21787297	21790669	3372
D1061_1_g9	3R	21821255	21824309	3054
D1061_2_c12/D1061_2_d9	3R	21833392	21839172	5780
D1061_2_d12	3R	21850899	21854331	3432
D794_1_d8	3R	25106535	25109594	3059
D798_1_h7	3R	25719613	25722367	2754
D802_1_b3	3R	26356268	26358853	2585
D803_2_e10	3R	26620544	26624503	3959
D810_1_d7	3R	27514649	27516778	2129
D810_2_g9	3R	27528694	27532134	3440
D810_1_d6	3R	27536479	27539356	2877
D1186_3_b8	4	526918	530249	3331

8.2. Expression profiling of lmd

Table IV - Expression profiling of lmd.

Differentially expressed genes with fold change > 1.6 (corresponds to $\log_2 = 0.68$) and $FDR < 1\%$ at one or more time-points). Median values of four independent repeats (\log_2).

FBgn	Symbol	5-6 h	6-7 h	7-8 h	8-9 h	9-10 h	10-11 h
FBgn0020766	Aats-phe	-0.46	-0.50	-0.20	-0.76	-1.39	-1.25
FBgn0014454	Acp1	-0.94	-1.25	-0.55	-0.60	-0.30	-0.17
FBgn0000044	Act57B	-0.88	-0.60	-0.74	-0.96	-1.04	-0.22
FBgn0000046	Act87E	-0.20	-0.15	-0.02	-0.77	-0.77	-0.17
FBgn0000667	Actn	0.13	0.33	0.17	0.15	0.12	0.78
FBgn0036752	Adgf-A	0.35	0.85	0.16	0.04	-0.06	-0.59
FBgn0000055	Adh	-0.52	-0.26	-0.19	0.41	0.98	1.29
FBgn0046812	AGO2	0.41	0.85	0.90	0.35	0.26	0.57
FBgn0000064	Ald	-0.02	0.65	0.59	1.02	0.68	1.13
FBgn0015569	alpha-Est10	1.13	0.50	0.37	0.76	0.69	1.89
FBgn0003885	alphaTub84D	-0.32	-0.12	0.34	-0.34	-0.76	-0.48
FBgn0003886	alphaTub85E	-0.45	-0.42	0.28	-0.20	-0.76	-0.29
FBgn0000075	amd	-0.53	-0.08	0.06	-0.15	0.18	0.70
FBgn0033366	Ance-4	0.14	0.45	0.38	0.76	0.54	0.83
FBgn0035076	Ance-5	0.06	0.00	-0.06	0.18	0.29	0.81
FBgn0026150	ApepP	-0.76	-1.42	-0.50	-0.28	-0.28	-0.15
FBgn0000116	Argk	-0.69	0.15	-0.26	-1.61	-1.75	-2.56
FBgn0038369	Arpc3A	-0.21	0.11	-0.12	-0.36	-0.70	-0.43
FBgn0000120	Arr1	-0.47	0.59	2.25	0.12	-0.35	1.11
FBgn0000140	asp	-0.41	-0.73	-0.63	-0.59	-0.69	-0.33
FBgn0000147	aur	0.24	-0.18	-0.56	-0.68	-0.87	-0.79
FBgn0004587	B52	-0.82	-0.99	0.44	-0.70	-1.01	-0.32
FBgn0025463	Bap60	-0.58	0.02	0.52	-0.29	-0.76	-0.37
FBgn0014127	barr	0.10	-0.15	-0.27	-0.49	-0.68	-0.48
FBgn0000165	Bc	-0.13	0.73	0.39	0.87	0.82	0.64

FBgn	Symbol	5-6 h	6-7 h	7-8 h	8-9 h	9-10 h	10-11 h
FBgn0063765	BcDNA:AT03385	0.37	0.82	0.61	1.21	0.82	0.67
FBgn0063292	BcDNA:AT28829	-0.57	-0.59	-0.60	-1.09	-0.36	-1.20
FBgn0063249	BcDNA:GH14618	-0.84	-1.29	-1.47	-1.54	-1.26	-1.93
FBgn0047290	BcDNA:GM02002	-0.06	-0.43	-1.00	-0.82	-0.56	-0.69
FBgn0063019	BcDNA:RE43210	-0.17	-0.31	-0.74	-0.55	-0.38	-0.41
FBgn0047095	BcDNA:RE54004	-0.20	-0.39	-0.56	-0.39	-0.24	-0.72
FBgn0063664	BcDNA:RH07382	-0.65	-0.35	-0.56	-0.65	-0.81	-1.06
FBgn0063660	BcDNA:RH25742	-0.81	-0.41	-0.61	-0.72	-0.84	-1.13
FBgn0063653	BcDNA:RH61266	0.93	0.90	0.83	0.20	1.15	0.13
FBgn0045760	BcDNA:SD02026	-1.81	-1.73	-1.45	-1.36	-0.88	-1.35
FBgn0046991	BcDNA:SD03311	2.03	1.49	1.24	1.34	1.08	1.20
FBgn0061365	BcDNA:SD08734	1.24	1.18	1.08	0.91	0.77	0.58
FBgn0008635	betaCop	0.09	0.52	0.70	-0.06	-0.20	0.10
FBgn0010395	betaInt-nu	-0.18	-0.19	-0.53	-0.54	-0.46	-1.20
FBgn0003888	betaTub60D	-0.39	0.22	-0.16	-0.55	-0.40	-1.33
FBgn0003890	betaTub97EF	0.14	0.04	0.21	-0.19	-0.74	-0.33
FBgn0027348	bgm	0.10	0.63	0.92	0.90	0.68	0.37
FBgn0002638	Bj1	-0.07	0.09	0.41	-0.35	-0.91	-0.78
FBgn0000216	Brd	0.03	-0.48	-0.91	-1.48	-1.63	-1.34
FBgn0025458	Bub1	-0.08	-0.28	-0.27	-0.44	-0.96	-0.53
FBgn0021742	C901	-0.06	-0.11	-0.07	-0.01	0.24	0.70
FBgn0000250	cact	-0.47	-0.69	-0.23	-0.02	-0.17	0.03
FBgn0030741	CalpC	0.45	0.52	0.58	0.24	0.20	0.79
FBgn0010014	CanB	-0.11	0.01	-0.13	0.14	0.65	0.91
FBgn0015614	CanB2	-0.22	-0.10	-0.11	0.39	0.55	0.93
FBgn0026257	cav	-0.27	-0.48	-0.55	-0.65	-0.81	-0.87
FBgn0004106	cdc2	-0.11	-0.21	-0.25	-0.38	-0.75	-0.72
FBgn0027491	Cdk5alpha	0.01	0.24	0.03	1.12	0.82	0.72
FBgn0015618	Cdk8	-0.36	-0.69	-0.53	-0.29	-0.38	-0.24
FBgn0000277	CecA2	0.41	0.66	0.49	0.90	0.69	0.87
FBgn0038028	CG10035	-0.78	-1.50	-0.83	-1.26	-1.91	-0.85
FBgn0033942	CG10112	-2.07	-1.10	-0.29	1.19	1.16	2.20
FBgn0036353	CG10171	0.15	0.30	0.37	0.68	0.76	1.13
FBgn0033968	CG10200	0.09	0.08	0.07	0.74	0.69	1.14
FBgn0037439	CG10286	0.04	-0.15	-0.11	-0.64	-0.87	-0.91
FBgn0031868	CG10354	1.15	1.46	1.19	0.97	0.68	1.31
FBgn0036549	CG10516	0.30	0.58	0.53	0.68	0.62	0.84
FBgn0037044	CG10585	-0.06	0.07	-0.08	-0.18	0.42	1.46
FBgn0035621	CG10591	-1.18	1.21	1.25	1.88	1.81	1.47
FBgn0045761	CG10618	0.01	0.20	0.09	0.54	0.54	1.16
FBgn0032726	CG10621	0.99	1.04	1.28	0.43	0.14	0.27
FBgn0036290	CG10638	-0.39	-0.58	-0.69	-0.61	-0.38	-0.62
FBgn0046302	CG10650	0.02	0.10	0.06	0.95	0.73	1.19
FBgn0032833	CG10664	-0.90	-0.57	0.71	-0.06	-0.81	-0.72
FBgn0032754	CG10700	-0.36	-0.25	0.24	-0.01	0.33	-0.68
FBgn0033821	CG10799	0.01	-0.08	-0.03	0.04	0.21	0.71
FBgn0027930	CG1102	0.43	0.67	0.51	0.66	0.73	0.73
FBgn0030094	CG11042	0.99	0.97	1.06	0.53	0.18	0.63
FBgn0030511	CG11158	-0.01	-0.15	-0.23	-0.43	-0.31	-1.15
FBgn0039800	CG11314	0.66	0.56	0.78	0.76	0.65	0.74
FBgn0035542	CG11347	-0.52	0.11	0.36	0.37	-0.17	0.70
FBgn0034200	CG11395	0.01	0.17	-0.08	0.34	0.39	0.70
FBgn0037165	CG11437	-0.11	1.02	0.97	1.36	1.14	0.56
FBgn0040623	CG11500	-0.64	-0.79	-0.60	-0.57	-0.49	-0.66
FBgn0039859	CG11539	-1.37	-1.51	-1.51	-2.21	-1.07	-2.35
FBgn0036194	CG11652	0.42	-1.27	-0.62	-0.10	-0.77	-0.63
FBgn0040551	CG11686	-0.36	0.07	-0.14	0.97	0.98	0.72
FBgn0037239	CG11739	-0.36	0.73	0.29	0.88	0.63	0.77
FBgn0030294	CG11750	0.83	0.90	0.82	0.46	0.25	0.41

FBgn	Symbol	5-6 h	6-7 h	7-8 h	8-9 h	9-10 h	10-11 h
FBgn0037611	CG11755	-0.39	-0.68	-0.59	-0.73	-0.85	-0.68
FBgn0037615	CG11760	-0.21	-0.32	-0.22	-0.39	-0.60	-0.87
FBgn0039264	CG11786	-0.27	-0.10	-0.14	0.63	0.98	1.60
FBgn0033519	CG11825	1.53	-1.62	-1.00	-1.36	-1.66	-1.00
FBgn0039332	CG11910	-0.04	0.16	0.03	0.93	0.94	1.46
FBgn0035464	CG12006	0.11	-0.21	-0.37	-0.84	-1.22	-1.09
FBgn0035430	CG12009	-0.02	-0.03	0.00	0.24	0.26	0.89
FBgn0038220	CG12207	-0.25	-0.51	-0.09	-0.75	-0.74	-0.78
FBgn0038002	CG12256	-0.05	-0.01	-0.09	0.15	0.09	0.75
FBgn0038489	CG12265	0.13	-0.30	-0.32	-0.53	-0.91	-0.88
FBgn0040808	CG12487	-0.09	-0.71	-0.47	-1.41	-1.33	-1.59
FBgn0036872	CG12519	-0.32	-0.45	-0.19	-0.22	-0.17	0.84
FBgn0040666	CG12848	0.33	0.51	0.79	0.31	0.46	0.37
FBgn0033945	CG12868	0.10	0.92	0.55	1.21	0.92	0.74
FBgn0033521	CG12896	1.71	-0.25	0.66	0.02	0.15	0.89
FBgn0033554	CG12938	-0.12	-0.36	-0.36	-0.60	-0.83	-0.93
FBgn0030771	CG13011	1.05	0.30	-0.03	-1.14	-0.85	-1.58
FBgn0040794	CG13056	0.99	1.61	1.77	2.12	2.09	2.30
FBgn0032789	CG13083	0.59	0.38	0.52	1.20	1.15	2.47
FBgn0033721	CG13159	-2.20	0.84	0.44	0.90	0.85	0.52
FBgn0033608	CG13220	-0.10	-0.02	0.49	-0.09	-0.55	-0.69
FBgn0035930	CG13307	0.04	0.06	0.04	0.32	0.27	0.69
FBgn0033855	CG13333	-0.19	0.04	0.42	-0.38	-0.81	-0.64
FBgn0029531	CG13362	-0.23	0.28	0.53	1.06	0.97	0.77
FBgn0030559	CG13404	-0.87	-1.08	-1.13	-0.96	-0.84	-0.89
FBgn0038901	CG13419	-0.01	0.03	0.04	0.22	0.32	0.91
FBgn0039795	CG1342	-0.28	0.26	0.11	1.25	0.79	1.68
FBgn0034514	CG13427	-0.66	-0.47	-0.38	-0.76	-1.03	-1.30
FBgn0036503	CG13454	0.10	-0.51	-0.79	-1.22	-0.83	-0.69
FBgn0040809	CG13465	-0.11	-0.74	-0.37	-1.39	-1.57	-1.59
FBgn0034760	CG13512	-0.36	-0.35	-0.17	-0.28	0.08	-0.77
FBgn0030151	CG1354	0.27	0.47	0.71	0.11	-0.12	0.04
FBgn0040660	CG13551	-0.78	-0.78	0.08	-0.06	-0.22	-0.03
FBgn0034928	CG13562	0.10	0.03	-0.03	0.23	0.25	0.80
FBgn0039176	CG13610	0.27	-0.27	-0.42	-0.58	-0.84	-0.79
FBgn0039200	CG13616	-0.01	0.29	0.03	0.63	0.94	0.70
FBgn0040600	CG13631	-0.09	-0.05	0.09	0.37	0.31	2.09
FBgn0036773	CG13698	-0.28	0.18	0.15	0.78	0.84	0.65
FBgn0035578	CG13707	0.03	0.05	0.05	0.34	0.37	0.95
FBgn0033341	CG13746	-0.41	-0.40	0.48	-0.34	-0.70	-0.55
FBgn0031897	CG13784	-0.39	-0.77	-0.65	-0.22	-0.11	0.18
FBgn0035325	CG13806	-0.24	-0.07	-0.02	0.53	0.50	1.13
FBgn0035313	CG13810	1.43	1.10	0.37	0.55	0.52	1.05
FBgn0036956	CG13813	-0.13	-0.07	0.01	0.41	0.65	1.13
FBgn0039041	CG13838	-0.04	0.11	-0.19	-0.57	-0.63	-1.12
FBgn0038971	CG13845	0.97	0.51	0.28	0.76	0.66	0.80
FBgn0035173	CG13907	0.62	0.64	0.68	0.40	0.43	0.80
FBgn0035209	CG13914	0.07	-0.10	-0.20	-0.73	-0.96	-1.08
FBgn0025712	CG13920	0.08	1.05	1.05	0.61	0.04	-0.01
FBgn0030277	CG1394	-0.13	-0.08	0.08	0.15	0.34	1.26
FBgn0031807	CG13981	-0.19	0.23	0.13	1.11	1.00	1.62
FBgn0031792	CG13983	0.00	0.07	0.09	0.73	0.62	1.32
FBgn0036359	CG14105	0.09	0.02	0.10	0.52	0.46	0.99
FBgn0036351	CG14107	-0.02	0.08	-0.28	0.31	0.91	1.75
FBgn0036352	CG14110	-0.71	0.63	0.61	1.84	1.77	1.58
FBgn0036193	CG14135	-1.17	-1.37	-0.72	-0.43	-0.86	-0.82
FBgn0035994	CG14179	1.04	1.15	0.88	0.65	0.24	0.43
FBgn0031037	CG14207	1.11	1.12	0.89	0.27	0.20	0.04
FBgn0032022	CG14275	0.53	1.98	0.80	-0.23	-0.26	0.14

FBgn	Symbol	5-6 h	6-7 h	7-8 h	8-9 h	9-10 h	10-11 h
FBgn0039620	CG1443	0.05	0.03	-0.04	0.22	0.33	1.03
FBgn0033046	CG14470	0.00	-0.02	0.13	0.39	0.43	0.85
FBgn0034228	CG14479	0.08	0.93	0.62	0.26	-0.01	-0.14
FBgn0034281	CG14490	0.03	-0.01	-0.11	-0.40	-0.18	-0.71
FBgn0039611	CG14528	0.03	0.08	0.01	0.32	0.35	0.68
FBgn0040398	CG14629	0.89	1.84	0.97	1.20	1.02	0.84
FBgn0037835	CG14687	0.61	0.71	-0.30	-0.95	-0.86	-1.31
FBgn0037819	CG14688	-0.51	-1.21	-0.88	-1.27	-1.35	-0.70
FBgn0033275	CG14756	-0.47	0.28	0.29	0.97	0.86	0.37
FBgn0026871	CG14781	-1.03	-0.52	0.43	-0.80	-0.79	0.00
FBgn0035750	CG14826	0.09	0.26	0.09	0.35	0.41	0.80
FBgn0032362	CG14928	-0.19	-0.07	-0.01	0.35	0.31	1.34
FBgn0035428	CG14960	0.04	0.17	0.05	0.98	0.95	1.24
FBgn0034430	CG15119	-0.11	-0.15	0.26	-0.32	-0.68	-0.74
FBgn0030322	CG15220	-0.25	-0.39	0.16	-0.65	-1.02	-1.13
FBgn0029681	CG15239	-0.04	0.00	0.02	0.31	0.11	0.98
FBgn0030040	CG15347	-0.57	0.49	0.41	1.00	0.77	0.74
FBgn0040930	CG15352	-0.07	0.06	-0.06	-0.26	-0.36	-0.73
FBgn0031549	CG15415	-0.53	-0.78	-0.88	-0.70	-0.85	-0.58
FBgn0031610	CG15436	0.00	-0.20	-0.33	-0.58	-0.53	-0.80
FBgn0032489	CG15480	-0.64	-0.81	-1.04	-0.84	-1.20	-0.89
FBgn0034168	CG15614	-0.05	0.84	0.88	0.61	-0.02	-0.22
FBgn0031635	CG15626	-0.55	-0.29	0.19	-0.34	-0.65	-0.73
FBgn0031627	CG15630	0.11	0.03	0.05	0.15	0.32	0.76
FBgn0030309	CG1572	0.02	-0.25	-0.35	0.20	0.53	0.70
FBgn0031910	CG15818	0.03	0.00	0.11	0.36	0.42	1.17
FBgn0032136	CG15828	0.53	0.45	0.63	0.48	0.47	0.91
FBgn0038132	CG15887	-0.33	-0.24	-0.22	0.31	0.31	1.57
FBgn0033182	CG1621	-0.15	-0.47	-0.06	-0.23	-0.65	-0.69
FBgn0033453	CG1667	-1.10	-1.06	-0.78	-0.78	-0.58	-0.31
FBgn0039897	CG1674	-0.21	-0.34	-0.50	0.02	-0.24	-0.88
FBgn0029768	CG16752	0.32	0.54	0.66	0.46	0.75	0.20
FBgn0035348	CG16758	0.04	0.36	0.55	0.73	0.57	0.21
FBgn0029659	CG16782	0.00	-0.02	-0.12	-0.17	-0.28	-0.95
FBgn0039574	CG16918	0.08	0.32	0.72	1.13	1.23	1.62
FBgn0040732	CG16926	1.84	1.46	0.53	0.88	0.47	0.62
FBgn0025621	CG16989	0.69	0.86	0.70	0.06	0.08	0.22
FBgn0031117	CG1702	-0.20	0.04	0.06	0.22	0.40	0.80
FBgn0036546	CG17033	-0.40	-0.31	0.42	-0.53	-0.82	-0.58
FBgn0039051	CG17109	-0.08	-0.08	0.10	0.30	0.25	0.84
FBgn0039045	CG17119	-0.10	0.14	0.17	0.30	0.31	0.71
FBgn0035144	CG17181	-0.25	0.72	0.41	-1.03	-1.04	-0.86
FBgn0027500	CG17286	0.30	0.15	0.04	-0.49	-0.81	-0.59
FBgn0039915	CG1732	0.11	0.01	0.12	0.30	0.42	0.86
FBgn0032713	CG17323	-0.09	0.81	0.82	0.75	0.40	0.41
FBgn0035640	CG17498	-0.57	-0.53	-0.08	-0.63	-0.98	-0.95
FBgn0034352	CG17669	1.36	1.01	0.71	1.20	0.72	0.79
FBgn0038718	CG17752	-1.31	-1.47	-1.30	-1.61	-0.90	-1.49
FBgn0037433	CG17919	0.09	0.07	0.05	0.36	0.57	0.93
FBgn0030365	CG1796	-0.92	-0.93	-0.35	-0.89	-0.89	-0.93
FBgn0032189	CG18145	-0.20	-0.60	-0.60	-0.35	-0.76	-0.31
FBgn0035725	CG18156	0.35	-0.41	-0.51	-0.47	-0.74	-0.90
FBgn0033836	CG18278	-1.13	-0.64	-0.52	-0.84	-0.63	-0.72
FBgn0036873	CG18294	-0.43	-0.28	-0.29	-0.23	-0.12	1.15
FBgn0034382	CG18609	0.05	0.06	0.19	0.22	0.24	0.86
FBgn0040964	CG18661	-1.12	-1.16	-1.19	-1.37	-1.17	-1.49
FBgn0040599	CG18669	0.06	0.02	0.10	0.08	0.23	0.69
FBgn0035398	CG1869	-0.21	0.11	-0.01	0.53	0.66	0.75
FBgn0042185	CG18769	-0.34	-0.41	-0.21	-0.87	-0.58	-1.05

FBgn	Symbol	5-6 h	6-7 h	7-8 h	8-9 h	9-10 h	10-11 h
FBgn0039869	CG1890	-0.31	-0.26	0.02	-0.13	-0.44	-0.72
FBgn0037468	CG1943	-1.05	-0.90	0.33	-0.76	-1.35	-0.93
FBgn0039886	CG2003	0.00	0.24	0.05	0.41	0.53	0.80
FBgn0039664	CG2006	-0.43	-0.40	-0.06	-0.50	-0.52	-0.73
FBgn0037289	CG2016	0.02	-0.06	0.03	0.37	0.44	1.09
FBgn0033205	CG2064	0.24	0.76	0.46	0.56	0.31	0.79
FBgn0039873	CG2191	1.02	-0.67	-0.92	-0.53	-0.95	-0.66
FBgn0029990	CG2233	-0.53	-0.38	-0.31	0.66	0.71	0.58
FBgn0029994	CG2254	0.69	1.90	1.72	1.95	1.72	2.23
FBgn0039665	CG2310	-0.32	0.07	0.33	-0.18	-0.84	-0.57
FBgn0032969	CG2528	0.05	-0.18	-0.76	-0.51	-0.15	-0.33
FBgn0030394	CG2560	0.10	-0.02	0.15	0.44	0.67	1.06
FBgn0037478	CG2656	-0.43	-0.54	-0.70	-0.58	-0.60	-0.47
FBgn0035090	CG2736	0.00	0.01	-0.08	0.25	0.41	0.87
FBgn0037534	CG2781	-0.08	-0.04	-0.21	0.30	1.00	0.83
FBgn0031263	CG2789	-0.87	-0.40	-0.22	-0.42	-0.52	-1.00
FBgn0030186	CG2962	-0.98	-0.76	0.14	0.77	1.52	2.80
FBgn0050069	CG30069	-0.01	0.01	-0.02	0.95	1.40	0.91
FBgn0050148	CG30148	0.03	0.13	0.14	0.96	0.88	2.05
FBgn0050384	CG30384	-0.37	0.23	-0.08	0.64	0.65	1.01
FBgn0050392	CG30392	1.03	1.12	0.78	0.75	0.69	0.56
FBgn0050437	CG30437	-0.14	-0.12	-0.11	0.15	0.72	0.91
FBgn0050492	CG30492	1.08	0.79	0.55	0.68	0.59	0.87
FBgn0050502	CG30502	0.14	0.21	0.00	0.61	0.78	0.73
FBgn0029807	CG3108	0.01	-0.20	-0.34	0.10	0.82	1.37
FBgn0051300	CG31300	-0.13	0.25	0.21	0.68	0.99	0.26
FBgn0051323	CG31323	0.04	-0.02	-0.11	0.18	0.40	0.80
FBgn0038198	CG3153	-0.21	-0.05	0.03	0.90	0.81	1.46
FBgn0051997	CG31997	-0.08	-0.13	-0.18	0.86	1.14	1.54
FBgn0051999	CG31999	-0.08	-0.06	-0.30	-0.28	-0.31	-1.04
FBgn0045770	CG32063	0.17	0.92	0.61	0.70	0.54	1.02
FBgn0034569	CG3221	-0.40	-0.35	-0.78	-0.78	-0.61	-0.46
FBgn0031434	CG3227	-0.25	-0.49	-0.45	-0.53	-0.76	-0.69
FBgn0052369	CG32369	-0.02	-0.19	-0.17	-0.46	-0.43	-0.81
FBgn0052412	CG32412	-0.02	0.11	0.02	0.33	0.19	0.83
FBgn0031629	CG3244	-0.93	-0.37	-0.30	0.60	1.48	0.93
FBgn0052649	CG32649	-0.32	-0.05	-0.02	0.05	0.24	0.70
FBgn0052756	CG32756	0.10	-0.03	-0.15	-0.30	-0.40	-0.68
FBgn0053006	CG33006	0.16	0.94	0.68	0.16	-0.05	-0.05
FBgn0053056	CG33056	-0.05	0.04	0.03	0.56	0.41	0.90
FBgn0053143	CG33143	0.13	0.74	0.26	-1.15	-1.07	-0.99
FBgn0040609	CG3348	-0.17	-0.08	0.17	-0.28	-0.87	-1.51
FBgn0034792	CG3499	0.81	0.78	0.81	0.23	0.05	0.37
FBgn0038250	CG3505	-0.25	0.05	0.04	0.55	0.41	1.33
FBgn0038467	CG3590	0.47	0.50	0.72	0.41	0.14	0.24
FBgn0031418	CG3609	-0.74	0.21	0.43	0.66	0.64	0.75
FBgn0040397	CG3655	0.92	1.18	0.60	0.41	0.63	1.13
FBgn0027521	CG3679	-0.54	-0.53	-0.70	-0.97	-1.02	-1.14
FBgn0040349	CG3699	0.51	-0.11	0.08	0.44	0.55	0.68
FBgn0034951	CG3860	-0.07	0.21	0.10	0.40	0.34	0.69
FBgn0038292	CG3987	-0.03	0.14	0.00	0.71	0.93	0.73
FBgn0037801	CG3999	0.50	-0.65	-0.13	0.64	0.72	1.10
FBgn0038017	CG4115	-1.10	0.14	0.08	1.55	1.40	2.36
FBgn0030745	CG4239	0.00	-0.05	-0.08	-0.13	-0.11	-0.79
FBgn0034761	CG4250	-0.07	-0.13	-0.23	-0.45	-0.44	-0.98
FBgn0014092	CG4278	-0.53	-0.15	-0.16	-0.42	-0.45	-0.70
FBgn0025632	CG4313	-0.15	0.14	0.46	1.23	0.83	0.55
FBgn0030452	CG4330	0.38	0.69	0.69	0.19	0.07	0.19
FBgn0039075	CG4393	0.10	0.19	0.25	0.58	0.51	0.72

FBgn	Symbol	5-6 h	6-7 h	7-8 h	8-9 h	9-10 h	10-11 h
FBgn0039073	CG4408	-1.21	-1.45	-0.63	-0.73	-0.53	-0.98
FBgn0034128	CG4409	1.80	1.38	0.91	0.99	0.74	0.89
FBgn0040984	CG4440	-0.33	-0.69	-0.39	-1.19	-1.67	-1.77
FBgn0032105	CG4454	-0.84	-0.79	0.10	-0.63	-1.09	-0.82
FBgn0029838	CG4666	-0.45	-0.24	-0.34	0.55	1.13	1.44
FBgn0033815	CG4676	0.18	-0.30	-0.43	-0.72	-0.84	-0.70
FBgn0037992	CG4702	-0.17	0.05	0.03	1.73	1.36	2.44
FBgn0039024	CG4721	0.00	-0.03	-0.05	0.19	0.30	0.73
FBgn0043456	CG4747	1.04	1.52	1.20	0.18	0.07	0.46
FBgn0027600	CG4778	0.03	0.12	0.20	0.40	0.31	0.74
FBgn0032618	CG4826	0.04	0.15	0.00	0.31	0.20	0.86
FBgn0030803	CG4880	-0.63	-0.81	-0.44	-0.77	-0.70	-0.72
FBgn0036616	CG4893	0.15	-0.17	-0.12	0.17	0.74	0.78
FBgn0034145	CG5065	-0.11	0.29	0.19	0.63	0.71	0.43
FBgn0031320	CG5126	-0.43	-0.34	-0.22	-0.47	-0.61	-0.76
FBgn0035957	CG5144	-0.52	-0.21	-0.13	-0.51	-0.60	-0.96
FBgn0038476	CG5175	-0.40	-0.58	-0.66	-0.70	-1.11	-0.89
FBgn0031908	CG5177	-0.42	-0.36	-0.85	-0.38	-0.44	-1.77
FBgn0034365	CG5335	-0.16	0.42	0.21	0.88	0.99	0.52
FBgn0032242	CG5355	-0.39	-0.83	-0.68	-0.32	-0.41	-0.07
FBgn0032213	CG5390	-0.11	0.44	0.09	0.64	0.48	1.45
FBgn0039521	CG5402	-0.13	-0.04	0.05	0.52	1.00	0.78
FBgn0032436	CG5418	0.00	0.10	-0.07	0.18	0.30	0.79
FBgn0034887	CG5428	0.23	0.29	0.09	0.30	0.24	0.83
FBgn0034888	CG5431	-0.06	-0.06	-0.18	0.48	0.53	1.00
FBgn0038384	CG5470	-0.06	-0.17	0.06	0.32	0.52	0.91
FBgn0034364	CG5493	-0.22	0.81	-0.25	-1.24	-0.47	0.13
FBgn0027565	CG5498	-0.79	-0.78	-0.73	-0.50	-0.45	-0.27
FBgn0039560	CG5514	0.51	0.73	0.83	0.51	0.34	0.57
FBgn0034158	CG5522	0.18	-0.61	-0.86	-0.16	-0.34	-0.10
FBgn0034902	CG5532	-0.79	-0.71	0.13	-0.27	-0.60	-0.71
FBgn0035639	CG5537	-0.23	0.00	0.34	-0.48	-0.74	-0.65
FBgn0034914	CG5554	-1.49	-0.95	-0.18	-1.06	-1.26	-1.10
FBgn0032200	CG5676	-0.28	-0.66	-0.31	-0.42	-0.44	-0.71
FBgn0039172	CG5677	-0.01	-0.03	-0.03	0.27	0.27	1.13
FBgn0032197	CG5694	-0.02	-0.14	-0.13	0.35	0.29	1.26
FBgn0034310	CG5733	-0.38	-0.86	-0.78	-0.66	-0.94	-0.64
FBgn0034299	CG5757	-0.19	-0.40	-0.29	-0.46	-0.43	-0.75
FBgn0039198	CG5768	-0.09	0.05	0.09	0.53	0.54	1.41
FBgn0034290	CG5773	1.84	1.55	1.16	1.24	0.99	0.98
FBgn0038516	CG5840	0.42	0.16	0.28	0.41	0.62	0.81
FBgn0038511	CG5873	-0.10	0.20	0.33	0.52	0.76	1.08
FBgn0039379	CG5886	0.08	0.12	-0.13	-0.48	-0.56	-0.93
FBgn0039139	CG5933	-0.37	-0.85	-0.46	-0.20	-0.41	0.00
FBgn0031913	CG5958	1.21	1.58	1.09	0.57	0.42	0.74
FBgn0038056	CG5961	-0.35	-0.72	-0.66	-0.89	-0.50	-0.78
FBgn0038676	CG6026	-0.08	0.06	-0.01	0.25	0.35	1.58
FBgn0036182	CG6084	-0.26	-0.10	-0.04	0.45	0.86	1.79
FBgn0036542	CG6112	-0.03	-0.38	-0.61	-0.99	-0.52	-0.96
FBgn0038407	CG6126	0.36	0.87	0.42	0.43	0.30	0.38
FBgn0032252	CG6232	-0.12	-0.04	-0.15	0.17	0.21	0.80
FBgn0038071	CG6234	-0.43	-0.76	-0.24	0.04	-0.45	0.01
FBgn0034276	CG6385	-0.08	-0.05	-0.04	0.46	0.54	1.12
FBgn0027889	CG6386	-0.15	-0.27	-0.04	-0.84	-0.76	-0.72
FBgn0032287	CG6415	-0.03	-0.07	0.15	0.70	0.41	0.76
FBgn0034162	CG6426	-0.05	-0.05	0.03	0.24	0.34	0.79
FBgn0039213	CG6668	0.13	0.36	0.70	0.26	0.14	0.25
FBgn0033887	CG6704	0.06	-0.05	-0.04	0.38	0.31	1.24
FBgn0032394	CG6746	-0.04	-0.34	-0.32	0.09	0.08	0.68

FBgn	Symbol	5-6 h	6-7 h	7-8 h	8-9 h	9-10 h	10-11 h
FBgn0032292	CG6750	0.40	0.63	0.86	0.48	0.19	0.16
FBgn0036031	CG6761	0.06	-0.09	-0.04	0.07	0.24	0.68
FBgn0032400	CG6770	-0.36	-0.20	-0.05	0.90	0.82	0.16
FBgn0037913	CG6783	-0.29	0.74	0.66	0.71	0.53	0.56
FBgn0032399	CG6785	-0.19	-0.03	0.09	0.25	0.23	1.06
FBgn0030882	CG6835	-0.39	-0.33	-0.09	NA	-0.39	-0.77
FBgn0036815	CG6874	0.22	-0.27	-0.44	-0.50	-0.62	-0.78
FBgn0030955	CG6891	1.83	2.04	1.54	1.63	1.41	1.48
FBgn0036800	CG6897	-0.02	-0.69	-0.77	-0.55	-0.78	-0.54
FBgn0030958	CG6900	0.56	1.29	0.89	1.48	1.29	1.29
FBgn0036261	CG6906	-0.30	-0.16	-0.04	0.30	0.45	0.78
FBgn0037956	CG6959	0.31	0.97	0.85	0.75	0.30	0.37
FBgn0039008	CG6972	-0.19	-0.13	-0.25	-0.20	-0.55	-1.26
FBgn0036945	CG6981	-0.46	0.32	0.22	1.29	0.73	0.40
FBgn0038972	CG7054	-0.76	-0.93	-0.26	-0.66	-0.33	-0.25
FBgn0031961	CG7102	-0.25	-0.53	-0.92	-0.55	-0.62	-0.50
FBgn0031947	CG7154	-0.32	-0.47	-0.87	-0.57	-0.53	-0.56
FBgn0038574	CG7212	-0.29	-0.72	-0.63	-0.63	-0.72	-0.57
FBgn0031971	CG7224	0.17	-1.11	-0.31	-0.84	-1.58	-2.26
FBgn0031970	CG7227	-0.09	0.02	0.03	1.03	0.94	1.29
FBgn0032286	CG7300	0.07	-0.06	0.17	0.35	0.64	0.98
FBgn0031977	CG7380	0.00	-0.34	-0.34	-0.52	-0.63	-0.78
FBgn0036927	CG7433	-1.04	-0.72	-0.47	0.20	0.12	0.75
FBgn0038533	CG7523	-0.20	-0.29	-0.22	-0.40	-0.75	-0.98
FBgn0035798	CG7526	-0.18	-0.12	-0.23	-0.03	-0.15	-0.73
FBgn0036738	CG7542	-0.09	-0.15	-0.12	-0.34	-0.18	-0.80
FBgn0038610	CG7675	-0.74	0.77	0.48	1.35	1.36	0.68
FBgn0033633	CG7759	0.01	0.09	-0.17	-0.37	-0.60	-1.12
FBgn0032021	CG7781	-0.07	0.10	-0.08	0.12	0.31	0.68
FBgn0039704	CG7802	0.17	0.95	0.86	0.74	0.30	1.11
FBgn0039736	CG7912	-0.25	-0.72	-0.67	-1.03	-0.70	-1.03
FBgn0037607	CG8036	-0.35	0.74	1.06	0.59	0.42	0.58
FBgn0034011	CG8160	-0.09	-0.01	-0.07	-0.01	0.41	0.81
FBgn0030864	CG8173	0.07	-0.21	-0.03	-0.66	-0.79	-0.78
FBgn0033367	CG8193	0.25	0.85	0.96	0.28	-0.39	-0.15
FBgn0030683	CG8239	-0.03	-0.38	-0.43	0.17	-0.08	0.78
FBgn0037718	CG8286	0.58	0.78	0.28	0.51	0.42	0.54
FBgn0034143	CG8303	-0.14	-0.07	-0.12	0.17	0.23	0.97
FBgn0034142	CG8306	0.42	0.31	-0.19	0.39	0.48	0.74
FBgn0037723	CG8327	0.73	0.45	0.27	0.70	0.62	0.76
FBgn0037634	CG8359	-0.06	-0.48	-0.66	-0.92	-0.59	-0.82
FBgn0037664	CG8420	-0.22	0.02	0.35	1.21	0.68	0.91
FBgn0037670	CG8436	0.08	-0.29	-0.48	-0.62	-0.88	-0.79
FBgn0033917	CG8503	-0.07	0.19	0.01	-0.51	-0.72	-1.20
FBgn0037759	CG8526	-0.44	-0.77	-0.62	-0.51	-0.48	-0.33
FBgn0035773	CG8580	-0.11	-0.21	-0.08	-0.55	-0.75	-0.71
FBgn0033921	CG8589	-0.53	-0.92	-0.74	-0.65	-0.46	-0.43
FBgn0033271	CG8708	-0.05	0.09	0.21	0.60	0.49	0.69
FBgn0033764	CG8776	0.44	0.61	0.73	1.24	0.80	0.85
FBgn0028955	CG8788	-0.41	-0.43	0.33	-0.07	-0.62	-0.75
FBgn0031663	CG8891	-1.44	-0.83	-0.31	0.04	0.21	0.24
FBgn0031886	CG8902	-0.08	-0.41	-0.50	-0.70	-0.70	-0.70
FBgn0035199	CG9134	-0.19	-0.14	-0.10	0.35	0.55	0.88
FBgn0035194	CG9187	-0.10	-0.02	-0.09	-0.69	-0.73	-1.05
FBgn0038180	CG9307	0.01	0.06	0.07	0.43	0.53	0.73
FBgn0032879	CG9317	-0.28	0.05	1.06	-0.10	-0.31	0.42
FBgn0032895	CG9335	-0.01	0.08	-0.02	0.43	0.52	0.79
FBgn0032897	CG9336	-0.10	1.23	0.62	1.16	0.88	0.89
FBgn0032899	CG9338	-0.07	0.97	0.82	1.21	0.87	0.81

FBgn	Symbol	5-6 h	6-7 h	7-8 h	8-9 h	9-10 h	10-11 h
FBgn0035094	CG9380	0.28	0.14	-0.13	0.91	0.67	1.09
FBgn0037063	CG9391	0.03	-0.04	0.04	0.61	0.48	0.68
FBgn0037715	CG9399	-0.36	-0.62	-0.19	-0.71	-0.79	-0.59
FBgn0034438	CG9416	0.09	0.67	0.66	1.08	0.68	0.96
FBgn0037730	CG9444	0.29	0.24	0.19	0.41	0.35	0.75
FBgn0036875	CG9449	1.80	1.41	0.60	1.05	0.88	0.60
FBgn0033115	CG9460	0.01	0.04	0.08	0.45	0.37	0.70
FBgn0030587	CG9522	-0.07	-0.01	-0.14	0.19	0.33	1.18
FBgn0032087	CG9568	-0.34	-0.15	-0.33	0.13	0.91	1.22
FBgn0036433	CG9628	-0.46	0.92	0.36	0.78	0.35	0.23
FBgn0036857	CG9629	1.20	0.94	0.19	0.68	0.72	1.05
FBgn0031483	CG9641	-0.11	-0.16	-0.23	-0.71	-0.68	-0.98
FBgn0031515	CG9664	1.11	0.77	0.13	0.52	0.27	0.43
FBgn0030159	CG9689	-0.72	0.24	0.30	1.23	1.00	0.92
FBgn0036661	CG9705	-0.23	-0.53	-0.30	-0.65	-0.37	-0.77
FBgn0037669	CG9740	0.03	-0.42	-0.39	-0.57	-0.73	-0.71
FBgn0038149	CG9796	-1.00	0.71	0.64	0.65	0.40	-0.14
FBgn0037637	CG9836	0.67	0.61	0.77	0.46	0.21	0.16
FBgn0031453	CG9894	-0.39	-0.40	0.78	-0.65	-0.90	-0.10
FBgn0030755	CG9906	0.59	0.97	0.96	0.36	0.37	0.49
FBgn0035726	CG9953	-0.66	-0.93	-0.58	-0.51	-0.67	-0.46
FBgn0023395	Chd3	0.20	-0.19	-0.53	-0.42	-0.61	-0.70
FBgn0035499	Chd64	-0.47	0.39	0.12	1.07	0.79	0.80
FBgn0000337	cn	1.14	0.16	-0.25	-0.93	-1.05	-0.60
FBgn0015622	Cnx99A	0.56	1.02	1.17	0.35	0.56	0.65
FBgn0063757	CR32366	0.01	-0.19	-0.25	-0.50	-0.55	-0.88
FBgn0047242	CR32646	-0.18	0.95	0.76	0.89	0.83	0.36
FBgn0053327	CR33327	-0.22	-0.13	0.21	0.81	0.78	0.50
FBgn0000405	CycB	-0.04	0.11	0.11	-0.50	-0.97	-1.15
FBgn0015625	CycB3	-0.45	-0.52	-0.48	-0.99	-1.45	-1.38
FBgn0053503	Cyp12d1-d	0.46	0.01	-0.38	-0.77	-0.25	-0.73
FBgn0038095	Cyp304a1	0.13	0.16	-0.13	0.53	0.55	2.01
FBgn0035618	Cyp307a1	-1.15	-1.05	-0.15	-0.15	-0.33	0.04
FBgn0037601	Cyp313b1	-0.08	-0.05	-0.01	0.20	0.27	0.86
FBgn0010019	Cyp4g1	-0.66	-0.31	-0.15	0.54	0.68	1.85
FBgn0033304	Cyp6a13	0.04	0.06	0.02	0.25	0.39	1.10
FBgn0033978	Cyp6a23	0.03	0.22	0.29	0.73	0.58	0.90
FBgn0013772	Cyp6a8	0.77	1.33	0.87	0.66	-0.12	0.27
FBgn0015040	Cyp9c1	0.04	0.04	0.07	0.32	0.49	1.03
FBgn0038037	Cyp9f2	0.04	0.57	0.31	1.13	0.92	0.74
FBgn0038034	Cyp9f3Psi	0.04	0.11	0.13	0.85	0.58	0.60
FBgn0035141	Cypl	-0.80	-0.69	0.09	-0.34	-0.50	-0.38
FBgn0000406	Cyt-b5-r	-0.17	-0.44	-0.66	-0.84	-0.80	-0.41
FBgn0010316	dap	0.60	0.71	0.23	-0.32	-0.88	-0.49
FBgn0028381	decay	-0.08	0.02	0.06	0.44	0.68	0.75
FBgn0035964	Dhpr	-0.13	-0.20	0.14	0.06	0.16	0.74
FBgn0000449	dib	-0.49	-0.70	-0.77	-0.63	-0.76	-0.46
FBgn0000454	Dip-B	-0.47	-0.34	-0.07	0.42	0.47	0.71
FBgn0039802	dj-1beta	-1.23	-0.67	-0.03	-0.82	-0.71	-1.07
FBgn0022338	dnk	-0.14	-0.20	0.22	-0.29	-0.60	-0.76
FBgn0020306	dom	0.21	0.74	0.66	0.04	-0.04	0.14
FBgn0015929	dpa	-0.28	-0.14	0.68	-0.30	-0.82	-0.57
FBgn0002183	dre4	-0.52	-0.64	-0.10	-0.61	-0.64	-0.72
FBgn0035434	dro5	-0.96	-1.98	-1.54	-2.93	-2.83	-3.28
FBgn0010381	Drs	-0.34	-0.78	-0.76	-1.42	-1.41	-1.86
FBgn0011764	Dsp1	-0.45	-0.18	-0.37	-0.81	-0.92	-1.11
FBgn0028737	Ef1beta	-0.94	-0.84	-0.03	-0.53	-1.01	-0.82
FBgn0003731	Egfr	0.76	0.78	0.68	0.53	0.36	0.97
FBgn0040227	eIF-3p66	-0.37	-0.20	0.59	0.01	-0.79	-0.24

FBgn	Symbol	5-6 h	6-7 h	7-8 h	8-9 h	9-10 h	10-11 h
FBgn0000565	Eip71CD	-0.02	-0.22	-0.07	-0.41	-0.75	-0.82
FBgn0000570	elav	-0.21	0.02	-0.07	-0.55	-0.43	-0.75
FBgn0010435	emp	-0.01	0.14	0.03	0.41	0.61	0.72
FBgn0034433	endoB	0.48	0.85	0.58	1.16	0.90	1.25
FBgn0000579	Eno	-0.01	0.04	0.08	-0.09	-0.83	-1.12
FBgn0013953	Esp	0.09	-0.46	-0.51	-0.10	-0.68	-0.68
FBgn0000636	Fas3	0.00	1.01	1.14	0.72	0.12	0.09
FBgn0026721	fat-spondin	-0.13	0.58	0.64	0.68	0.55	0.75
FBgn0032820	fbp	-0.56	0.24	0.21	0.75	0.43	0.02
FBgn0033079	Fmo-2	0.12	-0.12	-0.22	0.07	0.28	1.03
FBgn0040222	fne	-0.12	0.56	0.34	0.71	0.41	0.26
FBgn0025373	Fpps	0.09	-0.58	-0.77	-0.20	-0.78	-0.60
FBgn0016081	fry	-0.28	-0.49	-0.61	-0.70	-0.79	-0.50
FBgn0036485	FucTA	0.13	0.18	0.11	0.44	0.45	0.70
FBgn0001086	fzy	-0.02	-0.32	-0.38	-0.48	-0.85	-0.67
FBgn0010223	Galpha73B	0.26	0.23	0.06	0.62	0.40	0.74
FBgn0028968	gammaCop	0.70	0.75	0.88	0.58	0.47	0.55
FBgn0026077	Gasp	-0.69	0.36	-0.05	1.24	1.25	1.61
FBgn0004868	Gdi	0.18	0.28	0.69	0.25	-0.02	-0.09
FBgn0033081	geminin	0.25	0.16	0.30	-0.46	-0.70	-0.70
FBgn0027341	Gfat1	-0.38	0.03	-0.09	0.71	1.38	1.29
FBgn0027657	glob1	1.33	1.39	0.69	1.25	1.47	1.49
FBgn0001114	Glt	-0.21	-0.13	0.03	0.99	0.72	1.81
FBgn0034603	Glycogenin	-0.18	-0.02	-0.03	-0.54	-0.28	-0.84
FBgn0004919	gol	-0.29	0.02	-0.59	-1.05	-0.89	-0.88
FBgn0039520	Gr98a	1.84	2.19	2.08	2.11	2.07	2.74
FBgn0001148	gsb	-0.27	-0.83	-0.72	-0.82	-1.14	-0.80
FBgn0010041	GstD5	-0.03	0.35	0.46	0.84	0.69	1.16
FBgn0034335	GstE1	0.02	0.10	0.49	0.85	0.81	1.19
FBgn0010391	Gtp-bp	0.20	0.46	0.70	0.34	0.06	0.23
FBgn0004461	gwl	-0.32	-0.43	-0.62	-0.42	-0.76	-0.40
FBgn0001174	halo	-1.10	-0.79	-0.39	-0.45	-0.51	-0.27
FBgn0040211	hgo	-0.09	0.00	-0.05	0.07	0.24	0.83
FBgn0030900	Him	0.39	0.64	1.13	0.98	0.89	0.81
FBgn0061209	His2B:CG17949	2.10	2.85	2.66	3.19	3.52	3.57
FBgn0002609	HLHm3	0.88	0.92	0.46	-0.13	-0.24	-0.32
FBgn0002631	HLHm5	-0.22	-0.68	-0.55	-0.79	-0.34	-0.63
FBgn0002734	HLHmdelta	0.13	-0.56	-0.86	-0.93	-0.97	-0.87
FBgn0002735	HLHmgamma	-0.17	-0.53	-0.56	-0.67	-0.95	-0.81
FBgn0004362	HmgD	0.05	0.03	0.28	-0.19	-0.46	-0.83
FBgn0010611	Hmgs	0.33	0.67	0.52	0.54	0.77	1.49
FBgn0001208	Hn	-0.03	0.19	-0.03	0.90	1.04	1.48
FBgn0030082	HP1b	-0.60	-0.54	0.10	-0.57	-0.70	-0.82
FBgn0001217	Hsc70-2	-1.11	-0.87	-0.67	-0.51	-0.42	-0.53
FBgn0001219	Hsc70-4	-0.34	0.25	2.15	-0.08	-0.44	1.16
FBgn0001223	Hsp22	-2.77	-1.22	-0.23	-0.71	-1.14	-0.31
FBgn0001224	Hsp23	-1.43	-1.27	-0.48	-1.07	-0.92	-0.24
FBgn0001226	Hsp27	-1.19	-0.83	-0.17	-0.29	-0.36	-0.59
FBgn0013275	Hsp70Aa	-2.08	-1.41	-0.37	-0.70	-0.90	0.05
FBgn0024227	ial	0.08	0.16	0.20	-0.49	-0.86	-0.60
FBgn0019972	Ice	-0.47	-0.24	0.36	-0.39	-0.93	-0.52
FBgn0020415	Idgf2	-0.23	-0.30	-0.02	0.82	0.78	1.49
FBgn0001250	if	0.56	0.72	0.75	0.74	0.67	0.64
FBgn0033835	IM10	-0.18	-0.05	-0.04	0.09	0.37	0.71
FBgn0001254	ImpE2	-0.60	-0.26	-0.02	0.73	0.99	1.19
FBgn0001256	ImpL1	-0.57	-0.14	-0.18	1.53	1.49	1.60
FBgn0001257	ImpL2	-0.50	-0.75	-0.08	-0.72	-1.56	-1.24
FBgn0001258	ImpL3	0.07	-0.06	0.05	-0.50	-0.93	-1.30
FBgn0011603	ine	0.05	-0.02	0.02	0.10	0.21	0.96

FBgn	Symbol	5-6 h	6-7 h	7-8 h	8-9 h	9-10 h	10-11 h
FBgn0025885	Inos	-0.03	-0.31	-0.06	-0.86	-0.85	-0.61
FBgn0001276	ix	-0.14	-0.38	-0.53	-0.47	-0.70	-0.58
FBgn0028841	jhamt	-0.08	-0.20	-0.36	-1.18	-1.66	-3.28
FBgn0010053	Jheh1	0.02	0.11	0.08	0.76	0.42	0.82
FBgn0034406	Jheh3	-0.45	0.11	0.10	0.87	0.76	0.63
FBgn0028425	JhI-21	-0.11	-0.26	-0.51	-0.44	-0.50	-0.68
FBgn0028424	JhI-26	0.12	0.26	0.29	0.69	0.52	0.18
FBgn0015396	jumu	0.31	-0.19	-0.55	-0.38	-0.71	-0.50
FBgn0028370	kek3	0.07	-0.70	-0.18	-0.63	-0.77	-1.33
FBgn0004378	Klp61F	0.11	-0.16	-0.74	-0.57	-0.73	-0.49
FBgn0028342	l(1)G0230	-0.80	-0.92	-0.57	-0.19	-0.36	-0.36
FBgn0002561	l(1)sc	-0.11	-0.51	-0.53	-0.73	-0.73	-0.49
FBgn0010488	l(2)01424	0.11	0.74	0.58	0.23	0.19	0.29
FBgn0010622	l(2)06496	-1.12	-0.61	-0.12	-0.54	-0.72	-0.60
FBgn0010786	l(3)02640	0.91	0.86	0.69	0.78	0.48	1.01
FBgn0002526	LanA	0.73	0.76	0.97	0.35	0.14	0.48
FBgn0002527	LanB1	0.66	0.80	0.78	0.62	0.38	0.47
FBgn0016032	lbn	-0.18	0.42	0.30	1.03	0.73	0.71
FBgn0041203	LIMK1	0.36	0.69	0.80	0.58	0.89	0.17
FBgn0039039	lmd	0.19	0.93	0.52	-0.29	-0.27	-0.54
FBgn0039114	Lsd-1	0.08	0.49	0.39	0.54	0.34	0.87
FBgn0010602	lwr	-0.63	-0.53	0.27	-0.49	-0.79	-0.56
FBgn0004425	LysB	1.20	0.95	0.59	0.78	0.51	0.34
FBgn0002629	m4	-0.36	-0.73	-0.53	-0.98	-0.79	-0.96
FBgn0002632	m6	-0.12	1.20	0.91	1.61	1.50	1.18
FBgn0010342	Map60	0.18	-0.05	0.06	-0.55	-0.69	-0.39
FBgn0017577	Mcm5	-0.41	-0.69	-0.34	-0.68	-1.17	-0.82
FBgn0043069	MESK4	0.23	0.57	0.78	1.03	0.84	0.84
FBgn0004228	mex1	-0.04	0.43	0.31	1.35	1.10	1.10
FBgn0011643	Mlp60A	-0.90	-1.10	-1.48	-0.35	-0.40	-0.80
FBgn0026409	Mpcp	-0.93	-0.46	0.28	-0.22	-1.07	-0.89
FBgn0030556	mRNA-capping-enzyme	0.08	0.01	0.01	0.31	0.25	1.10
FBgn0039555	mRpS22	-0.16	-0.34	0.14	-0.39	-0.57	-0.84
FBgn0035534	mRpS6	-0.25	-0.51	-0.43	-0.47	-0.44	-0.90
FBgn0027949	msb1l	-0.04	-0.31	0.24	-0.75	-1.04	-0.82
FBgn0002775	msl-3	-1.30	-1.11	-0.37	-0.62	-0.35	-0.98
FBgn0002868	MtnA	-0.28	-0.08	0.09	0.89	1.08	1.18
FBgn0010246	Myo61F	-0.03	0.24	0.08	0.69	0.79	0.78
FBgn0017565	Nacalpa	-0.49	-0.10	0.67	-0.24	-0.70	-0.53
FBgn0002924	ncd	0.06	-0.05	0.25	-0.47	-0.69	-0.71
FBgn0002931	net	-1.09	-0.31	-0.34	-0.50	-0.59	-1.10
FBgn0002939	ninaD	0.02	0.05	-0.21	-0.62	-0.50	-1.13
FBgn0016685	Nlp	-0.15	-0.20	0.13	-0.74	-0.58	-0.66
FBgn0005771	noc	-0.38	-0.32	-0.52	-0.62	-0.73	-0.90
FBgn0032946	nrv3	0.41	0.53	0.36	0.50	0.96	0.67
FBgn0029147	NtR	0.58	0.84	0.40	0.52	0.48	0.48
FBgn0036640	nx2	0.03	-0.55	-0.93	-1.10	-1.05	-1.07
FBgn0034468	Obp56a	-0.27	0.10	0.50	1.16	1.07	0.95
FBgn0039678	Obp99a	0.20	0.32	0.14	-0.37	-0.42	-0.87
FBgn0040296	Ocho	-0.32	-0.63	-0.42	-0.75	-1.08	-0.83
FBgn0033901	O-fut1	-0.65	-0.99	-0.80	-0.23	-0.67	-0.32
FBgn0002997	ome	-0.07	0.01	0.00	0.66	0.66	0.96
FBgn0015271	Orc5	-0.34	-0.84	-0.55	-0.30	-0.82	-0.54
FBgn0019952	Orct	0.56	0.78	0.63	0.73	0.53	0.53
FBgn0040279	Osi14	-0.26	-0.11	-0.23	0.18	0.45	1.17
FBgn0037424	Osi15	-1.08	-0.23	-0.61	0.73	0.86	2.16
FBgn0037429	Osi19	-0.29	-0.03	-0.10	0.03	0.62	1.98
FBgn0027527	Osi6	-0.48	-0.55	-0.45	1.04	1.04	1.83

FBgn	Symbol	5-6 h	6-7 h	7-8 h	8-9 h	9-10 h	10-11 h
FBgn0037414	Osi7	-0.55	-0.14	-0.22	0.54	0.29	1.57
FBgn0037416	Osi9	-0.10	0.07	-0.13	0.04	0.22	1.26
FBgn0060296	pain	-0.08	-0.02	-0.02	0.20	0.32	0.76
FBgn0020389	Paps	-0.17	0.34	0.80	0.41	0.20	-0.04
FBgn0011692	pav	-0.11	-0.53	-0.93	-1.14	-1.08	-1.14
FBgn0004401	Pep	-0.78	-0.29	0.55	-0.49	-0.92	0.36
FBgn0040959	Peritrophin-15a	1.01	0.37	0.73	0.72	1.34	-0.04
FBgn0036529	pgant8	0.24	0.30	0.18	0.26	0.55	0.99
FBgn0003076	Pgm	-0.53	-0.29	-0.55	-0.82	-0.74	-1.09
FBgn0039779	PH4alphaSG2	-0.03	0.14	-0.11	-0.29	-0.44	-0.78
FBgn0016054	phr6-4	-0.09	-0.25	-0.29	-0.55	-0.61	-0.70
FBgn0003087	pim	0.00	-0.43	-0.52	-0.64	-0.91	-1.31
FBgn0003114	plu	-0.77	-0.85	-0.22	-0.59	-0.26	-0.88
FBgn0003124	polo	0.25	0.08	-0.39	-0.65	-0.76	-0.99
FBgn0014269	prod	-0.16	-0.04	0.27	-0.59	-0.68	-0.60
FBgn0015282	Pros26.4	0.90	0.78	0.78	0.51	0.37	0.61
FBgn0033520	Prx2540-1	1.76	-0.17	0.70	-0.01	0.13	0.90
FBgn0033518	Prx2540-2	1.78	-0.18	0.66	0.17	0.15	1.01
FBgn0003187	qua	-0.13	0.14	-0.04	0.55	0.52	0.93
FBgn0033881	RacGAP50C	0.23	-0.18	-0.50	-0.57	-1.05	-0.78
FBgn0024194	rasp	-0.32	-0.64	-0.75	-0.86	-0.94	-1.00
FBgn0010256	Rbp2	-1.00	-0.51	-0.66	-1.37	-0.92	-1.15
FBgn0017551	Rca1	-0.03	-0.21	0.09	-0.42	-0.72	-0.66
FBgn0016724	RfaBp	0.81	1.06	0.85	0.68	0.44	0.62
FBgn0032244	RfC3	-0.29	-0.76	-0.40	-0.51	-0.76	-0.40
FBgn0010173	RpA-70	0.13	-0.25	-0.06	-0.30	-0.72	-0.48
FBgn0003276	RpII140	-0.20	-0.60	-0.38	-0.35	-0.68	-0.39
FBgn0022981	rpk	-0.47	-0.70	-0.85	-0.90	-0.69	-0.93
FBgn0015288	RpL22	0.52	0.89	0.84	0.34	-0.04	0.24
FBgn0003279	RpL4	-0.93	-0.54	0.93	-0.34	-1.04	-0.68
FBgn0031035	RpS10b	-0.44	-0.39	0.73	-0.14	-0.60	0.01
FBgn0038277	RpS5b	-0.79	-0.98	0.15	-0.74	-1.15	-1.29
FBgn0003292	rt	-0.03	-0.03	0.11	0.42	0.42	0.77
FBgn0037672	sage	0.69	0.80	0.01	-0.65	-0.61	-0.36
FBgn0003313	sala	-0.29	-0.52	-0.32	-0.57	-0.54	-0.83
FBgn0035471	Sc2	-0.39	0.04	0.27	0.84	0.54	0.57
FBgn0025682	scf	0.34	0.66	0.70	0.30	0.40	0.53
FBgn0037889	scpr-A	-0.08	-0.24	-0.74	-1.13	-1.04	-1.27
FBgn0037888	scpr-B	0.06	-0.13	-0.46	-0.93	-0.77	-0.85
FBgn0037879	scpr-C	-0.07	-0.20	-0.73	-1.65	-1.21	-1.70
FBgn0004243	scra	-0.25	0.22	0.29	-0.40	-0.74	-0.60
FBgn0026361	sep5	-0.32	-0.99	-0.65	-0.72	-0.80	-0.68
FBgn0014879	Set	-0.15	-0.08	0.09	-0.38	-0.74	-0.76
FBgn0035772	Sh3beta	0.80	1.31	1.07	0.97	1.16	1.02
FBgn0003411	sisA	0.16	-0.04	0.01	-0.82	-1.01	-0.41
FBgn0010083	SmB	-0.70	-0.42	0.54	-0.46	-1.05	-0.81
FBgn0027783	SMC2	0.11	-0.21	-0.53	-0.40	-0.74	-0.42
FBgn0016983	smid	0.02	-0.39	-0.75	-0.41	-0.26	-0.26
FBgn0016940	snRNP69D	-0.49	-0.46	0.27	-0.40	-0.81	-0.64
FBgn0035710	SP1173	-0.08	0.44	-0.03	0.56	0.44	0.74
FBgn0024294	Spn43Aa	-0.79	1.72	1.32	1.01	0.87	0.52
FBgn0003495	spz	0.01	0.07	0.03	0.21	0.46	0.81
FBgn0020377	Sr-CII	-0.46	-1.12	-1.11	-0.56	-0.90	-0.65
FBgn0024285	Srp54	-0.55	-0.60	-0.08	-0.45	-0.81	-0.60
FBgn0051641	stai	-0.16	0.05	0.06	0.68	0.61	0.73
FBgn0003525	stg	0.09	0.09	0.36	-0.41	-0.78	-0.93
FBgn0033782	sug	-0.12	-0.08	0.02	-0.60	-0.95	-0.89
FBgn0013343	Syx1A	0.13	-0.11	-0.70	0.06	0.37	0.09
FBgn0011291	Taf11	-0.17	-0.42	-0.38	-0.49	-0.48	-0.69

FBgn	Symbol	5-6 h	6-7 h	7-8 h	8-9 h	9-10 h	10-11 h
FBgn0031506	Tdp1	-0.66	-1.04	-0.96	-0.98	-0.96	-1.01
FBgn0043472	tef	0.13	-0.12	-0.12	-0.27	-0.65	-0.69
FBgn0003701	thr	-0.18	-0.58	-0.84	-0.60	-0.77	-0.49
FBgn0025879	Timp	-0.05	0.12	-0.08	0.07	0.28	0.74
FBgn0003714	tko	-0.76	0.12	0.10	-0.38	-0.56	-0.88
FBgn0003720	tll	0.44	0.12	0.01	-0.25	-0.58	-0.68
FBgn0026320	Tom	-0.24	0.39	0.44	-0.29	-0.70	-0.61
FBgn0003732	Top2	-0.08	-0.63	-0.75	-0.46	-0.56	-0.42
FBgn0010423	TpnC47D	-1.24	-1.23	-1.50	-0.23	-0.13	-0.38
FBgn0026319	Traf1	-0.16	-0.39	0.07	-0.39	-0.66	-0.75
FBgn0046687	Tre1	0.17	0.19	0.18	0.66	0.45	0.73
FBgn0003748	Treh	-0.36	-0.23	-0.58	-0.53	-0.74	-1.06
FBgn0024361	Tsp2A	-0.06	-0.05	-0.01	0.61	0.81	0.76
FBgn0029506	Tsp42Ee	0.98	1.04	0.50	0.96	0.80	0.53
FBgn0033127	Tsp42Ef	-0.21	-0.14	-0.08	0.38	0.67	0.91
FBgn0035936	Tsp66E	-0.83	-0.34	-0.17	0.94	0.71	1.39
FBgn0026076	UBL3	0.43	0.45	0.46	0.55	0.43	0.76
FBgn0010288	Uch	-1.16	-1.10	-0.76	-0.35	-0.30	-0.13
FBgn0040260	Ugt36Bc	0.64	0.18	0.19	-0.09	-0.56	-0.92
FBgn0040091	Ugt58Fa	0.28	0.68	0.26	1.01	0.86	1.36
FBgn0013349	UTPase	-0.59	-0.64	0.00	-0.54	-1.04	-0.90
FBgn0027779	VhaSFD	0.43	0.09	-0.12	0.63	0.32	0.78
FBgn0038134	Wnt8	-0.16	-1.27	-0.74	-0.50	-0.66	-0.22
FBgn0030805	wus	0.01	0.12	0.25	0.45	0.29	0.91
FBgn0021872	Xbp1	0.41	1.06	0.81	0.36	0.31	0.45
FBgn0022959	yps	-0.14	0.43	0.91	-0.04	-0.49	0.35

8.3. Direct target genes of Imd and Mef2

Table V - Direct target genes list for Imd and Mef2, showing shared target genes.

Symbol	FBgn	Imd target	Mef2 target	Common
Act57B	FBgn0000044	yes	yes	yes
betaTub60D	FBgn0003888	yes	yes	yes
CG11825	FBgn0033519	yes	yes	yes
CG30349	FBgn0050349	yes	yes	yes
cnn	FBgn0013765	yes	yes*	yes
Dll	FBgn0000157	yes	no	no
Dp	FBgn0011763	yes	yes	yes
Imd	FBgn0039039	yes	yes	yes
m6	FBgn0002632	yes	yes	yes
mam	FBgn0002643	yes	yes*	yes
mbl	FBgn0053197	yes	yes	yes
mir-1	FBgn0046834	yes	yes	yes
pnr	FBgn0003117	yes	yes*	yes
prd	FBgn0003145	yes	no	no
Tina-1	FBgn0035083	yes	yes	yes
Tm1	FBgn0003721	yes	yes	yes
tou	FBgn0033636	yes	yes	yes
18w	FBgn0004364	yes	no	no

Symbol	FBgn	lmd target	Mef2 target	Common
ab	FBgn0259750	yes	yes	yes
Act87E	FBgn0000046	yes	yes	yes
aop	FBgn0000097	yes	yes	yes
asrij	FBgn0034793	yes	yes	yes
blow	FBgn0004133	yes	yes	yes
by	FBgn0000244	yes	no	no
CG1074	FBgn0037250	yes	no	no
CG11033	FBgn0037659	yes	yes	yes
CG12203	FBgn0031021	yes	yes	yes
CG13838	FBgn0039041	yes	yes	yes
CG14687	FBgn0037835	yes	yes	yes
CG14757	FBgn0033274	yes	yes	yes
CG17181	FBgn0035144	yes	yes	yes
CG30035	FBgn0050035	yes	yes	yes
CG31038	FBgn0051038	yes	yes	yes
CG32982	FBgn0052982	yes	yes	yes
CG4984	FBgn0034267	yes	yes	yes
CG5080	FBgn0031313	yes	yes	yes
CG9005	FBgn0033638	yes	yes	yes
CG9416	FBgn0034438	yes	yes	yes
chic	FBgn0000308	yes	yes	yes
CR18854	FBgn0042174	yes	yes*	yes
csul	FBgn0015925	yes	no	no
dome	FBgn0043903	yes	yes	yes
Dsp1	FBgn0011764	yes	yes	yes
Git	FBgn0033539	yes	yes	yes
Glycogenin	FBgn0034603	yes	yes	yes
gol	FBgn0004919	yes	yes	yes
HLHmgamma	FBgn0002735	yes	yes	yes
Hph	FBgn0086689	yes	yes	yes
hth	FBgn0001235	yes	yes	yes
jing	FBgn0086655	yes	yes	yes
jp	FBgn0032129	yes	yes	yes
lbl	FBgn0008651	yes	no	no
lola	FBgn0005630	yes	yes	yes
malpha	FBgn0002732	yes	yes	yes
Mef2	FBgn0011656	yes	yes	yes
MESK2	FBgn0043070	yes	no	no
mthl5	FBgn0037960	yes	no	no
ninaD	FBgn0002939	yes	yes	yes
Pak	FBgn0014001	yes	yes	yes
Pax	FBgn0041789	yes	yes	yes
Pfrx	FBgn0027621	yes	yes	yes
rib	FBgn0003254	yes	no	no
Rya-r44F	FBgn0011286	yes	yes	yes
shot	FBgn0013733	yes	yes*	yes
sns	FBgn0024189	yes	yes	yes
Srp54	FBgn0024285	yes	no	no
sug	FBgn0033782	yes	no	no
svp	FBgn0003651	yes	yes	yes
tal	FBgn0087003	yes	no	no
tsh	FBgn0003866	yes	yes	yes

Symbol	FBgn	<i>lmd</i> target	<i>Mef2</i> target	Common
ttk	FBgn0003870	yes	yes*	yes
Uch	FBgn0010288	yes	yes	yes
Hsp70Ab	FBgn0013276	yes	no	no
RpS26	FBgn0004413	yes	no	no
Ance-5	FBgn0035076	no	yes	no
ball	FBgn0027889	no	yes	no
bap	FBgn0004862	no	yes	no
bib	FBgn0000180	no	yes	no
bowl	FBgn0004893	no	yes	no
C15	FBgn0004863	no	yes	no
CG10641	FBgn0032731	no	yes	no
CG11755	FBgn0037611	no	yes	no
CG13011	FBgn0261245	no	yes	no
CG13335	FBgn0033857	no	yes	no
CG13784	FBgn0031897	no	yes	no
CG14207	FBgn0031037	no	yes	no
CG14612	FBgn0040670	no	yes	no
CG15027	FBgn0030611	no	yes	no
CG15105	FBgn0034412	no	yes	no
CG15353	FBgn0040718	no	yes	no
CG17124	FBgn0032297	no	yes	no
CG17273	FBgn0027493	no	yes	no
CG17836	FBgn0261113	no	yes	no
CG18446	FBgn0033458	no	yes	no
CG2010	FBgn0039667	no	yes	no
CG2165	FBgn0259214	no	yes	no
CG2246	FBgn0039790	no	yes	no
CG2791	FBgn0037533	no	yes	no
CG30015	FBgn0050015	no	yes	no
CG30460	FBgn0050460	no	yes	no
CG30492	FBgn0050492	no	yes	no
CG31365	FBgn0051365	no	yes	no
CG33108	FBgn0053108	no	yes	no
CG33505	FBgn0053505	no	yes	no
CG4239	FBgn0030745	no	yes	no
CG4567	FBgn0243517	no	yes	no
CG4572	FBgn0038738	no	yes	no
CG4679	FBgn0033816	no	yes	no
CG4829	FBgn0030796	no	yes	no
CG5174	FBgn0034345	no	yes	no
CG5177	FBgn0031908	no	yes	no
CG6900	FBgn0030958	no	yes	no
CG6904	FBgn0038293	no	yes	no
CG6930	FBgn0086910	no	yes	no
CG7655	FBgn0038536	no	yes	no
CG8147	FBgn0043791	no	yes	no
CG8173	FBgn0030864	no	yes	no
CG8315	FBgn0034058	no	yes	no
CG8557	FBgn0030842	no	yes	no
CG8713	FBgn0033257	no	yes	no
CG9296	FBgn0032059	no	yes	no
CG9626	FBgn0037565	no	yes	no

Symbol	FBgn	<i>lmd</i> target	<i>Mef2</i> target	Common
CG9663	FBgn0031516	no	yes	no
CG9752	FBgn0034614	no	yes	no
CG9837	FBgn0037635	no	yes	no
coro	FBgn0033109	no	yes	no
CycG	FBgn0039858	no	yes	no
DI	FBgn0000463	no	yes	no
Doa	FBgn0259220	no	yes	no
Dph5	FBgn0024558	no	yes	no
dpn	FBgn0010109	no	yes	no
dpp	FBgn0000490	no	yes	no
Drip	FBgn0015872	no	yes	no
drl	FBgn0015380	no	yes	no
Dys	FBgn0260003	no	yes	no
E(spl)	FBgn0000591	no	yes	no
E2f	FBgn0011766	no	yes	no
EcR	FBgn0000546	no	yes	no
esn	FBgn0028642	no	yes	no
eve	FBgn0000606	no	yes	no
eya	FBgn0000320	no	yes	no
Fas3	FBgn0000636	no	yes	no
fd64A	FBgn0004895	no	yes	no
fray	FBgn0023083	no	yes	no
gcl	FBgn0005695	no	yes	no
Gpdh	FBgn0001128	no	yes	no
gukh	FBgn0026239	no	yes	no
Him	FBgn0030900	no	yes	no
HLH54F	FBgn0022740	no	yes	no
HLHm3	FBgn0002609	no	yes	no
HLHm7	FBgn0002633	no	yes	no
HLHmbeta	FBgn0002733	no	yes	no
hoip	FBgn0015393	no	yes	no
htl	FBgn0010389	no	yes	no
hts	FBgn0004873	no	yes	no
Hus1-like	FBgn0026417	no	yes	no
if	FBgn0001250	no	yes	no
insc	FBgn0011674	no	yes	no
Keap1	FBgn0038475	no	yes	no
kn	FBgn0001319	no	yes	no
Kr	FBgn0001325	no	yes	no
KrT95D	FBgn0020647	no	yes	no
I(1)G0084	FBgn0087008	no	yes	no
I(2)k01209	FBgn0022029	no	yes	no
LanB1	FBgn0002527	no	yes	no
m4	FBgn0002629	no	yes	no
Mhc	FBgn0086783	no	yes	no
mib2	FBgn0086442	no	yes	no
Mlc2	FBgn0002773	no	yes	no
Mlp60A	FBgn0259209	no	yes	no
Mlp84B	FBgn0014863	no	yes	no
Mp20	FBgn0002789	no	yes	no
mtSSB	FBgn0010438	no	yes	no
NaCP60E	FBgn0085434	no	yes	no

Symbol	FBgn	<i>lmd</i> target	<i>Mef2</i> target	Common
nau	FBgn0002922	no	yes	no
NetA	FBgn0015773	no	yes	no
NetB	FBgn0015774	no	yes	no
neur	FBgn0002932	no	yes	no
Oda	FBgn0014184	no	yes	no
Odd	FBgn0002985	no	yes	no
Orc1	FBgn0022772	no	yes	no
osa	FBgn0003013	no	yes	no
pnt	FBgn0003118	no	yes	no
pont	FBgn0040078	no	yes	no
ps	FBgn0026188	no	yes	no
Ptx1	FBgn0020912	no	yes	no
rdo	FBgn0243486	no	yes	no
RfaBp	FBgn0087002	no	yes	no
rgr	FBgn0033310	no	yes	no
robo	FBgn0005631	no	yes	no
RpS5a	FBgn0002590	no	yes	no
run	FBgn0003300	no	yes	no
SdhB	FBgn0014028	no	yes	no
sli	FBgn0003425	no	yes	no
slp1	FBgn0003430	no	yes	no
Snr1	FBgn0011715	no	yes	no
so	FBgn0003460	no	yes	no
sog	FBgn0003463	no	yes	no
Sox14	FBgn0005612	no	yes	no
spi	FBgn0005672	no	yes	no
sqz	FBgn0010768	no	yes	no
Src42A	FBgn0004603	no	yes	no
Stat92E	FBgn0016917	no	yes	no
stg	FBgn0003525	no	yes	no
stumps	FBgn0020299	no	yes	no
tara	FBgn0040071	no	yes	no
Tig	FBgn0011722	no	yes	no
tkv	FBgn0003716	no	yes	no
tok	FBgn0004885	no	yes	no
trx	FBgn0003862	no	yes	no
twi	FBgn0003900	no	yes	no
Ubx	FBgn0003944	no	yes	no
up	FBgn0004169	no	yes	no
vkg	FBgn0016075	no	yes	no
wfs1	FBgn0039003	no	yes	no
wgn	FBgn0030941	no	yes	no
wupA	FBgn0004028	no	yes	no
zfh1	FBgn0004606	no	yes	no

9. References

- Adams, M. D., et al. (2000). The genome sequence of *Drosophila melanogaster*. *Science* **287**, 2185-95.
- Arnone, M. I., and Davidson, E. H. (1997). The hardwiring of development: organization and function of genomic regulatory systems. *Development* **124**, 1851-64.
- Artero, R. D., Castanon, I., and Baylies, M. K. (2001). The immunoglobulin-like protein Hibris functions as a dose-dependent regulator of myoblast fusion and is differentially controlled by Ras and Notch signaling. *Development* **128**, 4251-64.
- Balagopalan, L., Keller, C. A., and Abmayr, S. M. (2001). Loss-of-function mutations reveal that the *Drosophila* nautilus gene is not essential for embryonic myogenesis or viability. *Dev Biol* **231**, 374-82.
- Barolo, S., Carver, L. A., and Posakony, J. W. (2000). GFP and beta-galactosidase transformation vectors for promoter/enhancer analysis in *Drosophila*. *Biotechniques* **29**, 726, 728, 730, 732.
- Baylies, M. K., and Bate, M. (1996). twist: a myogenic switch in *Drosophila*. *Science* **272**, 1481-4.
- Baylies, M. K., Bate, M., and Ruiz Gomez, M. (1998). Myogenesis: a view from *Drosophila*. *Cell* **93**, 921-7.
- Berkes, C. A., and Tapscott, S. J. (2005). MyoD and the transcriptional control of myogenesis. *Semin Cell Dev Biol* **16**, 585-95.
- Black, B. L., and Olson, E. N. (1998). Transcriptional control of muscle development by myocyte enhancer factor-2 (MEF2) proteins. *Annu Rev Cell Dev Biol* **14**, 167-96.
- Blackwood, E. M., and Kadonaga, J. T. (1998). Going the distance: a current view of enhancer action. *Science* **281**, 61-3.
- Bour, B. A., Chakravarti, M., West, J. M., and Abmayr, S. M. (2000). *Drosophila* SNS, a member of the immunoglobulin superfamily that is essential for myoblast fusion. *Genes Dev* **14**, 1498-511.
- Bour, B. A., O'Brien, M. A., Lockwood, W. L., Goldstein, E. S., Bodmer, R., Taghert, P. H., Abmayr, S. M., and Nguyen, H. T. (1995). *Drosophila* MEF2, a transcription factor that is essential for myogenesis. *Genes Dev* **9**, 730-41.
- Bourgouin, C., Lundgren, S. E., and Thomas, J. B. (1992). Apterous is a *Drosophila* LIM domain gene required for the development of a subset of embryonic muscles. *Neuron* **9**, 549-61.
- Brand, A. H., and Perrimon, N. (1993). Targeted gene expression as a means of altering cell fates and generating dominant phenotypes. *Development* **118**, 401-15.
- Braun, T., Rudnicki, M. A., Arnold, H. H., and Jaenisch, R. (1992). Targeted inactivation of the muscle regulatory gene Myf-5 results in abnormal rib development and perinatal death. *Cell* **71**, 369-82.

- Breitling R, A. P., Amtmann A, Herzyk P. (2004). Rank products: a simple, yet powerful, new method to detect differentially regulated genes in replicated microarray experiments. *FEBS Lett* **573**, 83-92.
- Brugnera, E., Haney, L., Grimsley, C., Lu, M., Walk, S. F., Tosello-Tramont, A. C., Macara, I. G., Madhani, H., Fink, G. R., and Ravichandran, K. S. (2002). Unconventional Rac-GEF activity is mediated through the Dock180-ELMO complex. *Nat Cell Biol* **4**, 574-82.
- Callahan, C. A., Bonkovsky, J. L., Scully, A. L., and Thomas, J. B. (1996). derailed is required for muscle attachment site selection in *Drosophila*. *Development* **122**, 2761-7.
- Campos-Ortega, J. A., and Hartenstein, V. (1997). "The embryonic development of *Drosophila melanogaster*." Springer, Berlin ; New York.
- Canon, J., and Banerjee, U. (2003). *In vivo* analysis of a developmental circuit for direct transcriptional activation and repression in the same cell by a Runx protein. *Genes Dev* **17**, 838-43.
- Carmena, A., Buff, E., Halfon, M. S., Gisselbrecht, S., Jimenez, F., Baylies, M. K., and Michelson, A. M. (2002). Reciprocal regulatory interactions between the Notch and Ras signaling pathways in the *Drosophila* embryonic mesoderm. *Dev Biol* **244**, 226-42.
- Chen, E. H., and Olson, E. N. (2001). Antisocial, an intracellular adaptor protein, is required for myoblast fusion in *Drosophila*. *Dev Cell* **1**, 705-15.
- Chen, E. H., Pryce, B. A., Tzeng, J. A., Gonzalez, G. A., and Olson, E. N. (2003). Control of myoblast fusion by a guanine nucleotide exchange factor, loner, and its effector ARF6. *Cell* **114**, 751-62.
- Clark, A. G., et al. (2007). Evolution of genes and genomes on the *Drosophila* phylogeny. *Nature* **450**, 203-18.
- Cripps, R. M., Black, B. L., Zhao, B., Lien, C. L., Schulz, R. A., and Olson, E. N. (1998). The myogenic regulatory gene Mef2 is a direct target for transcriptional activation by Twist during *Drosophila* myogenesis. *Genes Dev* **12**, 422-34.
- Cripps, R. M., Lovato, T. L., and Olson, E. N. (2004). Positive autoregulation of the Myocyte enhancer factor-2 myogenic control gene during somatic muscle development in *Drosophila*. *Dev Biol* **267**, 536-47.
- Damm, C., Wolk, A., Buttgereit, D., Loher, K., Wagner, E., Lilly, B., Olson, E. N., Hasenpusch-Theil, K., and Renkawitz-Pohl, R. (1998). Independent regulatory elements in the upstream region of the *Drosophila* beta 3 tubulin gene (beta Tub60D) guide expression in the dorsal vessel and the somatic muscles. *Dev Biol* **199**, 138-49.
- Davidson, E. H. (2006). "The regulatory genome : gene regulatory networks in development and evolution." Elsevier/Academic Press, Amsterdam ; London.
- Davis, R. L., Weintraub, H., and Lassar, A. B. (1987). Expression of a single transfected cDNA converts fibroblasts to myoblasts. *Cell* **51**, 987-1000.
- Deng, H., Hughes, S. C., Bell, J. B., and Simmonds, A. J. (2009). Alternative requirements for Vestigial, Scalloped, and Dmef2 during muscle differentiation in *Drosophila melanogaster*. *Mol Biol Cell* **20**, 256-69.
- Doberstein, S. K., Fetter, R. D., Mehta, A. Y., and Goodman, C. S. (1997). Genetic analysis of myoblast fusion: blown fuse is required for progression beyond the prefusion complex. *J Cell Biol* **136**, 1249-61.

- Duan, H., and Nguyen, H. T. (2006). Distinct Posttranscriptional Mechanisms Regulate the Activity of the Zn Finger Transcription Factor *Lame duck* during *Drosophila* Myogenesis. *Mol Cell Biol* **26**, 1414-23.
- Duan, H., Skeath, J. B., and Nguyen, H. T. (2001). *Drosophila* *Lame duck*, a novel member of the Gli superfamily, acts as a key regulator of myogenesis by controlling fusion-competent myoblast development. *Development* **128**, 4489-500.
- Dworak, H. A., Charles, M. A., Pellerano, L. B., and Sink, H. (2001). Characterization of *Drosophila* *hibris*, a gene related to human nephrin. *Development* **128**, 4265-76.
- Elgar, S. J., Han, J., and Taylor, M. V. (2008). *mef2* activity levels differentially affect gene expression during *Drosophila* muscle development. *Proc Natl Acad Sci U S A* **105**, 918-23.
- Erickson, M. R., Galletta, B. J., and Abmayr, S. M. (1997). *Drosophila* myoblast city encodes a conserved protein that is essential for myoblast fusion, dorsal closure, and cytoskeletal organization. *J Cell Biol* **138**, 589-603.
- Frasch, M. (1995). Induction of visceral and cardiac mesoderm by ectodermal Dpp in the early *Drosophila* embryo. *Nature* **374**, 464-7.
- Furlong, E. E., Andersen, E. C., Null, B., White, K. P., and Scott, M. P. (2001a). Patterns of gene expression during *Drosophila* mesoderm development. *Science* **293**, 1629-33.
- Furlong, E. E., Profitt, D., and Scott, M. P. (2001b). Automated sorting of live transgenic embryos. *Nat Biotechnol* **19**, 153-6.
- Ganguly, A., Jiang, J., and Ip, Y. T. (2005). *Drosophila* WntD is a target and an inhibitor of the Dorsal/Twist/Snail network in the gastrulating embryo. *Development* **132**, 3419-29.
- Geisbrecht, E. R., Haralalka, S., Swanson, S. K., Florens, L., Washburn, M. P., and Abmayr, S. M. (2008). *Drosophila* ELMO/CED-12 interacts with Myoblast city to direct myoblast fusion and ommatidial organization. *Dev Biol* **314**, 137-49.
- Gilbert, S. F. (2006). "Developmental biology." Sinauer Associates Inc. Publishers, Sunderland, Mass.
- Gossett, L. A., Kelvin, D. J., Sternberg, E. A., and Olson, E. N. (1989). A new myocyte-specific enhancer-binding factor that recognizes a conserved element associated with multiple muscle-specific genes. *Mol Cell Biol* **9**, 5022-33.
- Gray, S., Cai, H., Barolo, S., and Levine, M. (1995). Transcriptional repression in the *Drosophila* embryo. *Philos Trans R Soc Lond B Biol Sci* **349**, 257-62.
- Gray, S., and Levine, M. (1996). Short-range transcriptional repressors mediate both quenching and direct repression within complex loci in *Drosophila*. *Genes Dev* **10**, 700-10.
- Hakeda-Suzuki, S., Ng, J., Tzu, J., Dietzl, G., Sun, Y., Harms, M., Nardine, T., Luo, L., and Dickson, B. J. (2002). Rac function and regulation during *Drosophila* development. *Nature* **416**, 438-42.
- Halfon, M. S., Carmena, A., Gisselbrecht, S., Sackerson, C. M., Jimenez, F., Baylies, M. K., and Michelson, A. M. (2000). Ras pathway specificity is determined by the integration of multiple signal-activated and tissue-restricted transcription factors. *Cell* **103**, 63-74.
- Hartenstein, V. (2006). The muscle pattern of *drosophila*. In "Muscle development in *drosophila*" (H. Sink, Ed.), pp. 207. Landes Bioscience/Eurekah.com ;

- Springer Science + Business Media, Georgetown, Tex.
New York, N.Y.
- Hasty, P., Bradley, A., Morris, J. H., Edmondson, D. G., Venuti, J. M., Olson, E. N., and Klein, W. H. (1993). Muscle deficiency and neonatal death in mice with a targeted mutation in the myogenin gene. *Nature* **364**, 501-6.
- Hinz, U., Wolk, A., and Renkawitz-Pohl, R. (1992). Ultrabithorax is a regulator of beta 3 tubulin expression in the Drosophila visceral mesoderm. *Development* **116**, 543-54.
- Hummel, T., Schimmelpfeng, K., and Klammt, C. (1999). Commissure formation in the embryonic CNS of Drosophila. *Dev Biol* **209**, 381-98.
- Ip, Y. T., Park, R. E., Kosman, D., Yazdanbakhsh, K., and Levine, M. (1992). dorsal-twist interactions establish snail expression in the presumptive mesoderm of the Drosophila embryo. *Genes Dev* **6**, 1518-30.
- Jakobsen, J. S., Braun, M., Astorga, J., Gustafson, E. H., Sandmann, T., Karzynski, M., Carlsson, P., and Furlong, E. E. (2007). Temporal ChIP-on-chip reveals Biniou as a universal regulator of the visceral muscle transcriptional network. *Genes Dev* **21**, 2448-60.
- Jia, J., and Jiang, J. (2006). Decoding the Hedgehog signal in animal development. *Cell Mol Life Sci* **63**, 1249-65.
- Jimenez, G., Paroush, Z., and Ish-Horowicz, D. (1997). Groucho acts as a corepressor for a subset of negative regulators, including Hairy and Engrailed. *Genes Dev* **11**, 3072-82.
- Kassar-Duchossoy, L., Gayraud-Morel, B., Gomes, D., Rocancourt, D., Buckingham, M., Shinin, V., and Tajbakhsh, S. (2004). Mrf4 determines skeletal muscle identity in Myf5:Myod double-mutant mice. *Nature* **431**, 466-71.
- Keller, C. A., Erickson, M. S., and Abmayr, S. M. (1997). Misexpression of nautilus induces myogenesis in cardioblasts and alters the pattern of somatic muscle fibers. *Dev Biol* **181**, 197-212.
- Kelly, K. K., Meadows, S. M., and Cripps, R. M. (2002). Drosophila MEF2 is a direct regulator of Actin57B transcription in cardiac, skeletal, and visceral muscle lineages. *Mech Dev* **110**, 39-50.
- Kesper, D. A., Stute, C., Buttgereit, D., Kreiskother, N., Vishnu, S., Fischbach, K. F., and Renkawitz-Pohl, R. (2007). Myoblast fusion in Drosophila melanogaster is mediated through a fusion-restricted myogenic-adhesive structure (FuRMAS). *Dev Dyn* **236**, 404-15.
- Kim, S., Shilagardi, K., Zhang, S., Hong, S. N., Sens, K. L., Bo, J., Gonzalez, G. A., and Chen, E. H. (2007). A critical function for the actin cytoskeleton in targeted exocytosis of prefusion vesicles during myoblast fusion. *Dev Cell* **12**, 571-86.
- Kramer, S. G., Kidd, T., Simpson, J. H., and Goodman, C. S. (2001). Switching repulsion to attraction: changing responses to slit during transition in mesoderm migration. *Science* **292**, 737-40.
- Kremser, T., Gajewski, K., Schulz, R. A., and Renkawitz-Pohl, R. (1999). Tinman regulates the transcription of the beta3 tubulin gene (betaTub60D) in the dorsal vessel of Drosophila. *Dev Biol* **216**, 327-39.
- Leptin, M. (1991). twist and snail as positive and negative regulators during Drosophila mesoderm development. *Genes Dev* **5**, 1568-76.
- Lilly, B., Galewsky, S., Firulli, A. B., Schulz, R. A., and Olson, E. N. (1994). D-MEF2: a MADS box transcription factor expressed in differentiating

- mesoderm and muscle cell lineages during *Drosophila* embryogenesis. *Proc Natl Acad Sci U S A* **91**, 5662-6.
- Lilly, B., Zhao, B., Ranganayakulu, G., Paterson, B. M., Schulz, R. A., and Olson, E. N. (1995). Requirement of MADS domain transcription factor D-MEF2 for muscle formation in *Drosophila*. *Science* **267**, 688-93.
- Lin, M. H., Nguyen, H. T., Dybala, C., and Storti, R. V. (1996). Myocyte-specific enhancer factor 2 acts cooperatively with a muscle activator region to regulate *Drosophila* tropomyosin gene muscle expression. *Proc Natl Acad Sci U S A* **93**, 4623-8.
- Lin, S. C., and Storti, R. V. (1997). Developmental regulation of the *Drosophila* Tropomyosin I (TmI) gene is controlled by a muscle activator enhancer region that contains multiple cis-elements and binding sites for multiple proteins. *Dev Genet* **20**, 297-306.
- Liotta, D., Han, J., Elgar, S., Garvey, C., Han, Z., and Taylor, M. V. (2007). The Him gene reveals a balance of inputs controlling muscle differentiation in *Drosophila*. *Curr Biol* **17**, 1409-13.
- Lodish, H. F., Berk, A., Zipursky, S. L., Matsudaira, P., Baltimore, D., and Darnell, J. E. (2000). "Molecular Cell Biology." Scientific American Books : Distributed by W.H. Freeman and Co., New York.
- Luo, L., Liao, Y. J., Jan, L. Y., and Jan, Y. N. (1994). Distinct morphogenetic functions of similar small GTPases: *Drosophila* Drac1 is involved in axonal outgrowth and myoblast fusion. *Genes Dev* **8**, 1787-802.
- Martin, B. S., Ruiz-Gomez, M., Landgraf, M., and Bate, M. (2001). A distinct set of founders and fusion-competent myoblasts make visceral muscles in the *Drosophila* embryo. *Development* **128**, 3331-8.
- Massarwa, R., Carmon, S., Shilo, B. Z., and Schejter, E. D. (2007). WIP/WASp-based actin-polymerization machinery is essential for myoblast fusion in *Drosophila*. *Dev Cell* **12**, 557-69.
- Menon, S. D., and Chia, W. (2001). *Drosophila* rolling pebbles: a multidomain protein required for myoblast fusion that recruits D-Titin in response to the myoblast attractant Dumbfounded. *Dev Cell* **1**, 691-703.
- Molkentin, J. D., Black, B. L., Martin, J. F., and Olson, E. N. (1995). Cooperative activation of muscle gene expression by MEF2 and myogenic bHLH proteins. *Cell* **83**, 1125-36.
- Morin, S., Charron, F., Robitaille, L., and Nemer, M. (2000). GATA-dependent recruitment of MEF2 proteins to target promoters. *Embo J* **19**, 2046-55.
- Morin, S., Pozzulo, G., Robitaille, L., Cross, J., and Nemer, M. (2005). MEF2-dependent recruitment of the HAND1 transcription factor results in synergistic activation of target promoters. *J Biol Chem* **280**, 32272-8.
- Nguyen, H. T., Bodmer, R., Abmayr, S. M., McDermott, J. C., and Spoerel, N. A. (1994). D-mef2: a *Drosophila* mesoderm-specific MADS box-containing gene with a biphasic expression profile during embryogenesis. *Proc Natl Acad Sci U S A* **91**, 7520-4.
- Nguyen, H. T., and Xu, X. (1998). *Drosophila* mef2 expression during mesoderm development is controlled by a complex array of cis-acting regulatory modules. *Dev Biol* **204**, 550-66.
- Nicholson, L., and Keshishian, H. (2006). Neuromuscular development: connectivity and plasticity. In "Muscle development in drosophila" (H. Sink, Ed.), pp. 207. Landes Bioscience/Eurekah.com ; Springer Science + Business Media, Georgetown, Tex.

- New York, N.Y.
- Olson, E. N., Perry, M., and Schulz, R. A. (1995). Regulation of muscle differentiation by the MEF2 family of MADS box transcription factors. *Dev Biol* **172**, 2-14.
- O'Neill, L. A. (2000). The interleukin-1 receptor/Toll-like receptor superfamily: signal transduction during inflammation and host defense. *Sci STKE* **2000**, RE1.
- Onel, S. F., and Renkawitz-Pohl, R. (2009). FuRMAS: triggering myoblast fusion in *Drosophila*. *Dev Dyn* **238**, 1513-25.
- Peterson, B. K., Hare, E. E., Iyer, V. N., Storage, S., Conner, L., Papaj, D. R., Kurashima, R., Jang, E., and Eisen, M. B. (2009). Big genomes facilitate the comparative identification of regulatory elements. *PLoS One* **4**, e4688.
- Price, M. A., and Kalderon, D. (1999). Proteolysis of cubitus interruptus in *Drosophila* requires phosphorylation by protein kinase A. *Development* **126**, 4331-9.
- Qiu, F., Brendel, S., Cunha, P. M., Astola, N., Song, B., Furlong, E. E., Leonard, K. R., and Bullard, B. (2005). Myofilin, a protein in the thick filaments of insect muscle. *J Cell Sci* **118**, 1527-36.
- Rau, A., Buttgerit, D., Holz, A., Fetter, R., Doberstein, S. K., Paululat, A., Staudt, N., Skeath, J., Michelson, A. M., and Renkawitz-Pohl, R. (2001). rolling pebbles (rols) is required in *Drosophila* muscle precursors for recruitment of myoblasts for fusion. *Development* **128**, 5061-73.
- Richards, S., et al. (2005). Comparative genome sequencing of *Drosophila pseudoobscura*: chromosomal, gene, and cis-element evolution. *Genome Res* **15**, 1-18.
- Richardson, B. E., Nowak, S. J., and Baylies, M. K. (2008). Myoblast fusion in fly and vertebrates: new genes, new processes and new perspectives. *Traffic* **9**, 1050-9.
- Riechmann, V., Irion, U., Wilson, R., Grosskortenhaus, R., and Leptin, M. (1997). Control of cell fates and segmentation in the *Drosophila* mesoderm. *Development* **124**, 2915-22.
- Rubin, G. M., and Lewis, E. B. (2000). A brief history of *Drosophila*'s contributions to genome research. *Science* **287**, 2216-8.
- Rudnicki, M. A., Braun, T., Hinuma, S., and Jaenisch, R. (1992). Inactivation of MyoD in mice leads to up-regulation of the myogenic HLH gene Myf-5 and results in apparently normal muscle development. *Cell* **71**, 383-90.
- Rudnicki, M. A., Schnegelsberg, P. N., Stead, R. H., Braun, T., Arnold, H. H., and Jaenisch, R. (1993). MyoD or Myf-5 is required for the formation of skeletal muscle. *Cell* **75**, 1351-9.
- Ruiz-Gomez, M., Coutts, N., Price, A., Taylor, M. V., and Bate, M. (2000). *Drosophila* dumbfounded: a myoblast attractant essential for fusion. *Cell* **102**, 189-98.
- Ruiz-Gomez, M., Coutts, N., Suster, M. L., Landgraf, M., and Bate, M. (2002). myoblasts incompetent encodes a zinc finger transcription factor required to specify fusion-competent myoblasts in *Drosophila*. *Development* **129**, 133-41.
- Ruiz-Gomez, M., Romani, S., Hartmann, C., Jackle, H., and Bate, M. (1997). Specific muscle identities are regulated by Kruppel during *Drosophila* embryogenesis. *Development* **124**, 3407-14.

- Rushton, E., Drysdale, R., Abmayr, S. M., Michelson, A. M., and Bate, M. (1995). Mutations in a novel gene, myoblast city, provide evidence in support of the founder cell hypothesis for Drosophila muscle development. *Development* **121**, 1979-88.
- Sandmann, T., Girardot, C., Brehme, M., Tongprasit, W., Stolz, V., and Furlong, E. E. (2007). A core transcriptional network for early mesoderm development in Drosophila melanogaster. *Genes Dev* **21**, 436-49.
- Sandmann, T., Jakobsen, J. S., and Furlong, E. E. (2006a). ChIP-on-chip protocol for genome-wide analysis of transcription factor binding in Drosophila melanogaster embryos. *Nat Protoc* **1**, 2839-55.
- Sandmann, T., Jensen, L. J., Jakobsen, J. S., Karzynski, M. M., Eichenlaub, M. P., Bork, P., and Furlong, E. E. (2006b). A temporal map of transcription factor activity: mef2 directly regulates target genes at all stages of muscle development. *Dev Cell* **10**, 797-807.
- Schafer, G., Weber, S., Holz, A., Bogdan, S., Schumacher, S., Muller, A., Renkawitz-Pohl, R., and Onel, S. F. (2007). The Wiskott-Aldrich syndrome protein (WASP) is essential for myoblast fusion in Drosophila. *Dev Biol* **304**, 664-74.
- Schroter, R. H., Buttgereit, D., Beck, L., Holz, A., and Renkawitz-Pohl, R. (2006). Blown fuse regulates stretching and outgrowth but not myoblast fusion of the circular visceral muscles in Drosophila. *Differentiation* **74**, 608-21.
- Schroter, R. H., Lier, S., Holz, A., Bogdan, S., Klambt, C., Beck, L., and Renkawitz-Pohl, R. (2004). kette and blown fuse interact genetically during the second fusion step of myogenesis in Drosophila. *Development* **131**, 4501-9.
- Sims, D., Bursteinas, B., Gao, Q., Zvelebil, M., and Baum, B. (2006). FLIGHT: database and tools for the integration and cross-correlation of large-scale RNAi phenotypic datasets. *Nucleic Acids Res* **34**, D479-83.
- Staehling-Hampton, K., Hoffmann, F. M., Baylies, M. K., Rushton, E., and Bate, M. (1994). dpp induces mesodermal gene expression in Drosophila. *Nature* **372**, 783-6.
- Stathopoulos, A., and Levine, M. (2002). Dorsal gradient networks in the Drosophila embryo. *Dev Biol* **246**, 57-67.
- Stronach, B. E., Renfranz, P. J., Lilly, B., and Beckerle, M. C. (1999). Muscle LIM proteins are associated with muscle sarcomeres and require dMEF2 for their expression during Drosophila myogenesis. *Mol Biol Cell* **10**, 2329-42.
- Strunkelnberg, M., Bonengel, B., Moda, L. M., Hertenstein, A., de Couet, H. G., Ramos, R. G., and Fischbach, K. F. (2001). rst and its paralogue kirre act redundantly during embryonic muscle development in Drosophila. *Development* **128**, 4229-39.
- Stute, C. (2004). The determination of the founder and fusion competent myoblasts of the visceral mesoderm of Drosophila melanogaster depends on Notch as well as on Jeb/Alk mediated RTK-signalling. Universität Marburg, Marburg.
- Taylor, M. V. (2006). Comparison of muscle development in drosophila and vertebrates. In "Muscle development in drosophila" (H. Sink, Ed.), pp. 207. Landes Bioscience/Eurekah.com ; Springer Science + Business Media, Georgetown, Tex. New York, N.Y.
- Turner, B. M. (2002). Cellular memory and the histone code. *Cell* **111**, 285-91.

- Tusher VG, T. R., Chu G. (2001). Significance analysis of microarrays applied to the ionizing radiation response. *Proc Natl Acad Sci U S A* **98**, 5116-5121.
- Vigoreaux, J. O. (2006). Molecular basis of muscle structure. In "Muscle development in drosophila" (H. Sink, Ed.), pp. 207. Landes Bioscience/Eurekah.com ; Springer Science + Business Media, Georgetown, Tex. New York, N.Y.
- Volk, T. (2006). Muscle attachment sites: where migrating muscles meet their match. In "Muscle development in drosophila" (H. Sink, Ed.), pp. 207. Landes Bioscience/Eurekah.com ; Springer Science + Business Media, Georgetown, Tex. New York, N.Y.
- Wang, G., and Jiang, J. (2004). Multiple Cos2/Ci interactions regulate Ci subcellular localization through microtubule dependent and independent mechanisms. *Dev Biol* **268**, 493-505.
- Wray, G. A., Hahn, M. W., Abouheif, E., Balhoff, J. P., Pizer, M., Rockman, M. V., and Romano, L. A. (2003). The evolution of transcriptional regulation in eukaryotes. *Mol Biol Evol* **20**, 1377-419.
- Yin, Z., Xu, X. L., and Frasch, M. (1997). Regulation of the twist target gene tinman by modular cis-regulatory elements during early mesoderm development. *Development* **124**, 4971-82.
- Zeitlinger, J., Zinzen, R. P., Stark, A., Kellis, M., Zhang, H., Young, R. A., and Levine, M. (2007). Whole-genome ChIP-chip analysis of Dorsal, Twist, and Snail suggests integration of diverse patterning processes in the Drosophila embryo. *Genes Dev* **21**, 385-90.
- Zhang, Y., Featherstone, D., Davis, W., Rushton, E., and Broadie, K. (2000). Drosophila D-titin is required for myoblast fusion and skeletal muscle striation. *J Cell Sci* **113** (Pt 17), 3103-15.

Acknowledgments

It is common to start the acknowledgements by thanking your supervisor for the opportunity to pursue a project in their lab, and I do thank Eileen Furlong for giving me this opportunity when I first came to EMBL years ago. In this case however, this would be an understatement and would not do justice to what the last few years of my PhD have been; I would like to thank Eileen for both her encouragement and determination to see me finish my PhD. This thesis would not have been possible without Eileen's tenacity, scientific guidance and understanding during these last difficult times.

I would also like to thank the members of my Thesis Advisory Committee (TAC) Pernille Rørth, Jan Ellenberg and Renate Renkawitz-Pohl for helpful discussions during our TAC meetings. I would further like to thank Renate for her encouragement, concern and helpful suggestions, both via mail and during my visits to Marburg.

This work would not have been possible without the endeavor of Thomas Sandmann. Thomas started this project and made priceless contributions to the very end, both scientifically and as a dear friend.

I am greatly indebted to Hilary Gustafson who made invaluable contributions in virtually every aspect of this work, from transgenic fly lines, to *in situ* probe synthesis and hybridization, and in many other projects along the years. Her friendship and calm presence meant a lot to me all this time.

It was a pleasure to share an aisle in the lab with Janus Jakobsen. We shared many discussions as well, from the trivial day-to-day bench questions to the greater scope of the projects and life in general. Janus was always a true friend, the first support and a source of joy and positive thinking.

I would also like to thank Martina Braun for her friendly presence in the lab, as well as technical assistance along the years, in particular with quantitative Real-Time PCR preparation and analysis.

Philippe Beaufils provided technical assistance during the early stages of my PhD and was a great tutor in the fields of cloning and fly work.

I would like to thank the past and present members of the Furlong lab for the warm working atmosphere, and in particular Lucia Kayserova who contributed with fluorescent *in situ* stainings and helped refreshing my memory about luciferase assays, and Junaid Akthar for discussions around luciferase assays, and generosity with his S2 cells and reagents.

This work could not have been performed without the generation of a large number of transgenic flies, and I would like to thank Ane-Marie Voie, Eva Löser and Teresa Jagla for all the plasmid injections.

My days at EMBL were much happier thanks to the great number of people with whom I had the pleasure to play music all this time; I thank you all.

I started my PhD together with Marlene Rau, and from the beginning to the end she was an ever-present and understanding friend, and I couldn't ask for more.

The very first person I met in my first hours in Heidelberg was Jean-Baptiste Coutelis. He has been the best friend you could ask for from that moment on, and I hope someday I will be able to return some of what he has given me all these years. Obrigado JB.

Deixo um agradecimento à comunidade portuguesa no EMBL, em particular à Sílvia Curado que me acolheu nos meus primeiros tempos em Heidelberg, ao Pedro Beltrão pela presença sempre amiga e reconfortante do companheiro de Coimbra, e à Sílvia Santos pelo carinho e apoio. Um obrigado também à Raquel Matos e Hédio Roque com quem passei bons momentos nestes últimos anos.

A Daniela Roesch-Ely, uma palavra de profunda gratidão. Obrigado.

Um obrigado pela paciência e carinho durante os meus tempos conturbados em Portugal aos meus amigos Mário Miguel e Ana Cunha, e também Vasco, Tiago, Tito, Luís e Anabela, companheiros de guitarradas e copos de tantos anos.

Os últimos passos da escrita desta tese foram dados no escritório da Norte Architectos / Green Lines Institute. Agradeço à Cristina, Rogério e Filipe terem-me acolhido no seu ótimo ambiente de trabalho.

À minha família agradeço do fundo do coração a compreensão e apoio, incondicional e sem questões. Ao Luís pelo companheirismo. À minha irmã Marlene que apanhou o primeiro avião quando precisei dela, como sempre. Ao meu Pai, porque é a única pessoa que diz “tem calma” e tudo pára, à minha Mãe, que tirou o tempo que foi preciso para estar comigo, por tudo, tudo, desde o primeiro dia.

E obrigado à Andreia, pela paciência, pelo carinho, por tudo que coube nestes anos e não cabe numa folha de papel...

Declaration

I declare that I wrote this study myself and carried out the experimental work described in it, without using any other sources and aids than those that are stated.

Marburg, May 2010.

Publications

Feng Qiu, Sigrun Brendel, **Paulo M. F. Cunha**, Nagore Astola, Bauzhen Song, Eileen E. M. Furlong, Kevin R. Leonard and Belinda Bullard

Myofilin, a protein in the thick filaments of insect muscle

Journal of Cell Science **118**, 1527-36

Paulo M. F. Cunha*, Thomas Sandmann*, E. Hilary Gustafson, Lucia Ciglar, Michael P. Eichenlaub, Eileen E.M. Furlong

* These authors contributed equally

Combinatorial binding leads to diverse regulatory responses: Lmd is a tissue-specific modulator of Mef2 activity

PLoS Genetics (In revision).

Curriculum Vitae

Paulo Miguel Fernandes Cunha

Av. D. Nuno Álvares Pereira, nº 85
Apartamento 61
4750-324 Barcelos
PORTUGAL

Mobile: +351 93 420 05 28
pmfcunha@gmail.com

Education:

2002 – B.Sci. Biochemistry (Faculty of Science and Technology of the University of Coimbra)

Licenciatura em Bioquímica (Faculdade de Ciências e Tecnologia da Universidade de Coimbra)

1996 – High School education completed at the *Escola Secundária Alcaides de Faria* – Barcelos

Publications

Gomes, A. R., **Cunha, P.**, Nuriya, M., Faro, C. J., Huganir, R. L., Pires, E. V., Carvalho, A. L., and Duarte, C. B. (2004).

Metabotropic glutamate and dopamine receptors co-regulate AMPA receptor activity through PKA in cultured chick retinal neurones: effect on GluR4 phosphorylation and surface expression.

J Neurochem **90**, 673-82.

Feng Qiu, Sigrun Brendel, **Paulo M. F. Cunha**, Nagore Astola, Bauzhen Song, Eileen E. M. Furlong, Kevin R. Leonard and Belinda Bullard (2005)

Myofilin, a protein in the thick filaments of insect muscle

Journal of Cell Science **118**, 1527-36

Paulo M. F. Cunha*, Thomas Sandmann*, E. Hilary Gustafson, Lucia Ciglar, Michael P. Eichenlaub, Eileen E.M. Furlong (2010)

* These authors contributed equally

Combinatorial binding leads to diverse regulatory responses: Lmd is a tissue-specific modulator of Mef2 activity

PLoS Genetics (accepted for publication).